

# UNIVERSITY OF KWAZULU-NATAL



## *MASTERS DISSERTATION*

### **Optimizing the protection of an auto-recloser in a DG integrated distribution network**

*Author:*

***Siyabonga Brian Gumede***

*Supervisors:*

***Dr. Akshay Kumar Saha***

*This dissertation submitted in fulfillment of the requirements  
for the degree of Masters of Science (MSc): Electrical Engineering*

School of Engineering

College of Agriculture, Engineering and Science

Durban, South Africa

***December 2022***

**UNIVERSITY OF KWAZULU-NATAL**



**Optimizing the protection of an auto-recloser in a DG integrated  
distribution network**

*Author:*

***Siyabonga Brian Gumede***

*Signed:*



*Date:* 12/07/2022

*Supervisor:*

***Dr. Akshay Kumar Saha***

School of Engineering

College of Agriculture, Engineering and Science

Durban, South Africa


***December 2022***

## PREFACE

The research contained in this thesis was completed by the candidate *Mr. Siyabonga Brian Gumede*, under the supervision of *Dr. Akshay Kumar Saha* in the Discipline of Electrical, Electronic, and Computer Engineering, School of Engineering, College of Agriculture, Engineering, and Science, University of KwaZulu-Natal (UKZN), Howard College Campus, Durban, South Africa. This thesis has not been submitted in any form to another university, and the results reported are due to investigations by the candidate. The entire contents of this work, except where the work of other researchers is acknowledged in the text, is the original work of the candidate.

As the candidate's supervisor, I agree/ do not agree the submission for this thesis.

*Dr. Akshay Kumar Saha*

*Signed* 

*Date: 29 November 2022*

# DEDICATIONS

I sincerely dedicate this thesis to the following;

To the Lord, my family and friends. A special gratitude to my late mother and father, ***Mrs. Ntombiyenkosi Gumede and Mr Jerry Gumede*** who gave their all to give me education; my brothers and sisters who have helped bring the family into stability through difficulties and my aunt, ***Mrs. Lindiwe Mashoane*** for being a mother to my family and staying with us.

# PLAGIARISM DECLARATION

I, Siyabonga Brian Gumede declare that:

1. This thesis is the first work of the writer and where work of other writers has been used, is accordingly recognized in the content.
2. The thesis has not been submitted in any form to any other Institute of Higher Learning.
3. This thesis does not include other persons' data, pictures, graphs or other information unless specifically acknowledged as being sourced from other persons.
4. Where other written sources have been quoted, then:
  - Their words have been re-written but the general information attributed to them has been referenced.
  - Where their exact words have been used, their writing has been placed inside quotation marks and referenced.
5. This thesis does not include text, graphics or tables copied and pasted from the Internet, unless specifically acknowledged, and the source being detailed in the thesis and in the References section.

*Siyabonga Brian Gumede*

*Signed:*

A black rectangular box redacting the signature of Siyabonga Brian Gumede.

*Date:* 12/07/2022

## DECLARATION 2: PUBLICATIONS

DETAILS OF CONTRIBUTION TO PUBLICATIONS that form part and/or include research presented in this thesis (include publications in preparation, submitted, in press and published and give details of the contributions of each author to the experimental work and writing of each publication):

Publication 1:

*S. B. Gumede and A. K. Saha, "A Comparison of a Recloser Performance in a Passive and Active Distribution System," 2021 International Conference on Electrical, Computer, Communications and Mechatronics Engineering (ICECCME), 2021, pp. 1-6, doi: 10.1109/ICECCME52200.2021.9590845.*

Publication 2:

*Gumede, S.B.; Saha, A.K. Optimizing Recloser Settings in an Active Distribution System Using the Differential Evolution Algorithm. Energies 2022, 15, 8514. <https://doi.org/10.3390/en15228514>*

*Siyabonga Brian Gumede*

*Signed:*



*Date:* 12/07/2022

## ACKNOWLEDGEMENTS

I would like to acknowledge my supervisor, **Dr. Akshay Kumar Saha** for continued guidance, motivation and opportunity in completing this research work and **Mr. Ncengizwe Hlambisa** for his continual help with IT troubleshooting.

I would like to show great gratitude to God and my family for the love and the support they have given throughout the course of this work; without their support I would be where I am. I am very grateful to everyone who contributed to the completion of this project and studies.

I also wish to express my gratitude to all my friends and other staff members of University of KwaZulu-Natal who rendered their help during the period of my studies.

# Abstract

The integration of distributed generation into distribution networks is growing as most of the distributed generators have a sustainable power supply and can be used to improve the voltage profile. However, the type of a distributed generator and location in the distribution network can determine how a voltage profile behaves in a distribution feeder. They also contribute fault current in a new or same direction as the fault current from the utility. With this change in the fault current, the existing protection scheme may mal-operate since the protection scheme was designed for fault current from the utility generator. One of the protection devices that can mal-operate is the auto-recloser. This is a device used for the self-remediation of the distribution network when there is a temporary fault.

The IEEE and IEC standard for the international use of auto-reclosers in voltages between 1000 V and 38 kV states that the minimum tripping current shall be stated by the manufacturer with a tolerance not exceeding  $\pm 10\%$  or 3 A, and the preferred operating sequence for auto-reclosers shall be; open - time delay of 0.5 seconds - close and open-second time delay 2 seconds - close and open - third-time delay of 5 seconds - close and open then lock out. However, these parameters can be violated when distributed generators are introduced into the distribution network. The change in the fault current may vary the operating time of the auto-recloser and it may not operate in this manner. The inverse time-current characteristics of the auto-recloser relay cause this. However, the operating time problem can be optimized.

The inverse time-current characteristic of the auto-recloser relay can be used to formulate the auto-recloser operating time problem. The settings can be optimized to reduce the time and mitigate mal-operations such as protection blinding, fuse and auto-recloser losing coordination, and sympathetic tripping. To optimize the settings, optimization algorithms can be applied.

In this research, the development of a single-shot auto-recloser is conducted. The IEEE 13-node and 34-node radial distribution feeders are used as a passive distribution network. The Wind Turbine and Solar Photovoltaic systems are distributed generators. MATLAB/Simulink is used for simulations, and the results obtained show that the integration of the distributed generators into a passive distribution network causes mal-operations in the auto-recloser when there is a fault. The factors that contribute to these mal-operations is the fault location, fault type, distributed generator type, distributed generator penetration and location. However, the auto-recloser shows improvement when the settings are optimized in these conditions.



# Contents

PREFACE .....	I
DEDICATIONS .....	II
PLAGIARISM DECLARATION .....	III
ABSTRACT .....	VI
LIST OF FIGURES .....	X
LIST OF TABLES .....	XII
NOMENCLATURE .....	XIII
CHAPTER 1 – INTRODUCTION .....	1
1.1. Background .....	1
1.2. Purpose of research .....	6
1.3. Objectives of research .....	7
1.4. Scope of research work .....	7
1.5. Limitations .....	8
1.6. Outline of chapters .....	8
CHAPTER 2 -THEORETICAL BACKGROUND AND LITERATURE REVIEW .....	10
2.1. Introduction .....	10
2.2. Application and operation of the auto-recloser .....	10
2.3. Auto-recloser mal-operation in active distribution networks .....	14
2.4. Optimizing the protection settings .....	20
2.5. Conclusion .....	22
CHAPTER 3 – METHODOLOGY .....	24
3.1. Introduction .....	24

3.2.	Modelling of the auto-recloser.....	24
3.3.	Circuit breaker control design.....	25
3.4.	Settings and operability design .....	25
3.5.	Auto-recloser performance evaluation.....	26
3.6.	Auto-recloser protection optimization approach.....	28
3.7.	Determination of the distribution network conditions .....	29
3.8.	Auto-recloser protection optimization case studies .....	33
3.9.	Conclusion .....	34
CHAPTER 4 AUTO-RECLOSER PERFORMANCE EVALUATION AND SETTINGS OPTIMIZATION .....		35
4.1.	Introduction.....	35
4.2.	Auto-recloser model.....	35
4.3.	Auto-recloser output .....	36
4.4.	Settings and operation.....	37
4.5.	Operating time and dead-time.....	38
4.6.	Application in a passive distribution network.....	39
4.7.	DG integration .....	41
4.8.	Comparison of auto-recloser performance.....	45
4.9.	Optimization framework.....	46
4.10.	Optimal settings and operation .....	49
4.11.	Conclusion .....	52
CHAPTER 5 OPTIMIZING AUTO-RECLOSER PROTECTION .....		53
5.1.	Introduction.....	53
5.2.	DG systems .....	53
5.3.	Integration.....	54
5.4.	DE modified schemes .....	54

5.5.	Case studies for optimal auto-recloser protection .....	55
5.6.	Case studies for the exponential scale factor application.....	67
5.7.	Discussion .....	73
5.8.	Conclusion .....	78
CHAPTER 6 CONCLUSION AND RECOMMENDATION FOR FUTURE RESEARCH WORKS .....		80
6.1.	Introduction.....	80
6.2.	Integration of DGs for the F1 fault location case studies.....	80
6.3.	Integration of DGs for the F2 fault location case studies.....	81
6.4.	Integration of DGs with exponential scale factor application for the F1 fault location case studies 81	
6.5.	Integration of DGs with exponential scale factor application for F2 fault location case studies ....	82
6.6.	Recommendation for future Research Work.....	82
REFERENCES .....		83

# List of Figures

Fig. 1-1 Characteristics of a distribution network [2] .....	2
Fig. 2-1 Control circuit of auto-recloser [18-19] .....	13
Fig. 2-2 Sympathetic tripping of an auto-recloser [50].....	19
Fig. 2-3 Loss of coordination between the auto-recloser and fuse [1] .....	19
Fig. 3-1 IEEE 13 node radial distribution test feeder with faults in node 34 and node 75 [62].....	27
Fig. 3-2 IEEE 13 node radial distribution test feeder with faults in node 34 and node 75 [62].....	28
Fig. 3-3 Application of the auto-recloser in the IEEE 34 node radial distribution feeder with DG [67] ....	30
Fig. 3-4 Distribution Network's voltage profiles .....	31
Fig. 4-1 Auto-recloser construction overview [73].....	36
Fig. 4-2 Control signal of the auto-recloser [75] .....	37
Fig. 4-3 Flow chart of the auto-recloser operation [1] .....	38
Fig. 4-4 Voltage profiles during a temporary and permanent fault at node 34 .....	40
Fig. 4-5 Current profile and control signals for R1 and R2 during a temporary and permanent fault at node 34 .....	40
Fig. 4-6 Current profile and control signals of R1 and R2 during a temporary and permanent fault at node 75 .....	41
Fig. 4-7 Voltage profiles for a temporary and permanent fault with DG integrated.....	43
Fig. 4-8 Current profile and control signals for R1 and R2 during a temporary and permanent fault at node 34 with DG.....	44
Fig. 4-9 Current profile and control signals for R1 and R2 during a temporary and permanent fault at node 75 with DG.....	45
Fig. 4-10 Comparison of the fast and delayed operation times for R1 in the four case studies.....	46
Fig. 4-11 Comparison of the fast and delayed operation times for auto-recloser R2 in the four case studies .....	46
Fig. 4-12 Comparison of the fast and delayed curves with conventional and optimal settings in case 3 and case 4.....	50
Fig. 4-13 Comparison of the not-optimized and optimized operation of auto-recloser R1 for a temporary fault .....	51
Fig. 4-14 Comparison of the not-optimized and optimized operation of auto-recloser R1 for a permanent fault .....	52
Fig. 5-1 Voltage profile with no DG for a temporary fault in the F1 fault location .....	57
Fig. 5-2 Auto-recloser pick-up activity for different schemes and settings in case study 1 .....	57

Fig. 5-3 Voltage profile with Solar PV system integration for a temporary fault in the F1 fault location	59
Fig. 5-4 Auto-recloser pick-up activity for different schemes and settings in case study 2	59
Fig. 5-5 Voltage profile with Solar PV and Wind Turbine system integration for a temporary fault in the F1 fault location	61
Fig. 5-6 Auto-recloser pick-up activity for Conventional, MDE1 and MDE3 schemes and settings in case study 3	61
Fig. 5-7 Voltage profile with no DG for a temporary fault in the F2 fault location	63
Fig. 5-8 Auto-recloser pick-up activity for MDE1 and MDE3 schemes and settings in case study 4	63
Fig. 5-9 Voltage profile with Solar PV system integration for a temporary fault in the F2 fault location	65
Fig. 5-10 Auto-recloser pick-up activity for MDE1 and MDE3 schemes and settings in case study 5	65
Fig. 5-11 Voltage profile with Solar PV and Wind Turbine system integration for a temporary fault in the F2 fault location	67
Fig. 5-12 Auto-recloser pick-up activity for MDE1 scheme and settings in case study 6	67
Fig. 5-13 Auto-recloser pick-up activity for MDE1 and MDE3 schemes and settings with exponential scale factor in case study 1	69
Fig. 5-14 Auto-recloser pick-up activity for MDE1 and MDE3 schemes and settings with exponential scale factor in case study 2	70
Fig. 5-15 Auto-recloser pick-up activity for MDE1 and MDE3 schemes and settings with exponential scale factor in case study 3	71
Fig. 5-16 Auto-recloser pick-up activity for MDE3 scheme and settings with exponential scale factor in case study 5	72
Fig. 5-17 Auto-recloser pick-up activity for MDE1 and MDE3 schemes and settings with exponential scale factor in case study 6	73
Fig. 5-18 Scheme and settings performance for temporary fault at F1 location	75
Fig. 5-19 Scheme and settings performance for temporary fault at F2 location	76
Fig. 5-20 Scheme and settings performance with an exponential scale factor for temporary fault at F1 location	76
Fig. 5-21 Scheme and settings performance with an exponential scale factor for temporary fault at F2 location	76

## List of Tables

Table 3-1 Voltages at the common couplings in per unit .....	31
Table 3-2 Fault currents for fault located in node 802 and node 826 .....	32
Table 4-1 Optimal settings.....	50
Table 5-1 DE Modified Schemes.....	55
Table 5-2 Conventional and Optimal Settings .....	55
Table 5-3 Auto-recloser operating times in case study 1 .....	56
Table 5-4 Auto-recloser operating times in case study 2 .....	58
Table 5-5 Auto-recloser operating times in case study 3 .....	60
Table 5-6 Auto-recloser operating times in case study 4 .....	62
Table 5-7 Auto-recloser operating times in case study 5 .....	64
Table 5-8 Auto-recloser operating times in case study 6 .....	66
Table 5-9 Auto-recloser operating times for exponential scale factor application in case study 1 .....	68
Table 5-10 Auto-recloser operating times for exponential scale factor application in case study 2.....	69
Table 5-11 Auto-recloser operating times for exponential scale factor application in case study 3.....	70
Table 5-12 Auto-recloser operating times for exponential scale factor application in case study 4.....	71
Table 5-13 Auto-recloser operating times for exponential scale factor application in case study 5.....	72
Table 5-14 Auto-recloser operating times for exponential scale factor application in case study 6.....	73

# Nomenclature

A	Ampere
AC	Alternating Current
ACO	Ant Colony Optimization
ANSI	American National Standards Institute
DC	Direct Current
DE	Differential Evolution
DG	Distributed Generation
Hz	Hertz
IEEE	Institute of Electrical and Electronics Engineers
IEC	International Electrotechnical Commission
kA	Kiloampere
kV	Kilovolts
kW	Kilowatts
MDE1	Modified Differential Evolution One
MDE2	Modified Differential Evolution Two
MDE3	Modified Differential Evolution Three
msec	Milliseconds
MVA	Mega Volt Ampere
PSO	Particle Swarm Optimization
PV	Photovoltaic
R	Resistance
R1	Auto-recloser One
R2	Auto-recloser Two
RMS	Root Mean Square
XC	Capacitive Reactance
XL	Capacitive Inductance
V	Volts

# Chapter 1 – Introduction

## 1.1. Background

Radial distribution networks can be defined as networks with one main generator supplying the distributors at just a single end [1]. An electric utility generates power from the generation system at the center of consumers and supplies this power downstream to substations. In substations, the voltage is stepped down by transformers to distribution voltage levels and supplied to radial distribution networks. The AC voltage system is generally used in the radial distribution network for the voltage supply [2].

The distribution network consists of a main feeder, lateral feeder and a service main. The main feeder is designed using its current carrying capacity and the lateral feeder is designed based on the voltage drops along the main feeder. The point where the lateral feeder or main feeder is connected is called a node. The node at the substation is called a reference node, this is a node for sending power from the substation. The point of connection between the main feeder and the lateral feeder is called a load node. This is a receiving node. A typical radial distribution voltage in the main and lateral feeders is between 1kV - 38kV [3]. The voltage at the node must be limited to  $\pm 6\%$  variation to the voltage of the consumer [2].

The main or lateral feeder has an impedance in ohms/m. The impedance of the feeder is made up of its resistance  $R$ , inductive reactance  $X_L$  and capacitive reactance  $X_C$  between two feeders. The section of the feeder between two nodes is called a branch. A branch has a  $R/X$  ratio; this determines the voltage drop in a feeder. Distribution feeders have a high  $R/X$  ratio and therefore have high voltage drops. Because of the high voltage drops, strategies are employed in the distribution network to support the voltage. These strategies are changing the tap position of the transformer, active power sharing and injection of reactive power [4].

A block diagram in Fig. 1-1 depicts how the distribution network can be constructed and the nature of the current. The simplest, less expensive and commonly used scheme of connection is the radial distribution network.



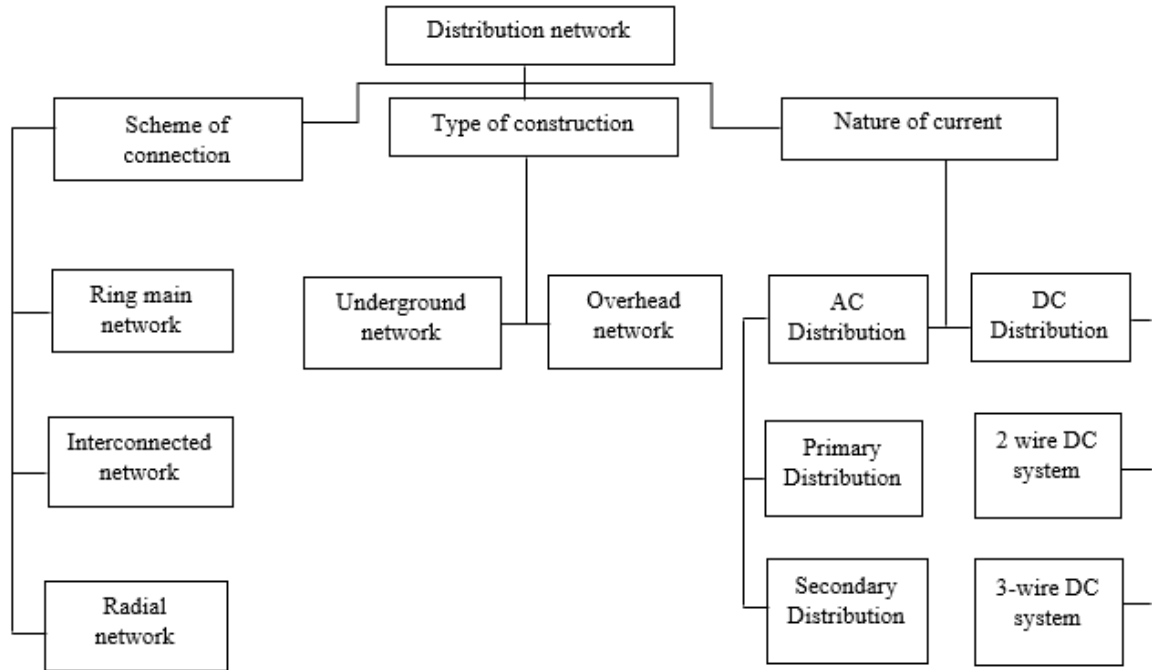


**Fig. 1-1 Characteristics of a distribution network [9]**

Radial distribution networks can have these feeders broken or clashing, failure in their insulation or lightning strikes. These are commonly called faults in the distribution network. These faults disrupt power distribution to consumers and decrease the reliability of the distribution network. Faults can be classed into three types depending on the duration. They can be permanent, semi-permanent, or temporary (i.e. transient). A permanent fault is a fault that does not self-clear and requires an operator to clear it, a semi-permanent fault is a fault that persists for certain period of time but eventually self-clears and a temporary fault is a fault that self-clears in a short period time. Many research studies have concluded that about 85% of these faults are temporary, and this has led power utilities to implement automatic reclosing in radial distribution networks. Automatic reclosing is for automating the reclosure of a circuit breaker [5]. This is to avoid long power interruptions in the power supply when there are temporary faults. This also enhances the reliability of the distribution network [6]. Underground feeder faults are considered as permanent faults and automatic reclosing is usually not applied for these feeders [7]. The name of the device that has the capability of automatically reclosing a circuit breaker in the main or lateral feeder is called an auto-recloser. This device is a circuit breaker that is equipped with an overcurrent relay and a reclosing control circuit, it can also receive signals from an overcurrent relay in the distribution network to perform its operation. It performs the operation of tripping the circuit breaker after an operating time and reclosing after a dead-time. The auto-recloser is often placed near a distribution substation [8-9].

The auto-recloser has to maintain its optimal operation for a continued reliable operation of the distribution

network [10]. The following five aspects are the requirements for an optimal operation of the auto-recloser.

- Selectivity requirement

Only the faulted segment of the feeder in the distribution network should be isolated.

- Security requirement

The auto-recloser must avoid unnecessary disconnection of lines due to increased currents on healthy lines.

- Redundancy requirement

The auto-recloser should act as primary protection and backup protection.

- Sensitivity requirement

The auto-recloser should be adjusted such that there is high redundancy without compromising selectivity.

- Dependability requirement

The auto-recloser must achieve its objective in changing network topology, network conditions, and fault conditions.

Radial distribution networks were traditionally passive with the specifications of the plant gears, and control gears including auto-reclosers being based on the assumption of a grid supply. This made protection settings easy to implement and optimal, but passive distribution networks can exhibit problems such as unstandardized voltage drops and inadequate power supply which may require building or integrating new generators [11]. Power utilities are integrating DGs into the distribution network for improving the voltage profile, deregulate the grid, and provide ancillary service to the utility. Other advantages of deploying this generation is that it has an environmentally-friendly generation which is sustainable [12-13].

DGs can be defined as small electric generators which normally use renewable energy resources to generate power. These newly deployed voltage sources in the distribution network can vary between a few kilowatts to several megawatts of power, and connected close to the load. They can be synchronous machines, asynchronous machines or fuel cells. Their power ratings normally range from 1kW to 50kW [14]. They can be operated in island mode (i.e. standing alone, apart from the utility grid) or grid-connected mode, and hybridized with energy storage systems to ensure a reliable, and stable power supply to the local loads.

The integration of DGs into a passive distribution network makes the distribution network decentralized

and changes the passive distribution network into an active distribution network. However, this additional generation of power affects the load flow and voltage stability [15].

On the integration of this generator, the utility generator and the DG voltages have to be synchronous [10]. This is advantageous in that there is a provision of voltage support [16]. There is a maximum allowable DG capacity for different distribution network configurations. There are three constraints in the distribution network when the capacity of a DG is increased, these are a continual operation of conventional protection coordination, decrease in line losses and preservation of distribution network voltage within limits [17].

There is a growing demand in the integration of the DG and there is more renewable generation integrated in the distribution network. Therefore, the penetration of DGs into the grid determines the amount of fault current contribution to the fault current that will flow through the auto-recloser. This change in the fault current can affect the normal operation of the auto-recloser using pre-programmed settings (i.e. conventional settings) [18]. The location, type and penetration of the DGs in the distribution network play a vital role in the operation of the auto-recloser because of this fault current contribution [19].

In the case of a fault occurring in active distribution networks, the prevailing practice was to isolate the DGs during that fault. However, the substantial increase in the penetration of DGs has led to a standard requiring them to remain grid-connected during a fault. This is because during the interruption there is a significant reduction of power which is unsuitable for the utility. The DGs can be enabled to have a fault ride-through or low voltage ride-through and remain grid-connected, this provides a continuous supply of voltage. The integration of DGs in distribution feeders changes the topology of the radial distribution network, this introduces another fault current source and direction in the distribution network. This can result in the variation of the fault current level that the auto-recloser is detecting. The auto-recloser can have a varied operating time because of the non-linear current dependent time characteristic. This leads to faster or delayed tripping signals of the auto-recloser [20].

In these cases, the auto-recloser is not operating according to the conventional settings and this is a mal-operation of the auto-recloser. The cause of auto-recloser mal-operation can be due to the number, capacity, type and location of the DGs. The location of the fault, type of a fault and network impedance also influences the auto-recloser to mal-operate. The three types of common mal-operations in the auto-recloser are [21-22]:

- Blinding of auto-recloser protection.
- Sympathetic tripping of the auto-recloser.

- Auto-recloser losing coordination with other protection devices.

The blinding of auto-recloser protection occurs when there is a decrease in the fault current detected by the auto-recloser and makes the operating time infinite [23]. When a DG is integrated into the distribution network, its contribution to the fault might decrease the fault current level, and this level is less than the pick-up current of the auto-recloser. The auto-recloser does not detect the fault current and does not operate to isolate the fault [18-19].

The sympathetic tripping of the auto-recloser occurs when the current in a healthy feeder increases and surpasses the auto-recloser's pick-up setting, the auto-recloser operates although there is no fault on the feeder. This can be due to the contribution of the DG to a fault if it is integrated in a healthy feeder, transient current increases or inrush currents [17, 24].

The auto-recloser can also lose coordination with other protection devices when there is detection of a higher current by the protection device than the auto-recloser. The current is outside the minimum and maximum bounds for the coordination to remain valid. The time delay becomes less than the fast mode of operation in the auto-recloser. The integration of a DG alters the fault current level detected by the auto-recloser and this depends on the location of the fault relative to the DG [24-25].

The reliability of the auto-recloser is dependent upon the mitigation or reduction of these mal-operations. The mitigation or reduction has been addressed in literature through the use of a directional protection method. This method addresses the reverse current of the DG, but this applies mostly to relays. Another method is to disconnect DGs before the auto-recloser operates, this should enable the auto-recloser to operate in pre-existing voltage and fault conditions. Another method is to determine the best DG location, and separating the distribution network into protection zones that are controlled by computer-based substation relays [7]. However, this method is complex and imposes a lot of expense [21]. Another method is to use a superconducting fault current limiter to reduce the current flowing into the auto-recloser. The superconducting fault current limiter is connected in series with the DG. The disadvantage with the superconducting fault current limiter is the lack of methodology in determining its optimum impedance and the high cost associated with it [26]. Using an adaptive protection scheme that updates settings on the auto-recloser based on the prevailing conditions of the distribution network, and the fault type has also been presented [20]. The auto-recloser adapts to the change of passive conditions to active conditions [12]. This method is normally applicable for networks with increasing penetration of distributed generation. This method also requires communication enabled remotely auto-reclosers and circuit breakers [8]. Adaptive protection schemes may require optimization algorithms in selecting optimal settings. Using microprocessor-based auto-reclosers instead of hydraulically controlled auto-reclosers which provide the

selection of optimal settings may mitigate or reduce the mal-operations. This also reduces complexity of selecting settings that adapt to network conditions. Metaheuristic optimization algorithms are commonly used in optimizing the settings provided by protection devices [27]. The selection of settings through these algorithms can enhance the performance of the auto-recloser when the distribution network has a grid-connected DG. These algorithms are population based and provide a method of obtaining optimal solutions through iterative steps. They can select the best solution to solve an optimization problem. They involve the formulation of linear and non-linear optimization problems. The DE algorithm has been ranked as one of the best algorithms for solving optimization problems. The advantage of using this algorithm is that it performs a stochastic search through the feasible region of solutions, is capable of handling non-linear and non-differentiable functions, and easily escapes from a local optimum [19].

## **1.2. Purpose of research**

The DG provides a voltage support to the distribution network and reduces the voltage drops. The DGs' grid-connected mode during fault conditions is beneficial to the utility and consumer because the loads that are unaffected have a voltage supply [29]. However, these generators tend to be intermittent, and the voltage does not remain in a steady state. These generators are normally installed with an energy storage system and a hybrid solution may be inadequate as the energy storage system needs to be charged. A quick reconnection of the utility generator may be necessary. Since the settings of the auto-recloser program the auto-recloser to make a selection between temporary and permanent faults, the fault current magnitude is also a factor in the calculation of the operating time, if there is a delay in operation and the faults seems permanent, other electrical equipment such as fuses may be impacted during the temporary fault. Therefore, to have an appropriate discrimination, quick isolation and quick restoration of service, appropriate settings need to be programmed when there is grid-connection and low voltage ride-through of the DG. Since the distribution network has also been reconfigured to include the additional generation, and this varies the magnitude and direction of the fault current [30], fault currents not isolated may stress electrical equipment not designed to handle this magnitude of the fault currents.

Therefore, the research focuses on the selection of feasible optimal settings in the auto-recloser when DGs are integrated. This is to optimize the protection of the auto-recloser for a temporary fault and change in voltage conditions. The proposed optimization algorithm is the DE algorithm. The research seeks to answer the following questions:

1. What is the cause of mal-operations in the auto-recloser when DG is integrated? What is the level of performance in these new voltage and fault conditions?

2. What are the optimal settings that will optimize this performance and reduce these mal-operations within the provided feasible settings?
3. How effective are the selected settings during the DG's low-voltage ride through?
4. What impact does the type and location of the DG on the performance of the auto-recloser?
5. Which DE scheme provides the most optimal settings for the protection of the auto-recloser in a DG integrated network?

### **1.3. Objectives of research**

This research aims to reduce auto-recloser mal-operations when a DG is integrated and explores the feasibility of using the DE algorithm to quickly search and select optimal settings in the auto-recloser. These settings are to minimize the operating time of the auto-recloser when a DG has a low voltage ride-through during a temporary fault. The following aspects are covered:

1. Modelling of the auto-recloser for investigation and analysis.
2. Application and evaluation of the auto-recloser performance in a passive distribution network.
3. Application and evaluation of the auto-recloser performance in an active distribution network.
4. Comparison of the auto-recloser performance in a passive and an active distribution network.
5. Formulation of the mal-operations and optimization of the auto-recloser settings.
6. Analysis of the performance of the auto-recloser between conventional and optimal settings.
7. Investigation of the effect of the optimal settings on the auto-recloser in an active distribution network.
8. Integrating two types of DGs in a passive distribution network.
9. Modifying the DE algorithm to optimize the protection of the auto-recloser.
10. Testing the auto-recloser in different case studies that include changing the DG location and type.  
The case studies also test changing the fault location and type.
11. Balance the exploration and exploitation of the algorithms that have best met the objective function.

### **1.4. Scope of research work**

The scope of research covered in this thesis is limited to the auto-recloser and the performance of settings in a passive and active distribution network. The validation of the optimal settings is limited to the Solar PV system, Wind Turbine system, and supplementary energy storage system. The following aspects are covered in detail:

1. Modelling the auto-recloser for investigation and analysis.

2. Evaluation of the auto-recloser performance in an active distribution system.
3. A comparison of auto-recloser performance.
4. The selection of optimal settings using the DE algorithm.
5. Application of the optimal settings and comparison.
6. Modifications of the DE algorithm.
7. Case studies for optimizing auto-recloser protection with optimal settings.
8. Comparison of different DE scheme settings and the operating times they computed.

## **1.5. Limitations**

1. The actual auto-recloser device is not available for application using a hardware-in-the-loop experiment and simulation. Therefore, there is no experimental data for validating with simulated data. The results serve as a visualization of real expectations from optimizing the auto-recloser protection in a DG integrated network.
2. There is no real distribution network that can be modelled and the auto-recloser applied to observe the performance of the auto-recloser.

## **1.6. Outline of chapters**

Chapter 2 presents a theoretical background and a literature review on the application of the auto-recloser in distribution networks. The chapter also reviews the voltage profile variation as a result of the integration of DGs, the mal-operations when there is DG integration in the distribution network and the optimization using the DE algorithm.

Chapter 3 presents the methodology for modelling the auto-recloser, evaluating its performance and optimizing the protection. The methodology provides details of the application of the auto-recloser in the IEEE 13 node distribution feeder and IEEE 34 node distribution feeder. The methodology provides details of the simulations performed for obtaining auto-recloser operating times in a passive distribution network and active distribution network when there are faults. The details for a method in optimizing auto-recloser protection are also provided.

Chapter 4 presents the design and application of the auto-recloser in a passive distribution network, application of the auto-recloser in an active distribution network, comparison of auto-recloser performance in passive and active distribution networks. The problem formulation, optimizing settings through the DE algorithm, and comparison of conventional settings with optimal settings is also conducted.

Chapter 5 presents the modified DE algorithm schemes and the settings they computed. Case studies are simulated to analyze the performance of optimal settings in different types and location of DG systems integrated. The case studies also investigate different fault locations and types.

Chapter 6 presents the summary of findings for the case studies performed in chapter 5 and concludes. Recommendations are presented on the use the modified DE for obtaining auto-recloser optimal settings to isolate temporary faults in an integrated DG network. Future research work is also proposed.



# **Chapter 2 -Theoretical Background and Literature Review**

## **2.1. Introduction**

In normal operating conditions of a radial distribution network, the direction of flow for the current is from the sub-station to the load point, and also during faulted conditions the direction of the current flow is from the sub-station to the fault point [8]. To have a functional overcurrent protection with automatic reclosing for a distribution feeder, the auto-recloser is equipped with a time-dial setting, a pick-up setting, a dead-time and a control circuit. The performance of the auto-recloser highly depends on the level of the over-current as this device is operates by the detection of the fault current level. The time-dial, pick-up, dead-time and control circuit all form a fully operational auto-reclosing protection scheme with the performance dependent on the time-current characteristics. According to [31], any protection scheme should execute protection in the minimum time possible and must be capable of meeting this time when the distribution network is passive or active. In the event of failing to meet the operation time requirement, the settings of the auto-recloser can be optimized with a robust algorithm such as a DE algorithm.

## **2.2. Application and operation of the auto-recloser**

Auto-reclosers are designed for substation or pole mounted applications. They are primarily applied for the isolation of a faulted feeder section and quick reconnection of that feeder. They are also applied for distribution network recon-figuration, which is the process of altering the network topology by changing the open or close status of the auto-recloser [32]. With these applications, auto-reclosers in a distribution network are able to improve the distribution network's reliability, provide switching and protective functions, and reduce sustained interruptions due to temporary faults [33]. The automatic reclosing of circuit breakers after a temporary fault avoids an unnecessary long power supply interruption to consumers. The auto-recloser should operate faster than all protection devices to check if the fault is temporary and reclose the circuit breaker in the case of a temporary fault. If the fault is permanent, the fuse should operate before the final shot of the auto-recloser and the auto-recloser operates as back-up protection. The auto-recloser can be applied either using a standard inverse, very inverse, extremely inverse, definite minimum time or definite time lag characteristics [9, 15].

### **2.2.1. Setting the auto-recloser**

A protection scheme is designed and implemented for over-voltage, under-voltage, over-frequency, under-

frequency and over-current conditions in the distribution network. The protection philosophy is well established for radial distribution networks [16]. The auto-recloser can be programmed to detect over-current conditions for these network topologies. The auto-recloser has a dual-time operation that utilizes two types of overcurrent relay operations. The design and application of these overcurrent relays are according to the time-current characteristics. The time-current characteristic curves are designed and programmed by using two parameters of the overcurrent relays. These parameters are the time-dial setting and the pick-up current setting which can be set at the machine interface. The time-dial and pick-up settings have a minimum and maximum range of settings to adjust the time delay before sending trip commands. This is the operating time of the auto-recloser. With the use of these parameters to adjust the operating time of the auto-recloser, the auto-recloser can be programmed to trip for a fault current flowing downstream from the utility generator, and to coordinate with other protection devices. It can be programmed to at least one fast mode of operation and one delayed mode of operation [5,8]. A common practice is for a temporary fault to be cleared before the final delayed mode of operation and lock-out. The dead-time is also programmed to allow for the de-ionization of the fault current before it recloses the feeder. The auto-recloser can open and isolate the fault and then reclose after the dead-time for up to four shots, it will then lock-out the circuit breaker in the final shot [9]. For coordination, the final delayed operation is set to be slower than the coordinated devices' operating time in order to provide backup protection to the device. With fuses, this meets the requirement of a fuse saving scheme in the distribution network [13].

According to [25], relays and auto-reclosers have a set of settings that are pre-calculated so that they fulfil primary and back-up protection requirements. Calculations are based on minimum and maximum fault currents. The auto-recloser has both a relaying and a reclosing capability. According to [8], the time-dial and pick-up settings of the auto-recloser are fixed based on the maximum load and fault current. This is done by selecting a fixed time-dial parameter and pick-up parameter for the fast and the delayed mode of operation. The dead-time of the auto-recloser is often programmed to make the circuit breaker remain open in the ranges of a 100 milliseconds to seconds before a reclosure attempt [17].

In [34], it is stated that in the substation's primary protection is provided by a circuit breaker and feeder relay or, in some cases, by an auto-recloser and a microprocessor-based auto-recloser control. It is stated that the auto-recloser relay is comprised of a series trip coil that releases the stored-energy trip mechanism when an overcurrent occurs, and a relay that has a closing solenoid which supplies the energy for contact closing. It is also stated that the use of microprocessor based auto-recloser controls is accurate and repeatable. The reset characteristic of these auto-recloser controls is accurate and repeatable as well. Microprocessor-based auto-recloser controls can be coordinated better and there are numerous choices for

coordination curves. The auto-recloser can then be programmed to have a characteristic curve and provide an intentional time delay, making coordination simpler between devices operating on the fast curve. The curve settings are simpler to change using the auto-recloser control software instead of having to physically change out mechanical parts. The auto-recloser control overcurrent elements operate on current signals after going through a 1-cycle cosine filter.

In [35], the cutout mounted auto-recloser operates with an open-close-open-dropout sequence and has a 5 second dead-time interval. The auto-reclosers at the feeder source or upstream were re-programmed from two-shot reclosing to one fast and one time delayed trip before lock-out. It is noted that the raising of the auto-recloser settings reduced the level of back-up protection afforded to other laterals in the main feeder not fitted with these auto-reclosers. All the temporary short-circuits that that were monitored by the auto-recloser were cleared by the auto-recloser before the first 5 second dead-time elapsed. No outage was experienced by the main feeder and the 5 second dead-time was the only outage experienced by the lateral feeders.

### **2.2.2. Auto-recloser control circuit**

According to [36], the control logic of the auto-recloser performs a vital role in maintaining a power supply. With the increasing need for the association between each of the auto-reclosers and advanced calculation devices, more and more auto-recloser controls are equipped with advanced features that are similar to modern digital protection relays. Typical advanced operations in auto-recloser controls are voltage protection, directional overcurrent, sync-check, as well as the latest application of pulse reclosing.

The protection and control operations of the auto-recloser are electronically controlled in an integrated and modularized control unit. The controlling circuit can be illustrated using the block diagram in Fig 2-1. [18-19]. The AC source is the supply to the auto-recloser, and normally rated at 230V AC or 110V DC. The RMS block is to measure the root mean square of the instantaneous current passing the auto-recloser. The peak of the current is computed by the gain block and sends it to the time-current characteristics block. The time-current characteristics block is for operating the auto-recloser in fast and delayed modes using the time-dial, pick-up setting and the peak of the current. This also allows the auto-recloser to be coordinated with other protection. The output of this block is the operating time of the auto-recloser. The relay is to energize the circuit breaker when the fault current is greater than the pick-up current, it switches between two binary values (i.e. 0 and 1). The time-delay block delays the binary outputs of the relay. It is in this block that the auto-recloser trips the circuit-breaker in fast mode or delayed mode [23-24].

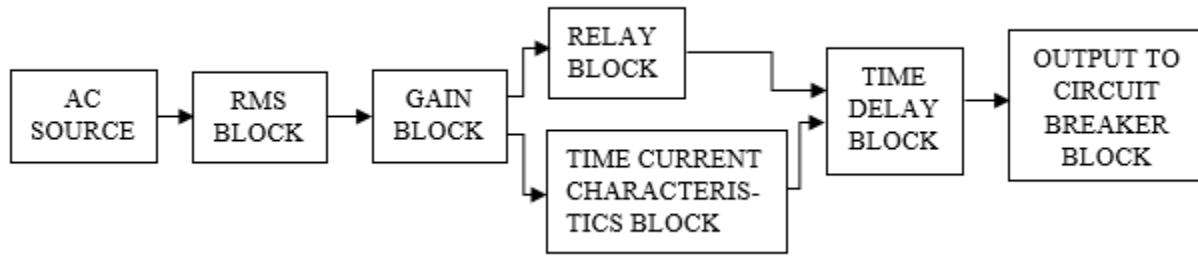


Fig. 2-1 Control circuit of auto-recloser [18-19]

### 2.2.3. Standards for application in distribution networks

Choosing optimal time-current curves in the auto-recloser for the selection of temporary faults in the distribution network must ensure that only a minimum number of customers are disconnected, and are not disconnected for long durations. The presence of a DG must not disconnect the customers unnecessarily. The IEEE Standard 1547-2003 states that: “Any distributed resource installation connected to a spot network shall not cause operation or prevent reclosing of any network protectors installed on the spot network. This coordination shall be accomplished without requiring any changes to prevailing network protector clearing time practices of the area electric power system” [26]. Auto-reclosers can be designed to trip and reclose all three-phases in low voltages ranging between 1 kV to 38 kV to achieve this purpose and adhere to the standard. For high voltages, the auto-recloser in the affected distribution feeders can be designed to trip and reclose individually [37]. The operator can either program the auto-recloser using the IEC 60255, ANSI/IEEE C37.112 or any user defined time-current characteristics.

### 2.2.4. Literature review on the application of an auto-recloser

According to [38], the auto-recloser installed in the distribution network can be a Single Pole Auto-Recloser (i.e. SPAR) or Three-Pole Auto-Recloser (i.e. TPAR), this will depend on the network necessity. The SPAR is applied for single-phase-to-ground faults and the TPAR is applied for all types of faults. In [39], the performance of the auto-recloser is evaluated by varying the phase of the fault, and the circuit topology that is faulted. The fault location is also varied on the transmission line. The study applies a SPAR for the transmission line as this is high voltage. Reference [40] uses a two instantaneous-one-time delay sequence and a one instantaneous-one-time delay sequence of the auto-recloser to provide a model for all other auto-reclosers. The control can be initiated between one to four times before locking out from repeating the open and reclosure sequence. The counting mechanism registers these operations and stops according to the programmed number of operations. The frequency of reclosing is according to system design. When there is a fault in the distribution network, the auto-recloser interrupts the fault current instantaneously or after a

time delay. The circuit breaker uses an arc-extinguishing medium to extinguish the arc between the contacts during the dead-time of the auto-recloser. In [41], it is stated that the first dead-time of the auto-recloser is usually about 100 milliseconds to 300 milliseconds. After the dead-time, the auto-recloser recloses, and there is a reclaim time, which can be defined as the time after the auto-recloser had a successful reclosing before another opening. If the fault still persists, the auto-recloser opens again after the reclaim time which is also the time delay of the auto-recloser. It recloses again after the second dead-time (of about 15 sec), it will repeat the same sequence for a third dead-time (of about 45 sec) and if the fault still persists, it locks-out (i.e. remains open until an operator recloses the breaker).

In [40], the application of the auto-recloser and its performance in a smart grid is conducted. The control circuit is observed in order to analyze the control signal sent to the circuit breaker under various fault conditions. It is determined that when a DG is present in the distribution network, the level of reactive power that is flowing into the distribution network is affected which affects the voltage. This causes the auto-recloser and fuse to lose coordination and the performance of the auto-recloser in the distribution network is degraded. Reference [42] simulates the operation of the auto-recloser, and the auto-recloser modelled as time-current characteristics consisting of fast and delayed time-current curves. When the tests of the model are done, the fault is assumed to start at 0.015 seconds and ends at 0.035 seconds, making the fault to have a duration of 0.02 seconds. This fault is classified as temporary. Depending on the operating time of the fast-curve, tripping of the circuit breaker can be fast or delayed, the auto-recloser will begin to operate at the time of the start of the fault with the addition the operating time of the auto-recloser. The circuit-breaker status is either 1 or 0, denoting the closed and opened status.

### **2.3. Auto-recloser mal-operation in active distribution networks**

In a three-phase balanced radial distribution network, the phase voltages are displaced by 120 degrees. In each node, there is power injected by the generators and power drawn by the load. The vectors of active power injection ( $P$ ), reactive power injection ( $Q$ ), voltage angle ( $\delta$ ) and voltage magnitude ( $V$ ) are found in the node. The current flowing in a branch between two nodes can be determined by equations 2.1 to 2.3 [37,43].

$$P_{(k)} = P_{G(k)} - P_{L(k)} \quad (2.1)$$

$$Q_{(k)} = Q_{G(k)} - Q_{L(k)} \quad (2.2)$$

$$I_{b(k)} = \frac{(P_{(k)} - jQ_{(k)})}{V_{b(k)}/\delta} \quad (2.3)$$

Where  $k$  is the node index;  $P_G$  is the active power received by the bus;  $P_L$  is the active power sent by the bus;  $Q_G$  is the reactive power received by the bus;  $Q_L$  reactive power sent by the bus.

The voltage in the next node is given by 2.4.

$$V_{b(k+1)} = V_{b(k)} - I_{b(k)}Z_{b(k)} \quad (2.4)$$

Where  $Z_{b(k)}$  is the impedance of the branch.

The impedance of the branch causes a voltage drop and power losses. Longer feeders increase losses since the impedance is determined per kilometre. Voltage and current profiles can be obtained from each node [44].

### 2.3.1. Fault current level

When a fault occurs in the distribution network, the fault current is limited by the generator impedance, transformer impedance and line impedance up to the location of the fault. However, the resistance in the line impedance is usually neglected since in most cases the reactance can be three times the resistance. The fault current is given by the generator voltage and the reactance of the network or percentage reactance. The short-circuit fault can be either symmetrical or unsymmetrical, a symmetrical fault is a fault that gives rise to equal phase fault currents displaced by 120 degrees and the example of a symmetrical fault is the three-phases shorted together or to ground. Unsymmetrical fault is a fault that gives rise to unequal currents with unequal displacement an example of such faults are single-phase-to-ground, phase-to-phase and double-phase-to-ground faults. There are three stages to a fault, the sub-transient, transient, and steady-state. The peak of the fault current during the sub-transient stage is the current detected and used to compute an operating time of the auto-recloser. The instantaneous short circuit fault current ( $i(t)_{ac}$ ) can be determined analytically using the equation 2.5 [16,43].

$$i(t)_{ac} = \sqrt{2}E_g \left[ \left( \frac{1}{X''} - \frac{1}{X'} \right) e^{\frac{-t}{T''}} + \left( \frac{1}{X'} - \frac{1}{X} \right) e^{\frac{-t}{T'}} + \frac{1}{X} \right] \sin(\omega t + \alpha - \frac{\pi}{2}) \quad (2.5)$$

Where  $E_g$  is the RMS line to neutral pre-fault generator terminal voltage;  $X''$  is the direct axis sub-transient reactance of the generator;  $X'$  is the direct axis transient reactance of the generator;  $X$  is the synchronous reactance of the generator;  $t$  is the duration of the short circuit;  $T''$  is the short-circuit sub-transient time

constant which is the duration of the sub-transient fault and  $T'$  is short-circuit transient time constant which is the duration of the temporary fault current.

At  $t = 0$ , when the fault is at a maximum current, the fault current can be theoretically determined using 2.6.

$$I'' = \frac{E_g}{X''} \quad (2.6)$$

Where  $I''$  is the sub-transient fault current.

Taking into consideration the transformers and feeders, the transformer is represented by its leakage reactance and the feeder by its series impedance. The Thevenin's impedance ( $Z_{TH}$ ) as viewed from the fault can then be determined and used to determine the sub-transient fault current ( $I_F''$ ) as in 2.7.

$$I_F'' = \frac{E_g}{Z_{TH}} \quad (2.7)$$

For a distribution network with many nodes, the nodal-impedance matrix ( $Z_{node}$ ) applies and the vector of node voltage at the fault ( $E_F$ ). The sub-transient fault current can be determined by 2.8 [43] and the short-circuit current can be determined by 2.9.

$$I_F'' = \frac{E_F}{Z_{node}} \quad (2.8)$$

$$I_{SC} = \frac{E_F}{Z_{node} + Z_{line}} \quad (2.9)$$

Each node has a lower voltage limit and an upper voltage limit [44]. The node voltage level in remote nodes is low because of the losses along the feeder, but is increased by the adjustment of the tap position of the transformer, or integration of DG systems. With the change in the topology caused by the integration of a DG, faults also affect the DG system. DG systems were initially configured to adhere to the IEEE 1547 grid code requirement during faults or temporary disturbances. These voltage sources are to be disconnected from the grid quickly during disturbances. However, according to [45], with the increasing penetration of DGs in the distribution network, grid codes are being modified in some high and extra high voltage grid connection standards (i.e. 1 kV to 60 kV) to enforce the DG to remain grid-connected during disturbances, and support the grid voltage by injecting reactive power. The DG system is then configured to deliver the maximum output power to the distribution network. The DG penetration level to the distribution network is determined by using (2.10). DG systems are integrated to supply loads locally and make the distribution network voltage dependent on the DG penetration level.

$$P_{\text{penetration-level}} = \frac{P_{DG}}{P_{Load}} \times 100\% \quad (2.10)$$

Where  $P_{DG}$  and  $P_{Load}$  are the power generated by the distributed generation and the power consumed by the loads.

The three modes can result to the voltage profile of the feeder due to the penetration of the DGs are the following [46]:

- *Flat voltage profile mode*: in this mode, the penetration rate is equal to 100%, i.e. the power consumed is equal to the output power of the DG and the voltage profile is constant throughout the entire feeder.
- *Rising voltage profile mode*: in this mode the penetration level exceeds 100%. The excess power is injected into the upstream network, which leads to a rising voltage profile in the feeder.
- *Falling voltage profile mode*: in this mode the penetration level below 100%. The voltage reduces in the feeder.

In [47], the relationship between the fault conditions and the variation in the voltage profile is investigated. Faults are initiated in different nodes of an active distribution network, it is determined that the DG added 2% voltage improvement at any severely affected node, however the integration altered the network's impedance matrix. With these two aspects, the variation in voltage profile and alteration of the distribution network's impedance, there is a variation in the fault current level that feeder. In [18], it is stated that the contribution of fault current to the fault current level by the synchronous based DGs ranges from 5 to 6 times their rated current. It is also stated that the contribution of fault current to the fault current level by the inverter based DGs ranges from 1.1 to 2 times their rated current. The fault can cause voltage drops in the distribution feeder reducing the power quality. This is dependent on the fault current magnitude and direction.

### 2.3.2. Auto-recloser operation time

Instrument transformers of the auto-recloser continuously monitor all the phase current, voltages and neutral current using the current transformers, voltage transformers and earth current sensitive current transformers. When the fault is sensed by the current transformer, the auto-recloser trips on the fast curve, this curve provides a fast operating time.

In [48], it is stated that modern microprocessor relays typically have multiple setting groups available, the settings can be easily changed by changing the active setting group. This change can move the time-current curve. It is explained that when the relay picks up, it starts timing and the change of setting groups can



reduce the tripping times of the relay which can be important in the coordination of the protection scheme devices. In [26], the operating time of the auto-recloser is expressed as an inverse function of the fault current flowing through it. The auto-recloser operates with an IEC/IEEE very inverse for the fast mode of operation and IEC/IEEE extremely inverse for the delayed mode of operation. These curves can be used as a hybrid or homogeneous to design a nonlinear function of the time and the current detected by the auto-recloser in the two modes of operation. A time current curve has three main operating regions, these regions are the overload region, adjustable instantaneous region, and instantaneous region. The last two regions are necessary to clear fault events while the overload region protects the system in cases of emergency operation

According to [49], two factors should be considered in programming auto-reclosers to act on suitable curves for optimal operating times, these factors are selecting suitable settings in order to have successful operations and limiting the effects of auto-reclosers operations such as over voltages. An optimal fast operating time of the auto-recloser should be between 100 milliseconds to 200 milliseconds within the instantaneous and adjustable instantaneous region [6,44]. With the integration of DGs, different types of DGs contribute different magnitudes of fault current and cause the fault current to be at different levels. The variation in the operating time due to the change in the fault current level will conform to the type, location and penetration of the DG relative to the fault. A double-fed induction generator wind turbine generates high sub-transient fault currents but gradually drops after the first-cycle, requiring a fast operation time of the auto-recloser for temporary faults within the first cycle [50].

### **2.3.3. Auto-recloser mal-operation**

When there is a high penetration of DGs in the grid, the fault current contribution from the DGs could affect the selectivity, sensitivity, security and selectivity of the overcurrent protection [25]. Since grid code standards require DGs to remain grid-connected during temporary faults [50], a fault can cause the auto-recloser on the unaffected feeder to exhibit sympathetic tripping. This is caused by the contribution of the DG to the fault if the distributed generator is integrated in that healthy feeder. Inrush currents and temporary current increases can also cause this mal-operation [33, 52]. Sympathetic tripping is depicted in Fig. 2-2. Another mal-operation of the auto-recloser that may also result with the integration of the DG is the blinding of auto-recloser protection. This occurs when the DG and the utility generator feed the fault in parallel [53]. When the DG is connected to the distribution network, the utility generator and the DG both contribute to the fault. The DG's contribution to the fault might decrease the fault current level, and it becomes less than the pick-up current setting of the auto-recloser. The auto-recloser then does not detect the fault current and it does not operate to isolate the fault [22, 49, 54].

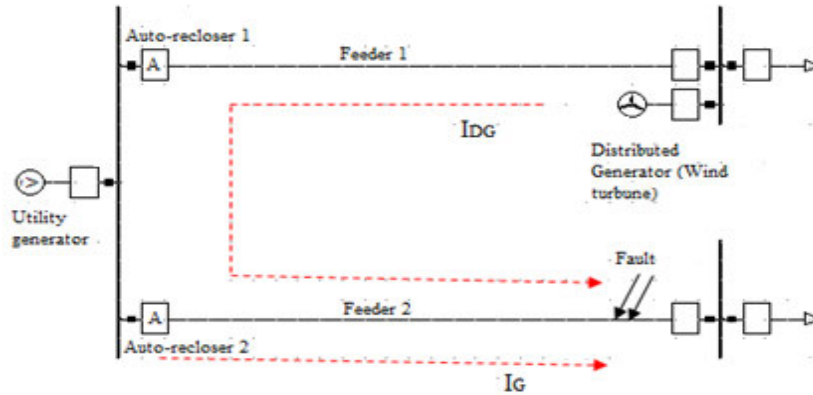


Fig. 2-2 Sympathetic tripping of an auto-recloser [50]

All protection scheme devices have to be coordinated for grid-connected mode operation in the expectation of large currents. This is because the penetration level of DGs compromises the coordination of the protection devices. The auto-recloser may not meet the selection of temporary faults in the coordination if the auto-recloser's trip command is delayed by more than 200 milliseconds [3]. In a traditional distribution network where the power flow is radial, and the auto-recloser and fuse detect the same fault current, the auto-recloser and the fuse are easily programmed to coordinate such that the auto-recloser operates faster than the fuses to check if the fault is temporary. This coordination is determined by the time delay calculated through the ratio of the fault current and the pick-up current setting of the auto-recloser. Depending on the location of the fault, the coordination can remain the same with the integration of the DG if the fault current is greater than the pick-up current. If the auto-recloser detects a smaller fault current compared to the fuse, the fast operating mode of the auto-recloser will have an increased time delay as compared to how it was conventionally programmed and the fuse may act first. This results in the fuse melting when the fault is temporary, this mal-operation is depicted in Fig. 2-3 [5].

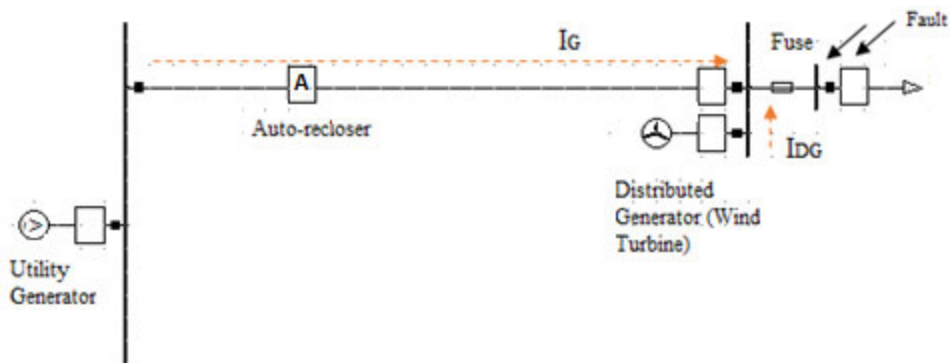


Fig. 2-3 Loss of coordination between the auto-recloser and fuse [5]

### **2.3.4. Literature review on the mal-operation of the auto-recloser**

According to [54], every protection device has an associated maximum distance that it can operate efficiently, this is known as the reach of the device. Because of the large distribution network which may have feeders that are kilometers long from the substation, it may be challenging to protect the whole feeder from the sub-station. In [52], it is stated that the two major impacts of a DG on existing protection schemes is the sympathetic tripping of the protection devices and protection blinding. In [50], a model of the wind farm is connected on the feeder and this modifies the fault current direction on the line resulting in a relay sympathetic trip. The contribution which causes a reduction in the fault current and the long distribution lines causes the reduction of reach or protection blinding.

According to [34], a traditional method to mitigate sympathetic tripping of inverse-time overcurrent relays was to raise the pick-up setting, increase the time-dial setting, or both. Although this mitigates sympathetic tripping, it decreases the sensitivity and speed of the auto-recloser. The study demonstrates that changing the curve setting of the fast curve can be used to successfully mitigate undesired operation of the auto-recloser and still prevent downline fuses from blowing. This requires additional options for fast curve selection, such as those available in a microprocessor-based recloser control.

In [54] and [55], an investigation of the auto-recloser and fuse losing coordination is conducted. In [55], for the first case, the auto-recloser only detects the current from the utility generator, while the fuse detects the current from the utility generator and DG. For the second case, the auto-recloser detects the fault current from the DG while the fuses detect the summation of the fault current from the substation and the DG, in both cases the fuse operates faster than the auto-recloser, and it melts. In [54], when there is no DG connected, the fault current detected by the auto-recloser and the fuse is the same and the auto-recloser operates faster than the fuse. A DG is integrated in between the auto-recloser and the fuse, which causes the fault current detected to differ. The current through the auto-recloser decreases and the current through the fuse increases and the fuse operates faster. The high powered energy storage systems are also stated to be the source of fault currents in the grid, according to [56], this also provides an inaccurate fault discrimination.

## **2.4. Optimizing the protection settings**

The optimization of auto-recloser protection is based on the mitigation or reduction of the mal-operations. The requirement includes optimizing selectivity, security, redundancy, speed and dependability of the auto-recloser. To achieve this, the operating time of the auto-recloser must be minimized to optimal levels for

the selectivity, redundancy and sensitivity requirements. The pick-up activity must be assessed for the security and dependability requirements. In order to minimize the operating time, optimal time-dial and pick-up settings should be selected while satisfying associated constraints. For solving the mal-operations problem and objective function, the DE algorithm has a metaheuristic nature which mimics the process of a natural selection. It starts with a set of candidate solutions or individuals which shall be the time-dial and pick-up settings. The initial population is randomly generated within the constraints of the decision variables and the objective function associated with each individual is calculated to produce a fitness function value. The selection the best decision variables according to the fitness function is the next step followed by the crossing over. The crossed-over decision variables are recombined at random positions, exchange information and produce new decision variables. The new decision variables are then mutated to produce optimal time-dial and pick-up settings according to the best combination of settings minimizing the fitness function [17].

### **2.4.1. Formulating the mal-operations**

The constraints in the auto-recloser settings limit the range of applicable settings for optimization. Only these settings provided are feasible to reduce the mal-operations. With this regard, the mal-operations of the auto-recloser can be formulated and the optimal solutions of these feasible settings obtained to address these mal-operations within the constraints. The time-dial and pick-up settings of the fast mode and delayed mode of operation can be considered as decision variables in an optimization algorithm. The optimal pick-up current settings are to be obtained between the maximum full load current and the minimum fault current that passes through the auto-recloser. The time-dial settings are to be selected between the minimum and the maximum setting range of the auto-recloser. The objectives considered for solving the problem can be either singular or multi objectives. For single objective optimization problems, the Pareto optimal solution is unique, the search focuses on the decision variable space and compute a single best solution. For multi-objective optimization problems, the Pareto optimal solutions take the most feasible solution which improves one objective function without affecting the rest. The Pareto optimal solutions are located in the bounds of feasible outcome region; these are called a Pareto frontier. Pareto-based algorithms search and select optimal solutions using the principle of dominance, this is by comparing two feasible solutions and only proceed with the most optimal one. The comparison checks which solution performs better in at least one objective and is no better than the other solution [57].

### **2.4.2. Literature review on the DE algorithm application**

The best minimum operating time possible in voltage conditions and fault conditions can be obtained by solving the protection blinding, sympathetic tripping and auto-recloser's loss of coordination mal-

operations as an optimization problem. In [58], a relay coordination problem is formulated to obtain the minimum possible operating time. The fitness function is defined as the summation of operating times of the primary overcurrent relays. It is solved using the DE algorithm and optimal relay settings are obtained with a standard inverse time-current characteristic model. The time-dial and pick-up settings are optimized for this model. The overcurrent relays had a long operating time when there was the Solar PV system integration, but they were optimized with settings obtained by the use of the algorithm. The optimal settings reduced the fitness function, which is the summation of the operating times of all primary relays. In [59], the coordination of inverse definite minimum time overcurrent relays is formulated as a constrained optimization problem, the objective is to minimize the total operating time of all the directional overcurrent relays. The optimization problem has twelve decision variables in the first case and twenty-eight decision variables in the second case, their optimal settings are obtained by the DE algorithm. The DE algorithm has the selection, crossover and mutation steps. The mutation operator affects the working of the DE algorithm. However, the DE algorithm converges before the iterations are completed and computes optimal values of the time-dial and pick-up settings, this can limit it from searching globally for a solution, and therefore can be modified. Optimal time-current characteristics curves are also presented for all optimization cases. In [28], the DE algorithm is stated as consistently being ranked one of the best search algorithms for globally searching an optimal solution in optimization problems. A mutation to the DE algorithm can be conducted and produce five modified schemes, the modification is made on the weighted difference and the scale factor can be varied following the Laplace distribution. The DE variant can be denoted as DE/X/Y/Z where X is the vector mutated; Y is the number of difference vectors used and Z is the cross over scheme. One of the performance metrics considered to determine the scheme that is reliable and efficient is the fitness function value. The schemes are applied to optimize the directional over-current relay settings by obtaining optimal time-dial and pick-up settings.

## 2.5. Conclusion

The application of automatic reclosing in a distribution network allows temporary faults to self-clear preceded by re-energizing the feeder and resume the power supply. This improves the reliability of the network. The auto-recloser also reduces the duration of a power interruption due the occurrence of unsolicited openings of the breaker. But the integration of the DG causes problems in the operation of the auto-recloser. Strategies have been developed to mitigate these problems, but they have proven not adequate. Since this is degrading the operation of the auto-recloser, there are more studies, investigations and experiments that need to be done to optimize the auto-recloser protection. The type, location and penetration of the DG should be considered in the operation of the auto-recloser. The location and type of

fault should also be considered in the operation of the auto-recloser. The three mal-operations that have been understood are blinding of auto-recloser protection, sympathetic tripping of the auto-recloser, and auto-recloser losing coordination with other protection devices. Mitigating or reducing these mal-operations of the auto-recloser in distribution networks integrated with DGs should optimize the protection of an auto-recloser. This shall be done through minimizing the operating time of the auto-recloser.

## **Chapter 3 – Methodology**

### **3.1. Introduction**

This chapter presents the methodology of optimizing the protection of an auto-recloser when the distribution network conditions change and the auto-recloser mal-operates because of the integration of a DG. MATLAB/Simulink/Simscape Power Systems is used to model the auto-recloser and model the distribution networks. The IEEE 13 node radial distribution network and IEEE 34 node radial distribution network are selected as the distribution networks for evaluating and optimizing the auto-recloser protection. The auto-recloser is applied on the passive and active distribution networks. The MATLAB Script is used to implement the code of the DE algorithm and to make modifications to the DE algorithm determining the most optimal settings. To select the best settings, the settings are applied to the auto-recloser under different voltage profiles introduced by the types of the DGs and the best performing optimal settings. These different cases for different voltage and fault conditions are performed using the IEEE 34 node radial distribution network. An exponential scale factor is applied to further to balance the exploration and exploitation of the schemes that provide better performance.

### **3.2. Modelling of the auto-recloser**

The auto-recloser consists of two solenoids, a trip solenoid and a close solenoid. The operation of the trip solenoid is modelled using MATLAB/Simulink/Simscape Power Systems environment by a relay with a trip functionality operating on time-current characteristics. A same duplicate relay is integrated to the first relay but can be programmed to trip at different times. This is to provide a fast and a delayed operating modes of the auto-recloser. The first relay is designed to trip on the fast curve of the auto-recloser and the second relay is to designed to trip on the delayed curve of the auto-recloser [60]. These curves have the ability to compute the operating time of the auto-recloser for both the fast operation and the delayed operation and send trip commands as an input to the circuit breaker. The relays have a time-current characteristic curve setting, current transformer ratio setting, time-dial setting and pick-up current setting. The choice of time-current characteristic curves ranges between definite to extremely inverse of the IEEE or IEC characteristic curves. The time-dial setting ranges between 0.05 to 1 with a step size of 0.05 and the pick-up setting ranges from 25 % to 200 % of the phase-to-ground or phase-to-phase current with a step size of 25%. The logical operator blocks, S-R flip flop blocks and a delay blocks provided by the SimPowerSystems Toolbox are connected to make the dead-time and perform the reclosing capabilities of the model [61]. In order to investigate the protection ability and performance of the modelled auto-recloser,

temporary and permanent faults are simulated on the feeders of the distribution networks and the following assumptions are made:

- The auto-recloser is microprocessor based.
- The auto-recloser provides a single-shot by sending a trip command for the fast operation and if the fault is permanent it will send a second trip command for the delayed operation before lock-out.
- The types of faults initiated on the distribution line are a three-phase-to-ground fault or a single-phase-to-ground fault.
- The IEEE 13 node radial distribution and IEEE 34 node radial distribution feeders are considered as radial distribution networks.
- Auto-reclosers are applied in two lateral feeders of the IEEE 13 node radial distribution network and on the beginning of the IEEE 34 radial distribution network main feeder.

### **3.3. Circuit breaker control design**

To model the signal of the auto-recloser which shall control the circuit breaker, the microprocessor output is designed and depicted to show how the state of the auto-recloser should change between 0 and 1 in the event of a temporary or permanent fault. The signal that it should feed to the circuit breaker is the control signal with a fast or delayed operating time and a dead-time. The closed state of the auto-recloser is logic high of a 1 for the circuit breaker and the opened state is the logic low of a 0 for the circuit breaker. The following control commands are received by the auto-recloser; a trip command, a dead-time, a close command, and a lock-out [1].

### **3.4. Settings and operability design**

The operation of the microprocessor is modelled by using the time-current characteristic equation. The two settings that are used to program the microprocessor is the time-dial setting and the pick-up setting. The aim is to ensure the response of the auto-recloser is selective, secure, redundant, sensitive and dependable when there is a temporary fault. The auto-recloser should be able to reclose after the dead-time and restore the power supply. The settings are designed for over-current conditions. A flow chart is designed to map the steps that the microprocessor needs to go through in order to fulfil its operation in the auto-recloser. The microprocessor is designed to count the number of attempts it performs and locks-out after the programmed number of attempts [14].



### **3.5. Auto-recloser performance evaluation**

This sub-section describes a method used to evaluate the performance of the auto-recloser applied in a passive distribution network and an active distribution network. It also describes how the analysis of the control circuit output is conducted when there is a change in the voltage profile, magnitude of the current and the direction of the current. The two evaluations are for an auto-recloser applied in a distribution network without a DG and in a distribution network with a DG. Simulations are performed for the signal fed into the circuit breaker after the detection of the rise in the feeder current. The voltage is also simulated to note the voltage profile of the feeder in a passive and active distribution network [61].

#### **3.5.1. Auto-recloser simulation in a passive distribution network**

Auto-reclosers are applied with the time-dial set as 0.1 for the fast operating mode curve and 0.6 for the delayed operating mode curve. These are taken as the conventional time-dial settings. The pick-up current is set to a 150% for both trip commands, this is the conventional pick-up current setting. The distribution network is the IEEE 13 node radial distribution feeder, which is a three-phase, radial distribution feeder having pre-existing voltage level. The radial distribution feeder is fed by a step-up transformer of 5 kVA, 4.16 /12.45 kV grounded wye, and distributes power to various constant currents, constant impedance, and constant power loads. A single line diagram of this distribution feeder is depicted in Fig. 3-2. MATLAB/Simulink/Simscape Power Systems utilized to model this topology, study the worst-case fault current at nodes 34 and 75 and analyze the protection performance of the auto-reclosers under two types of fault durations [62].

Two fault locations are chosen for the evaluation of the auto-recloser performance when applied in these active and passive distribution networks. The fault duration is set between 0.1 sec and 0.2 sec when it is temporary. The fault is changed between temporary and permanent for the auto-recloser performance analysis [38]. The auto-recloser is applied in two lateral feeders in order to compare the protection and determine if it mal-operates when the DG is integrated into the network. Only the voltage and the current in the red-phase are monitored to ease the analysis and comparison of the results. The control circuit output signal is simulated to show how the state of the auto-recloser is changing between 0 and 1 in the event of a temporary and permanent fault. The signal that it sends to the circuit breaker is the control signal with a fast or delayed operating time after the fault was initiated. The control circuit output signals are analyzed [9]. Since this is the distribution network with a voltage of 12.45kV, the applied auto-recloser is a Three-Phase auto-recloser.

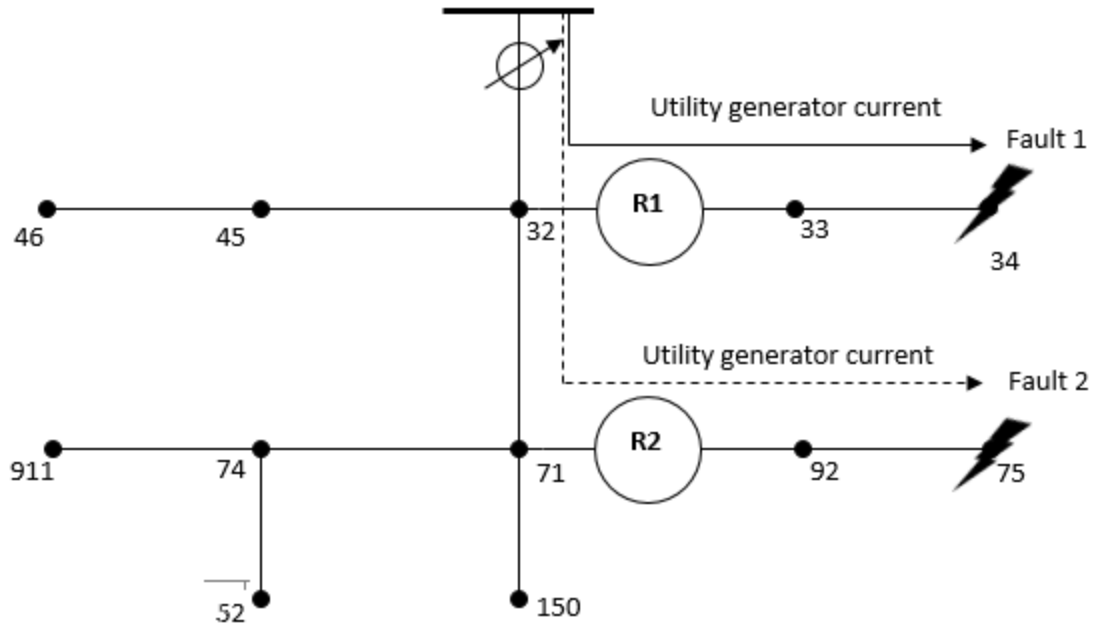


Fig. 3-1 IEEE 13 node radial distribution test feeder with faults in node 34 and node 75 [62]

### 3.5.2. Auto- recloser simulation in an active distribution network

The DGs are obtained from the SimPowerSystems toolbox. The chosen DGs for this sub-section is the Wind Turbine system and the energy storage system to supplement it. The Wind Turbine system is integrated in node 33 of the distribution network and the energy storage system is integrated in node 75 of the distribution network. In this sub-section, the performance of the auto-recloser is evaluated when the DG is integrated. The performance is analyzed to identify if the auto-recloser performs optimally with conventional settings [61]. Node 33 is the common coupling node for the Wind Turbine distributed generation system (i.e. DG 1) and node 75 is a common coupling node for the energy storage system (i.e. DG 2) [47]. The auto-reclosers are applied between nodes 32 and 33 (i.e. R1) and 71 and 92 (i.e. R2). The impact of the voltage support and fault current injection by the DG on the auto-recloser is assessed.

The simulations are performed for the two auto-reclosers by varying the fault location between two feeders. The first fault is initiated in node 34 of the active distribution network and the second fault is initiated in node 75 of the active distribution network. The first case is for the auto-recloser performance for a fault at node 34 with DG and the second case is for the auto-recloser performance for a fault at node 75 with DG. An analysis is performed in order to compare and identify mal-operations in the protection provided by the auto-recloser between the two distribution network topologies. The comparison of the results is done for four cases of the auto-recloser performance in order to detect any variance in the operating time and

determine the mal-operations. Three mal-operations are assessed and their causes. These mal-operations are protection blinding, sympathetic tripping, and loss of coordination between the auto-recloser and other protection devices [62].

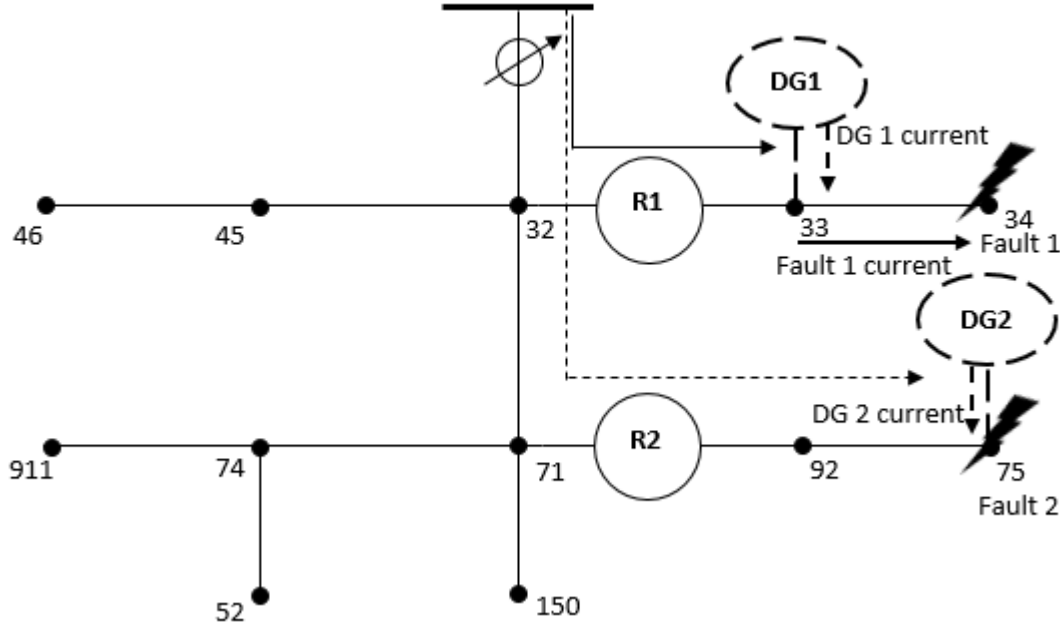


Fig. 3-2 IEEE 13 node radial distribution test feeder with faults in node 34 and node 75 [62]

### 3.6. Auto-recloser protection optimization approach

The code of the DE algorithm shall be written in the MATLAB Script using the MATLAB syntax. The function of this code is the objective function stated in the problem formulation. The objective function takes the time-dial setting and the pick-up setting as the inputs and outputs the optimal operating times with the relevant optimal time-dial and pick-up settings. The peak of the fault current is determined when there is an integration of the DG into the radial distribution network, this peak of the fault current is during the sub-transient state of the fault current. The extremely inverse time-current characteristics equation is used in the objective function for the minimizing of the operating time [63].

#### 3.6.1. Problem formulation

In order to obtain an objective function for the algorithm, the cause of the three mal-operations is investigated by comparison of the results between a distribution network without the DG and a distribution network with the DG. The cause of the mal-operations is the operating time, and the problems are

formulated. Since the operating time of the auto-recloser is determined by the time-current characteristic curves, the formula used is the time-current characteristic equation. The objective of applying the optimization algorithm is to quickly obtain optimal time-dial setting and the pick-up current setting [26]. The function is to be applied within the relevant constraints of the decision variables.

### **3.6.2. DE algorithm approach**

The decision to solve the problems and meet the objective using the DE algorithm approach is based on an analysis between three optimization algorithms. The optimization algorithms that were reviewed with their applications are PSO, ACO and DE algorithms. The factors that are used to determine the selection of a robust optimization algorithm are the capability of the algorithm to not converge early, therefore producing limited optimal settings, computation speed and searching globally for the optimal settings instead of remaining local [64]. The search space should provide more accurate solutions for the optimal settings. The DE algorithm was a more robust choice from the literature reviewed and the presented findings on the algorithms for the settings that are to be optimized when there is a DG integrated into the distribution network. The capability of the auto-recloser to optimally protect the network when there is a temporary and permanent fault are tested through comparing the optimal settings with the conventional settings. The new feeder current and the fault current detected by the auto-recloser when there is an integration of a DG is used as input to the function of the DE algorithm code. The code is run to obtain optimal time-dial and pick-up settings. These settings are implemented in the distribution network integrated with the DG and the operating time-current characteristics curves are obtained for the optimal settings. The optimized curves are compared with the not optimized curves to analyze the difference. Simulations are performed using the optimal settings and they are compared with the settings that were not-optimized [65].

## **3.7. Determination of the distribution network conditions**

To optimize the auto-recloser for a varied voltage and fault conditions caused by the integration of DGs into a distribution network, different types of DGs which either deliver active power or reactive power or consume active power or reactive power are connected to the feeder used as a network. This is to show that DGs can improve the voltage profile and evaluate the impact they have on the auto-recloser when there is a temporary fault in the distribution feeder [60, 66].

The IEEE 34 node distribution feeder is adopted as a benchmark passive distribution network for existing load flow and network conditions. The feeder has three-phases, two-phases and single-phase distribution lines. This feeder operates with a 12 MVA, 60Hz, 60/24.9kV step-down transformer in the sub-station. It

has various fixed and distributed constant current, constant impedance and constant power loads. The components of the feeder are protected by auto-recloser R1 for selecting temporary faults. The single line diagram of the feeder used as a distribution network is depicted in Fig. 3-4. The data for this feeder can be found in the IEEE Distribution Analysis Subcommittee article. The interfacing transformer for the Wind Turbine is a 0.48kV/24.9kV delta on the low voltage side, which is the Wind Turbine side and wye grounded on the high voltage side which is the distribution network side. The Wind Turbine and Solar PV systems are integrated as a phase-to-phase in the ungrounded three-phases section of the feeder. They are integrated in node 812 and node 860. The energy storage system is integrated as a single-phase to the second phase of the distribution feeder in node 856. These active distribution network conditions are simulated in MATLAB Simulink [63, 67].

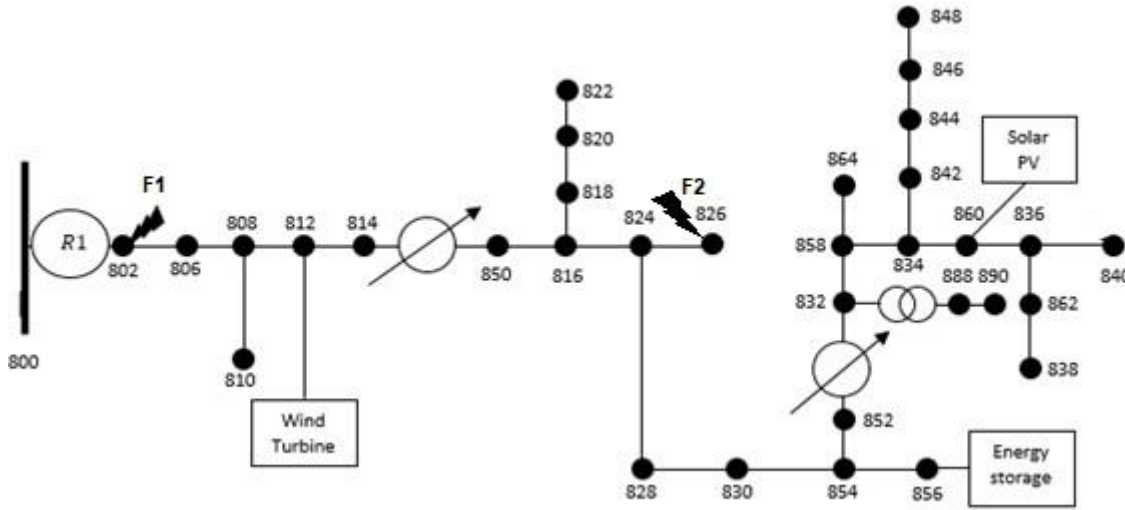


Fig. 3-3 Application of the auto-recloser in the IEEE 34 node radial distribution feeder with DGs [67]

### 3.7.1. Voltage conditions

The DG systems integrated in the distribution network depicted in Fig. 3-3 are configured to operate by supporting the voltage drops in the distribution network and improve the voltage profile. The configuration of both systems is conducted for their operation in the distribution network. The DGs are assumed to have a low-voltage ride through in the event of a fault. The energy storage system is integrated as a supplementary back-up for backing the DGs when there is no power injected. These all cause the voltage profiles to vary dependent on the type of DG. The investigation shall be conducted for six case studies of the integration and fault location. The base case study with no DG integration, the second case study with the integration of the Solar PV system and the third case study of the integration of the Solar PV system and Wind Turbine system. The fault location and type is varied for each case study. The difference in the

voltage profiles is noted as a result of the integration of the DG systems. Simulations on the protection of the auto-recloser are conducted under the varying voltage profiles to see performance of the auto-recloser with conventional settings and optimal settings [63].

The voltage profile of the distribution network is depicted in Fig. 3-4 for the case studies chosen when there is no fault on the distribution feeder. The distribution network's RMS voltage is 0,74235 p.u. before the integration of the DG. When the Solar PV system is integrated, the voltage profile shows a flat, falling and rising voltage profile mode. When the Wind Turbine system is integrated, the voltage profile shows a flat, falling and rising voltage profile mode as well. The integration of the Wind Turbine system or both DGs shows an increase in the level of the voltage compared to no DG and the Solar PV system integration. The voltages at the point of common couplings are given in Table 3-1.

**Table 3-1 Voltages at the common couplings in per unit**

Distributed generator	Node	RMS voltage (p.u.)
Solar photovoltaic system	860	0,6652
Wind turbine system	812	0,7945

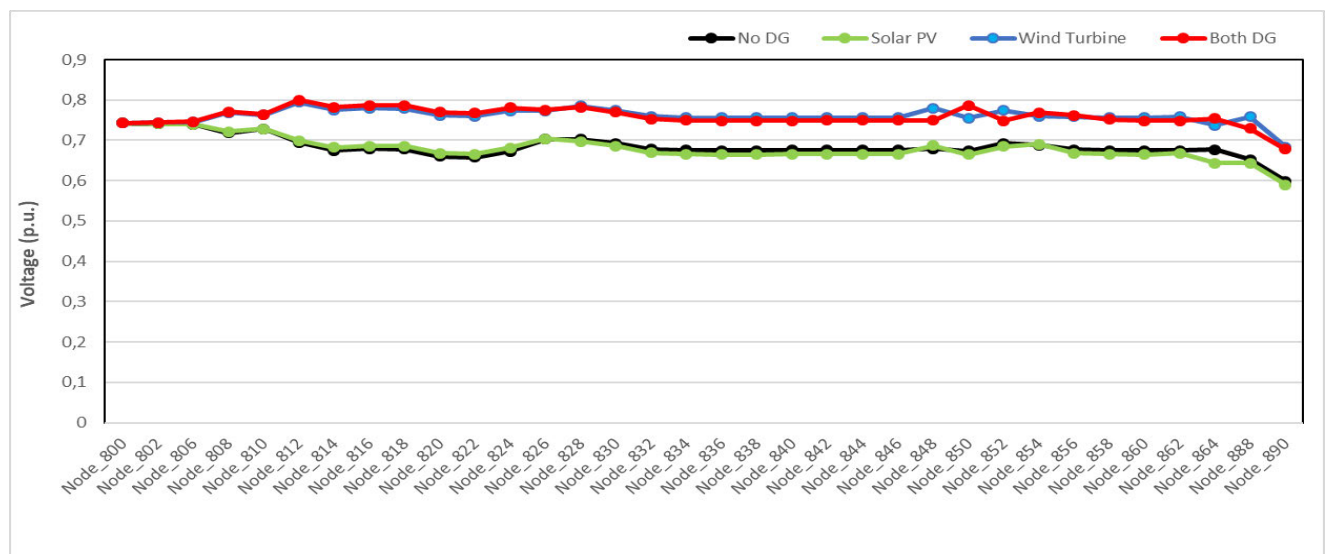


**Fig. 3-4 Distribution Network's voltage profiles**

### 3.7.2. Fault conditions

A short circuit was simulated to see the minimum and the maximum short circuit current that will flow in

all the nodes of the distribution network and in the node after the auto-recloser. This node shall be the subject of the voltage and current profile for the auto-recloser. This is taken as the installation point of the auto-recloser when there is no DG and when there is or are DGs integrated. The fault current variation that is detected by the auto-recloser in the installation point is investigated to find optimal settings [46].

For analysing fault conditions, two locations were chosen to observe the minimum and maximum fault current that will flow through the feeder when there is no DG and when there is DG integrated. For the minimum fault current detected by R1, the fault is simulated in node 826 and for the maximum fault current detected by R1, the fault is simulated in node 802. The fault in node 826 is a single-phase-to-ground fault and the fault in node 802 is a three-phase-to-ground fault. The fault currents are tabulated without the auto-recloser operation in Table 3-2. The fault current is determined when there is no DG integrated and when the Solar PV and Wind Turbine systems are integrated [66-67].

The table shows that the current that is passing between node 800 to node 802 is altered when there is an integration of a DG both near the auto-recloser and far from the auto-recloser. When there is a Solar PV system, there is a minor variation in the fault current compared to the fault current when no DG is integrated. When the Wind Turbine is integrated, the fault near the auto-recloser increases the current from 0.02 p.u. to 0.08 p.u. and when the fault that is far from the auto-recloser decreases the fault current from 0.08 p.u. to 0.05 p.u. When both DGs are integrated the current increases from 0.02 p.u. to 0.07 p.u. for the fault at node 802 near the auto-recloser and from 0.08 p.u. to 0.1 p.u. for the fault at node 826 far from the auto-recloser [66].

**Table 3-2 Fault currents for fault located in node 802 and node 826**

Node	No DG (p.u.)			Solar PV (p.u.)			Wind turbine (p.u.)			Both DG (p.u.)		
	I <sub>nom</sub>	I <sub>F1</sub>	I <sub>F2</sub>	I <sub>nom</sub>	I <sub>F1</sub>	I <sub>F2</sub>	I <sub>nom</sub>	I <sub>F1</sub>	I <sub>F2</sub>	I <sub>nom</sub>	I <sub>F1</sub>	I <sub>F2</sub>
800	0.014	0.73	0.08	0.0135	0.74	0.08	0.020	0.74	0.05	0.021	0.74	0.1
802	0.014	0.02	0.08	0.0135	0.02	0.08	0.020	0.08	0.05	0.021	0.07	0.1
806	0.014	0.02	0.08	0.0135	0.02	0.08	0.020	0.08	0.05	0.021	0.07	0.1
810	0.014	0.02	0.08	0.0135	0.02	0.08	0.020	0.08	0.00	0.021	0.07	0.0
812	0.014	0.00	0.00	0.0000	0.00	0.00	0.000	0.00	0.05	0.000	0.00	0.1
814	0.014	0.02	0.08	0.0136	0.01	0.08	0.020	0.08	0.10	0.021	0.07	0.1
816	0.014	0.02	0.08	0.0136	0.01	0.08	0.015	0.03	0.10	0.014	0.02	0.1
818	0.006	0.01	0.01	0.0136	0.00	0.01	0.015	0.02	0.01	0.014	0.02	0.0
820	0.005	0.01	0.01	0.0056	0.01	0.01	0.006	0.02	0.01	0.006	0.02	0.1
822	0.000	0.00	0.00	0.0048	0.00	0.00	0.005	0.02	0.00	0.005	0.00	0.0
824	0.010	0.01	0.07	0.0000	0.01	0.07	0.000	0.00	0.90	0.000	0.01	0.1
826	0.001	0.00	0.00	0.0000	0.01	0.00	0.012	0.02	0.00	0.010	0.00	0.1
828	0.011	0.06	0.08	0.0111	0.01	0.08	0.000	0.00	0.10	0.000	0.01	0.1
830	0.102	0.01	0.08	0.0106	0.01	0.08	0.012	0.01	0.10	0.012	0.01	0.1

832	0.010	0.01	0.07	0.0105	0.00	0.07	0.011	0.01	0.10	0.011	0.01	0.0
834	0.007	0.01	0.07	0.0067	0.00	0.07	0.011	0.01	0.10	0.011	0.00	0.0
836	0.001	0.00	0.08	0.0005	0.00	0.08	0.008	0.01	0.10	0.008	0.00	0.0
838	0.000	0.00	0.00	0.0000	0.00	0.00	0.001	0.00	0.00	0.001	0.00	0.0
840	0.000	0.00	0.00	0.0000	0.00	0.00	0.000	0.00	0.00	0.000	0.00	0.0
842	0.004	0.00	0.01	0.0042	0.00	0.02	0.005	0.00	0.01	0.005	0.00	0.0
844	0.003	0.00	0.01	0.0027	0.00	0.01	0.003	0.00	0.01	0.003	0.00	0.1
846	0.003	0.00	0.01	0.0027	0.02	0.01	0.003	0.00	0.01	0.003	0.02	0.1
848	0.000	0.00	0.00	0.0000	0.01	0.00	0.000	0.00	0.00	0.000	0.01	0.1
850	0.014	0.02	0.08	0.0136	0.01	0.08	0.015	0.02	0.10	0.014	0.01	0.0
852	0.010	0.01	0.08	0.0106	0.01	0.08	0.011	0.01	0.10	0.011	0.01	0.1
854	0.010	0.01	0.08	0.0106	0.01	0.08	0.011	0.01	0.10	0.011	0.01	0.1
856	0.000	0.00	0.00	0.0000	0.00	0.00	0.000	0.01	0.01	0.001	0.00	0.1
858	0.007	0.01	0.07	0.0073	0.00	0.07	0.008	0.01	0.10	0.008	0.00	0.1
860	0.001	0.00	0.06	0.0019	0.00	0.06	0.001	0.00	0.10	0.002	0.00	0.1
862	0.000	0.00	0.00	0.0000	0.00	0.00	0.000	0.00	0.00	0.000	0.00	0.0
864	0.000	0.00	0.00	0.0000	0.00	0.00	0.000	0.00	0.00	0.000	0.00	0.0
888	0.004	0.00	0.00	0.0036	0.00	0.00	0.004	0.00	0.00	0.004	0.00	0.0
890	0.004	0.00	0.00	0.0036	0.00	0.00	0.004	0.00	0.00	0.004	0.00	0.0

### 3.8. Auto-recloser protection optimization case studies

The simulations of the case studies shall be conducted in voltage conditions investigated in sub-section 3.7 and fault conditions investigated in sub-section 3.8. To obtain the best optimal settings of the DE algorithm in optimizing the auto-recloser protection under these network conditions, the DE algorithm is modified into three more schemes. The settings computed by each scheme shall be compared to determine which scheme and settings optimize the protection of the auto-recloser. The modification is performed in the mutation strategy of the original code in the DE algorithm [26, 68].

There are three case studies that the auto-recloser is optimized for, these cases are for a temporary fault isolation when there is no DG, a temporary fault isolation for a Solar PV system integration and a temporary fault isolation for the integration of a Solar PV and Wind Turbine systems. The main reason behind the case studies is to observe the protection of the auto-recloser with different settings, and analyze the fast operating time that can eliminate or reduce protection blinding, sympathetic-tripping and loss of coordination. A three-phase-to-ground and a single-phase-to-ground fault are simulated in different locations. The red phase of the distribution line is analyzed to observe the performance of the auto-recloser. The fault is initiated at 0.1 sec, and when the current rises from the rated current to its peak in all the cases, the auto-recloser is observed to see the operation time. The simulated fault is a temporary fault lasting for only 0.1 sec [66].



An exponential scale factor is applied to balance the exploration and exploitation of the schemes that provide the most optimal settings and optimize the auto-recloser protection. Simulations shall be performed to observe the improvements that might take place in the auto-recloser if there is a balance in exploring more candidate solutions that are not local and in exploiting the local candidate solutions using the selected schemes for the optimization of the auto-recloser protection [68]. The operating time of the auto-recloser is then compared for all the case studies. The comparison is done to see which settings give a better performance and optimize the protection of the auto-recloser.

### **3.9. Conclusion**

The selection of optimal settings that can optimize the protection of the auto-recloser shall be done through performance simulation of the auto-recloser and application of a robust optimization algorithm. The factors that are investigated which cause mal-operations in the auto-recloser are type and location of the DG system as well as the type and location of the fault. The following conclusions have been drawn from this chapter:

- The integration of a DG into the distribution network changes the fault current level, and this changes the operating time of the auto-recloser. The voltage profile is impacted by the integration of a DG, a change in the fault type and location. Mal-operations arise in the auto-recloser caused by the reverse current contribution, this affects the requirements that must be met in the operation of the auto-recloser.
- Voltage and fault conditions present different cases that can reduce the optimal operation of the auto-recloser. This can make the auto-recloser not meet the selectivity, security, redundancy, sensitivity and dependability requirements.
- An optimization algorithm can have shortcomings that can cause it to compute less optimal settings. It is necessary to assess these issues and refactor the algorithm to solve the issues for optimal computation.

The conclusions drawn in this chapter serve as a basis for the auto-recloser performance evaluation and settings optimization in chapter 4.

# **Chapter 4 Auto-Recloser Performance Evaluation and Settings Optimization**

## **4.1. Introduction**

An optimal protection of the auto-recloser depends on three-parameter settings viz. time-dial, pick-up and dead-time settings [12]. The settings design a fast time-current curve, re-closure time delay, and the delayed time-current curve. This has to meet the auto-recloser protection requirements, ensure a reduced power interruption duration and provide network security against temporary faults [61, 69]. In the case of the auto-recloser mal-operating and not meeting the requirements, various optimization algorithms can be utilized for selecting optimal settings. PSO, ACO, and DE algorithms are commonly applied for the protection scheme optimization to reduce the mal-operations. The following subsections present an auto-recloser model, performance evaluation and algorithm used for the optimization of auto-recloser protection when there is protection blinding, sympathetic tripping, and potential loss of coordination with other protection devices. The operating times are quantified, pick-up activities analyzed and issues identified through preliminary tests when the DG is integrated in the distribution network. The DE algorithm is evaluated for optimizing the auto-recloser protection by using it to select optimal time-dial and pick-up settings [21].

## **4.2. Auto-recloser model**

The auto-recloser's trip and automatic reclosing should provide optimal selectivity, security, redundancy, sensitivity, and dependability for the distribution network in the occurrence of a symmetrical or asymmetrical temporary fault [70]. It should trip and reclose only on faulted feeders and remain inactive in healthy feeders. The auto-recloser shall be microprocessor-based with embedded numerical relays, this allows the device to be time-graded with the fuse, sectionalizing links or other auto-reclosers for the provision of backup protection in permanent fault conditions [71]. The standard of the auto-recloser should comply with the IEC 62271-111 standard for design, operation, and application. As depicted in Fig. 4-1, the trip solenoid and the close solenoid are energized by the power supply in the auto-recloser to control the trip and reclosing operation. For symmetrical faults, the auto-recloser should be applied as a three-phase auto-recloser, with three-poles of the circuit breaker simultaneously tripping and reclosing. For asymmetrical faults, the auto-recloser should be applied as a single-phase auto-recloser, tripping one, two, or three poles of the circuit breaker independently and reclosing them independently. The auto-recloser shall be rated at a frequency of 60 Hz [72-73].

As depicted in Fig. 4-1, the analog to digital converter performs continuous to discrete (i.e. 0 and 1) conversions of the current signal from the analog current transformer, this is the current signal input into the microprocessor. All monitoring and control operations that energize the solenoids are performed in the microprocessor. It switches on or off the power supply of the solenoids independently [7,21,74]. The signal interface (i.e. human and machine interface) allows the operator to set the microprocessor according to the control requirements for the auto-recloser in the feeders. The calibration of the operating time for tripping is in conformance to the IEEE extremely inverse time-current characteristics curve. This is to program the auto-recloser to have a fast and delayed time-current curves for its timed responses [71].

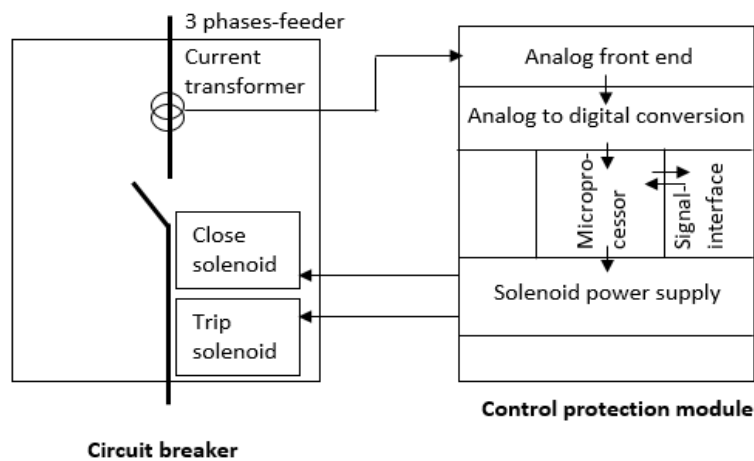


Fig. 4-1 Auto-recloser construction overview [73]

### 4.3. Auto-recloser output

The auto-recloser can allow between one to four reclosing attempts. It shall be according to the operator settings. It should only open and reclose according to settings and lock-out after the attempts have been completed [11]. Fig. 4-2 depicts the trip and close command in the control signal of the auto-recloser [75]. The auto-recloser outputs binary commands that are recognized by the circuit breaker which energize and de-energizes solenoids. When there is a temporary (i.e. transient) fault, the auto-recloser only operates in the red zone [24] and when there is a permanent fault, the auto-recloser operates in the blue zone. The time it takes to send a trip command is the operating time of the auto-recloser [76]. The calculation of the operating time is by the microprocessor. It converts numerical values of the time-dial and pick-up setting to operate the solenoids in a predetermined trip time.

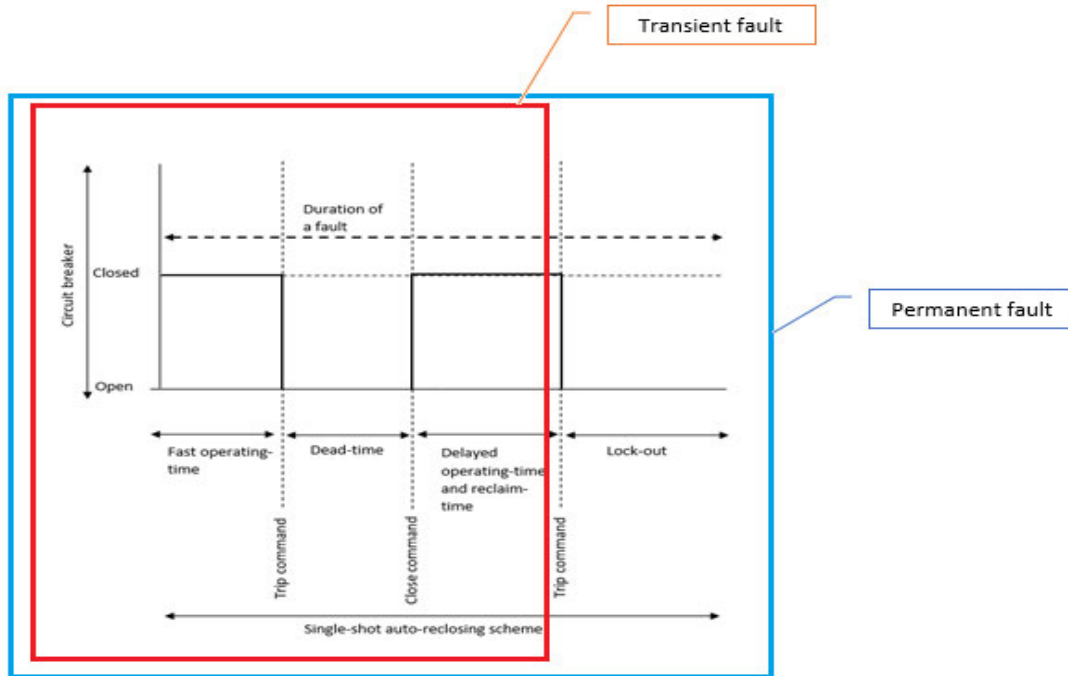


Fig. 4-2 Control signal of the auto-recloser [75]

#### 4.4. Settings and operation

Considering the voltage level and fault current level of the utility generator, the distribution network requires optimal adaptability of the auto-recloser settings to provide the distribution network with optimal selectivity, redundancy, security, sensitivity, and dependability [70]. The auto-recloser is required to operate with a high degree of availability which is dependent on the human-machine interface (i.e. HMI) settings of the device. The pick-up and time-dial settings are to be optimized in a selection based on the prevailing conditions of the distribution network. The settings are for overcurrent relay protection and automatic reclosing of the distribution feeders. Fig. 4-3 presents a flow chart for the operation of the auto-recloser when there is a temporary and permanent fault [1]. The count represents the increment of reclosing attempts performed by the auto-recloser. In this study, it is assumed that the auto-recloser performs a single attempt and lock-outs at the second attempt. The first trip is set to a time-dial setting of 0.1 and the second trip is set to a time-dial setting of 0.6. The pick-up setting of both relays is set to 150% of the distribution line current. These two parameters can also adjust time-current characteristics curves to determine the operation time of the auto-recloser [77].

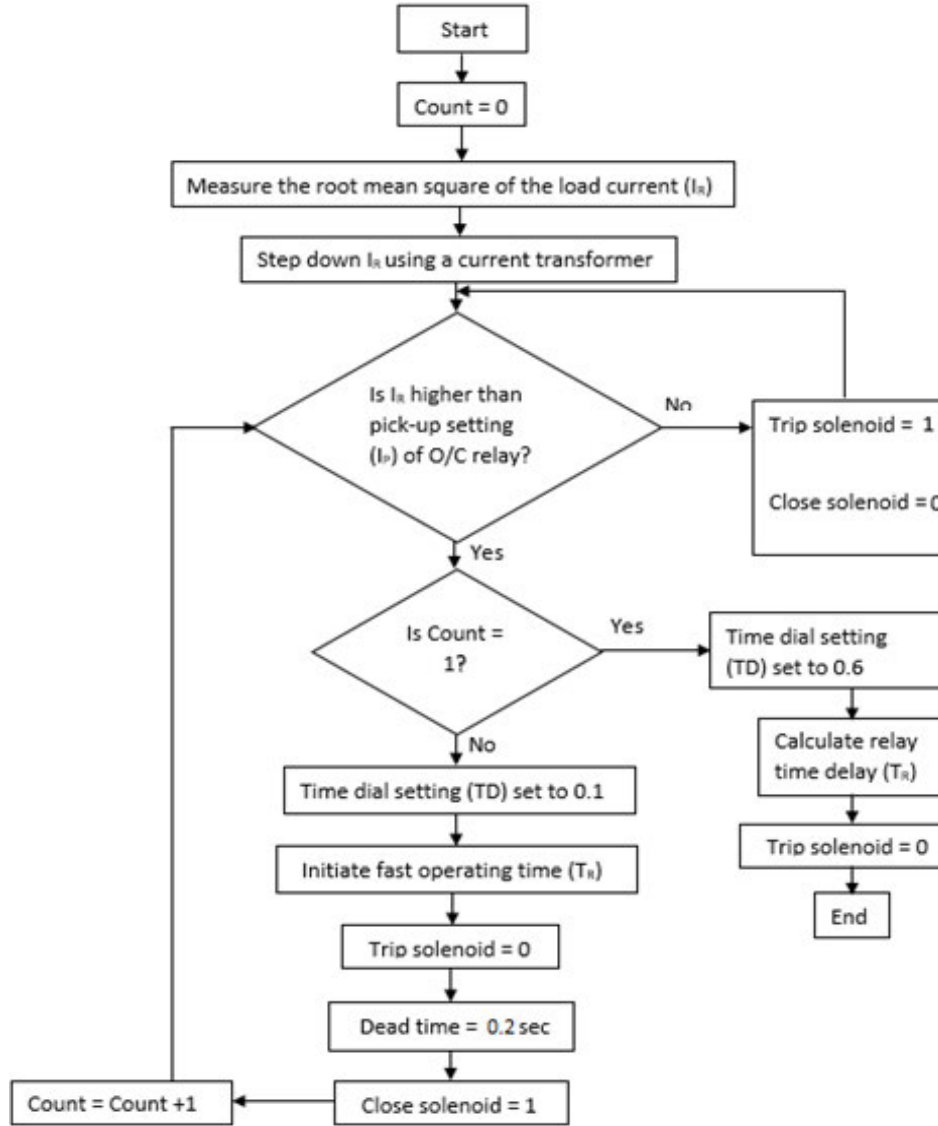


Fig. 4-3 Flow chart of the auto-recloser operation [1]

## 4.5. Operating time and dead-time

The equations used to calculate the operating time are presented from (4.1) to (4.3). Equation (4.1) is a non-linear function of the time-dial and the pick-up setting and mathematically defined by the IEEE C37.112. The time-dial and pick-up settings are chosen by the operator to design suitable fast or delayed time-current characteristic curves for controlling the circuit breaker's operating time [9, 57]. The delayed operating time is also the time-delay and reclaim time of the auto-recloser. A dead-time is set to allow the fault arc to be de-ionized and allow a temporary fault to self-clear. The length of the dead-time is selected using the equation depicted in (4.4) and (4.5), this is to ensure successful reclosing for faults not greater than 0.2 sec

in duration [78 - 79].

$$T_R = \left( \frac{A}{M^p - 1} + B \right) TD \quad (4.1)$$

$$M = \frac{I_R}{I_P} \quad (4.2)$$

$$I_R = \frac{I_L}{CT_{ratio}} \quad (4.3)$$

$$I_P = k \times I_R \quad (4.4)$$

$$t = 10.5 + \frac{V_{L-L}}{34.5} \text{ (cycles)} \quad (4.5)$$

$$t_{dead} = \frac{t}{f_G} \text{ (seconds)} \quad (4.6)$$

Where  $T_R$  is the operating time of the auto-recloser;  $TD$  is the time dial setting;  $M$  is the ratio of the current detected by the auto-recloser (i.e.  $I_R$ ) to the pick-up setting (i.e.  $I_P$ ); the parameters  $A$ ,  $B$ , and  $p$  are the constants for a particular time-current characteristic curve; the  $CT_{ratio}$  is the current transformer ratio;  $I_L$  is the distribution line current;  $k$  is the overload factor;  $t$  is the dead time expressed in cycles;  $V_{L-L}$  is the rated line-to-line voltage (kV);  $t_{dead}$  is the dead time in seconds and  $f_G$  is the rated frequency.

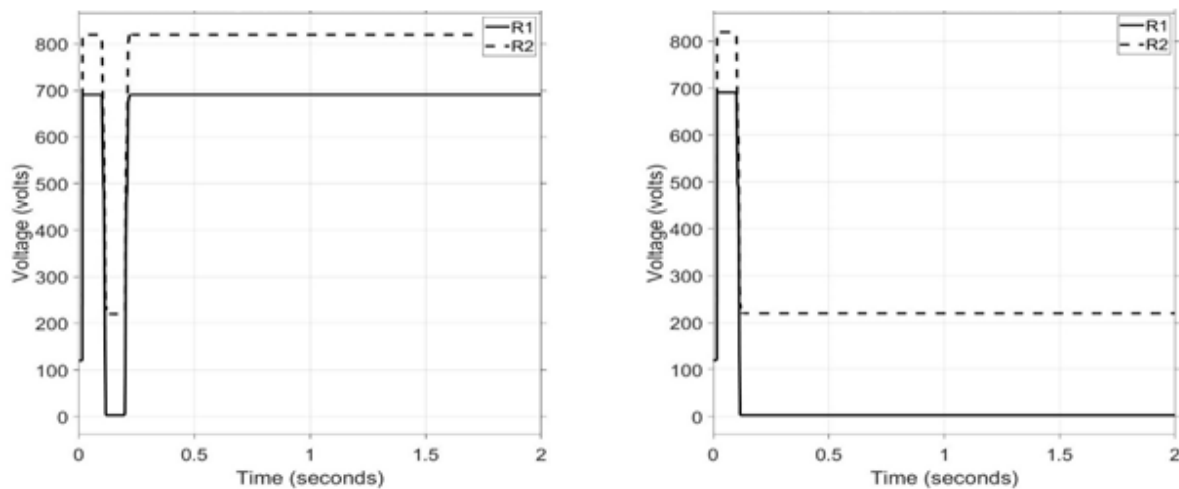
## 4.6. Application in a passive distribution network

The results for the evaluation of the auto-recloser performance when there is no DG are presented in this subsection. The analysis of the results is conducted in order to observe whether the faults are optimally cleared using the selected settings. The set-up for the simulations is depicted in Fig 3-1.

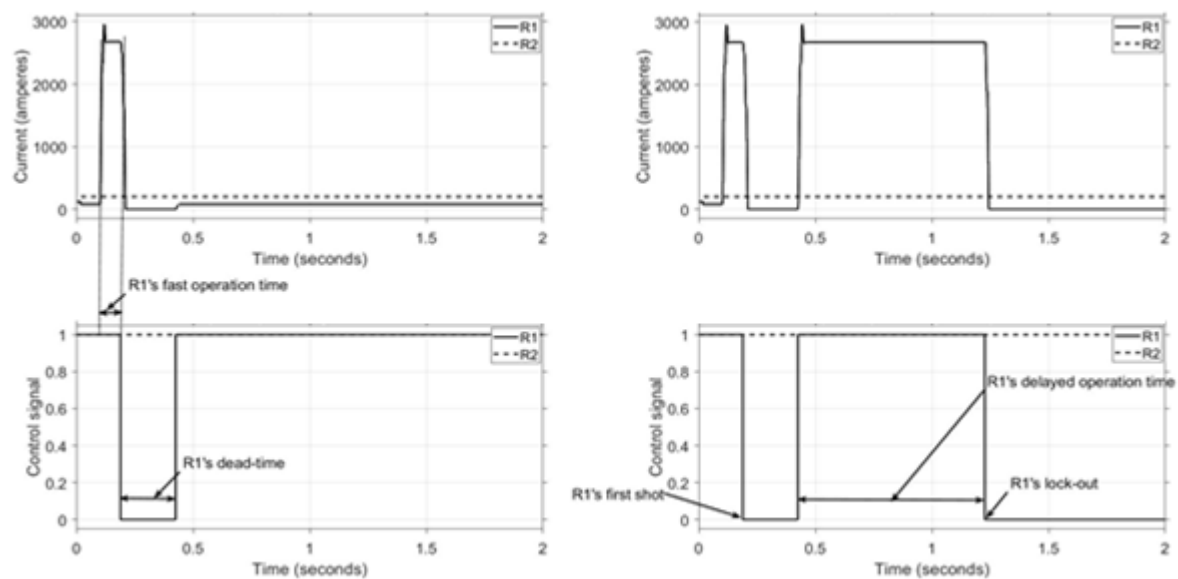
### 4.6.1. Auto-recloser performance for a fault at node 34

Fig. 4-4 shows the voltage profile at node 33 and node 92. There is a voltage drop at 0.1 sec and a voltage rise after a time of 0.1 sec when the fault is temporary for both auto-reclosers. There is also a voltage drop at 0.1 sec when the fault is permanent and the voltage is not restored for both auto-reclosers. This is a result of the short-circuit in node 34 and shows that a temporary fault causes a temporary drop and a permanent fault causes a permanent drop in the voltage level. Fig. 4-5 shows the current profile of the current detected by R1 and R2. For the feeder protected by R1, there is a line current of 80 A before the fault and a peak fault current of 2.951kA when there is a temporary or permanent fault. For the feeder protected by R2, there is a line current of 250 A and the line current remains at 250 A during fault conditions. The control signals of R1 and R2 shown in response to the current detected by each device are presented in Fig. 4-5. It can be observed that R1 trips after a fast operation time of 0.086 sec when the fault is temporary and isolates the

faulted section from the healthy section for a dead time of 0.200 sec. The fault clears within this period and R1 has a successful reclosure. R2 does not operate during this fault. When the fault duration is changed to permanent, it can be observed that R1 operates at the same time as when there was a temporary fault, which is 0.086 sec, it recloses after the dead time of 0.200 sec and operates again after a delayed operation time of 0.800 sec. After this final operation, R1 locks-out the circuit breaker, which can be observed that the fault did not clear. R2 again shows no operation. It can be observed that no auto-recloser is mal-operating [80].



**Fig. 4-4 Voltage profiles during a temporary and permanent fault at node 34**



**Fig. 4-5 Current profile and control signals for R1 and R2 during a temporary and permanent fault at node 34**

### 4.6.2. Auto-recloser performance for a fault at node 75

This case is simulated to compare the responses of the auto-reclosers when the fault is on a different feeder. This is to determine if the auto-reclosers maintain their performance when there is a change in the location of the fault. Fig. 4-6 shows the current profile for the fault at node 75. It can be observed that a peak fault current of 10.22 kA is detected by R2 for both the temporary fault and a permanent fault in node 75. The control signals of R1 and R2 are shown in response to the fault. It can be observed that R1 shows no rise in current and no operation. R2 trips after a fast operation time of 0.027 sec when the fault is temporary and recloses after the dead-time. When the fault is permanent, it is observed that R2 trips after a fast operation time of 0.027 sec as it did for a temporary fault and recloses after the dead-time, and trips again after a delayed operation time of 0.161 sec and locks-out. The auto-reclosers maintain their performance and exhibit no mal-operation [80].

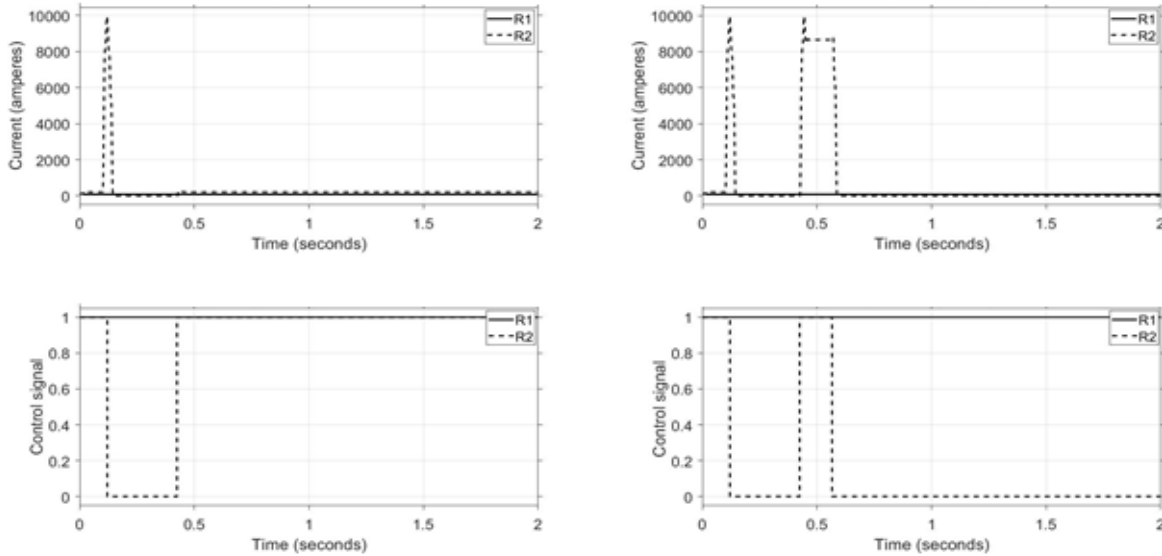


Fig. 4-6 Current profile and control signals of R1 and R2 during a temporary and permanent fault at node 75

## 4.7. DG integration

The integration of a DG changes the network topology. The new network topology can be represented mathematically by (4.7). The terminal voltages of the utility generator and the DG, their impedance, line impedance, and their current injection are presented in a 2x2 matrix by (4.7). Equation (4.8) to (4.9) is the Thevenin's impedance of the distribution network integrated with the DG when viewed from the location of the fault. The Thevenin's voltage and Thevenin's impedance determine the fault current level on the line to the fault as presented in (4.10) [62, 78-79,81]. Equations (4.11) to (4.12) are the current injections to the



fault by the two voltage sources. Equations (4.13) to (4.14) is the current detected by the auto-recloser dependent on the location of the DG relative to the fault [47,74,82]. The operation of the auto-recloser is subject to the following changes [18,58,83]:

- A decrease in the auto-recloser current can cause the operating time of the auto-recloser to be in excess compared to the fuses operating time according to the IEEE extremely inverse time-current characteristics curve.
- An increase in the auto-recloser current can cause the auto-recloser to trip unnecessarily on healthy a feeder thereby isolating that part of the distribution network without a fault.
- A drop in voltage on a healthy feeder can cause an increase in the auto-recloser current without the fault and can result in a trip. This drop is caused by a fault on an adjacent line.
- The location of the DG can vary the auto-recloser current since the impedance from the DG to the fault location can vary causing the current detected by the auto-recloser to vary.

$$\begin{bmatrix} V_g \\ V_{dg} \end{bmatrix} = \begin{bmatrix} Z_g + Z_l & (1-l)Z_l \\ (1-l)Z_l & Z_{dg} + (1-l)Z_l \end{bmatrix} \begin{bmatrix} I_g \\ I_{dg} \end{bmatrix} \quad (4.7)$$

$$Z_{th} = \frac{(Z_g + lZ_l) \times Z_{dg}}{(Z_g + lZ_l) + Z_{dg}} + (1-l)Z_l \quad (4.8)$$

$$l = \frac{p}{d} \quad (4.9)$$

$$I_{fault} = \frac{V_{th}}{\sqrt{3}Z_{th}} \quad (4.10)$$

$$I_{g,fault} = \frac{Z_{dg}}{(Z_g + lZ_l) + Z_{dg}} \times I_{fault} \quad (4.11)$$

$$I_{dg,fault} = \frac{Z_g + lZ_l}{(Z_g + lZ_l) + Z_{dg}} \times I_{fault} \quad (4.12)$$

$$I_R = I_{g,fault} + I_{dg,fault} \quad (4.13)$$

$$I_R = I_{g,fault} - I_{dg,fault} \quad (4.14)$$

Where  $V_g$  is the utility generator voltage;  $V_{dg}$  is the DG voltage;  $Z_g$  is the utility generator impedance;  $Z_{dg}$  is the DG impedance and  $Z_l$  is the network impedance.  $Z_{th}$  is the Thevenin's equivalent impedance of the active distribution network;  $p$  is the line impedance from utility generator to point of the DG;  $d$  is the all feeder impedance from the utility generator to the fault and  $I_{fault}$  is the fault current.

### 4.7.1. Auto-recloser performance for a fault at node 34 with DGs

This case is simulated to analyse the voltage profile, current profile, and operation of the auto-recloser when DGs is integrated into the passive distribution system. Fig. 4-7 depicts the voltage profiles in nodes 33 and 92 when the fault is temporary and permanent. It is observed that the voltage profile of node 33 is fluctuating which is caused by the integration of the Wind Turbine system. It is observed that a temporary fault causes a temporary drop in the voltage and a permanent fault causes a permanent drop in the voltage. Fig. 4-8 shows the current detected by R1 and R2. It is observed that there is a peak in the fault current detected by R1 of 2.930 kA when there is a temporary and a permanent fault at node 34. When the fault is temporary, R1 responds with a fast operation time of 0.182 sec followed by reclosure after the dead-time. When the fault is permanent, it responds again with a fast operation of 0.182 sec, recloses after the dead-time, and has a delayed operation time of 0.818 sec. There is an excess time delay of R1 for both fast and delayed operating times. For auto-recloser R2, it is observed that the current drops during fault conditions for both durations of the fault. R2 shows no response or mal-operation [80].

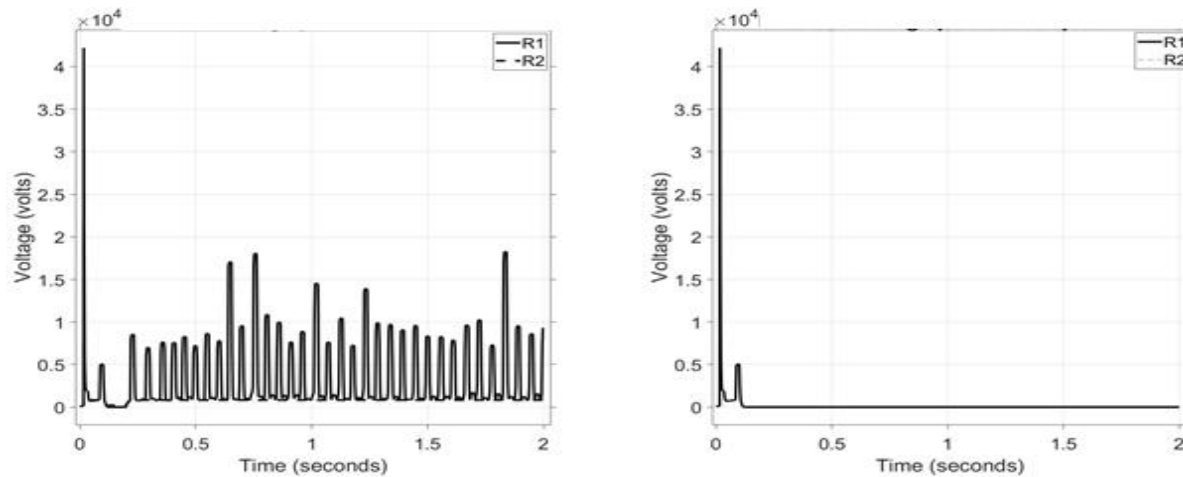


Fig. 4-7 Voltage profiles for a temporary and permanent fault with DGs integrated

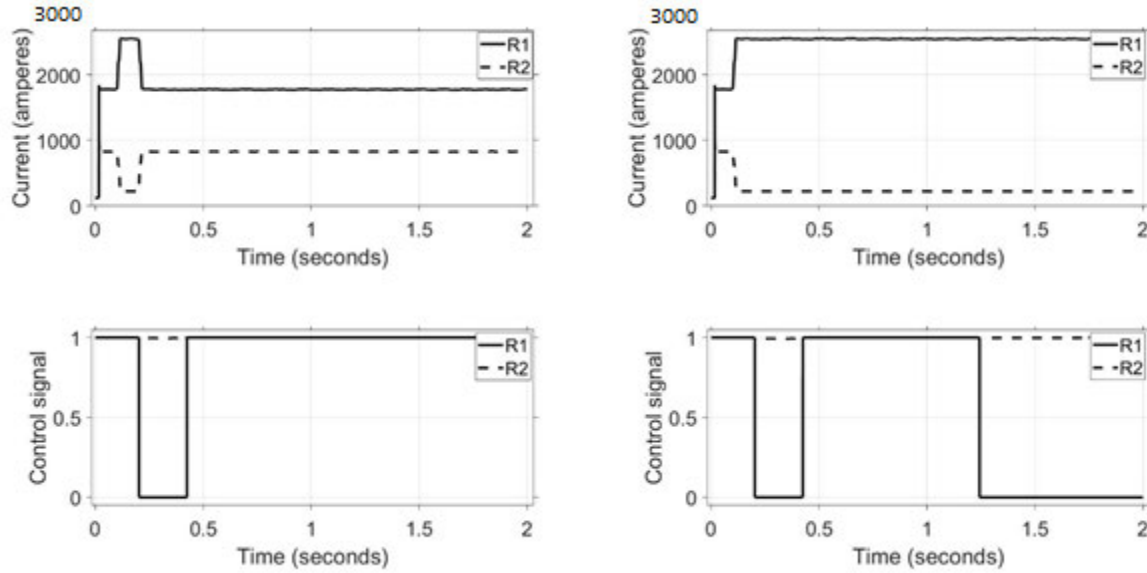


Fig. 4-8 Current profile and control signals for R1 and R2 during a temporary and permanent fault at node 34 with DGs

#### 4.7.2. Auto-recloser performance for a fault at node 75 with DGs

This case is simulated to compare the response of the auto-reclosers when the fault is on a different feeder. Fig. 4-9 shows the current profile of R1 and R2. It is observed that R1 has a drop in current to 836 A in both durations of the fault and R1 operates in a fast operation time of 0.184 sec for a temporary fault and recloses after the dead-time. For a permanent fault, it again operates after a fast operation time of 0.184 sec, recloses after the dead-time, and operates after a delayed operation time of 19.1 sec. However, the fault is not in node 34 where R1 is applied, but there is current flowing in this feeder initiating a trip. It can also be observed that R2 has a peak in the fault current of 1.649 kA when there is a temporary fault and a permanent fault at node 75. This auto-recloser operates after a fast operation time of 0.214 sec when the fault is temporary and recloses after the dead-time. When the fault is permanent, it operates again after a fast operation time of 0.214 sec, recloses after the dead-time, operates after a delayed operation time of 1.853 sec, and locks out. There is an excess in the operating time when compared to the passive distribution network operating times [80].

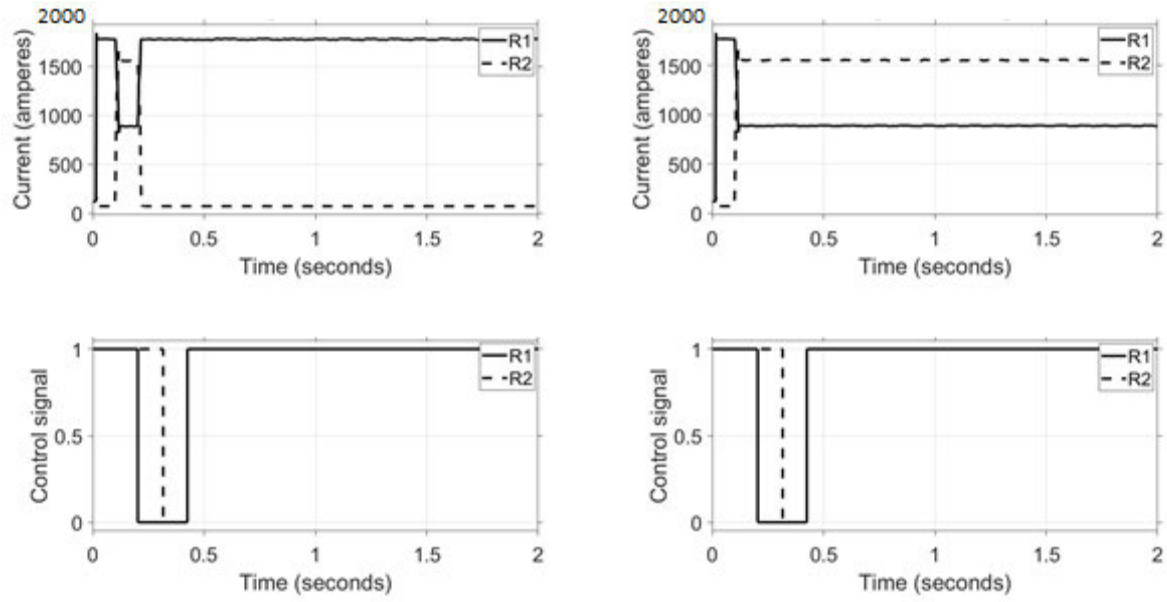


Fig. 4-9 Current profile and control signals for R1 and R2 during a temporary and permanent fault at node 75 with DGs

## 4.8. Comparison of auto-recloser performance

In Fig. 4-10, the operation times of R1 are compared for the four cases. The first case results can be used to grade the auto-recloser with other protection devices. The third case shows an increase of 109% for the fast operating time and 350% for the delayed operating time when compared to the first case. This can result in a loss of coordination, which is caused by the increased delays in operation. It shows that there was decreased dependability and can be loss of selectivity in terms of the requirements for the auto-recloser. Case four shows a trip in R1 when compared to the second case and there is no fault on the feeder. This trip is unwanted as the feeder is healthy. This is a sympathetic trip and the auto-recloser is failing the security, dependability, and selectivity requirement in a healthy feeder.

In Fig. 4-11, the operating times of R2 are compared. For the first case and the third case, R2 proves to operate optimally, the feeder is healthy and the auto-recloser does not exhibit a protection blinding or sympathetic tripping. The operating times have not increased from the conventional settings in the passive distribution network. The current contribution of the DG has not affected the operation of this auto-recloser, it has not affected its security, dependability, and selectiveness. In the second case, R2's fast operating time is 0.03 sec and delayed operating time is 0.161 sec, the auto-recloser performs optimally in this case. However, In the fourth case, the fast operating time is 0.214 sec, this is a 613% increase in the operating time when compared to the second case. This can cause a loss of coordination between the auto-recloser and other protection devices. There is also a 1049% increase in the delayed operating time when compared

to the second case.

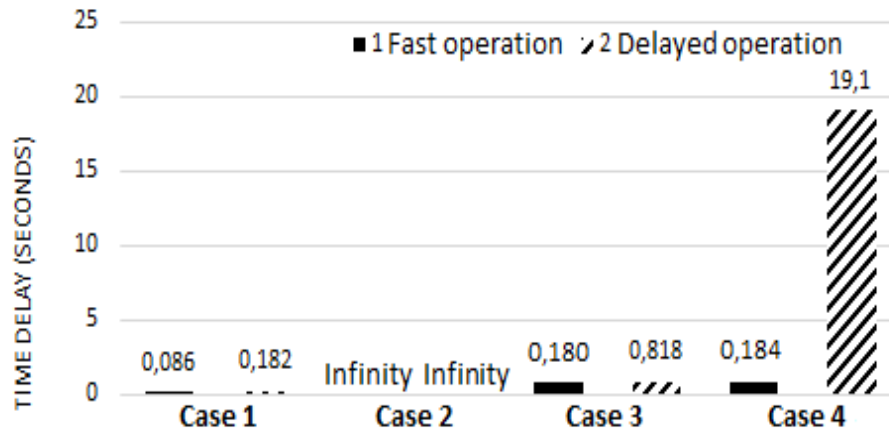


Fig. 4-10 Comparison of the fast and delayed operation times for R1 in the four case studies

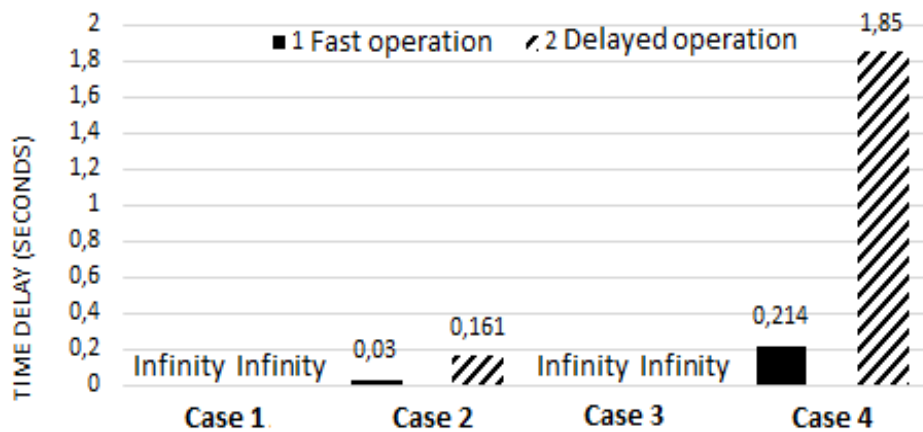


Fig. 4-11 Comparison of the fast and delayed operation times for auto-recloser R2 in the four case studies

## 4.9. Optimization framework

The search and selection of optimal settings for an auto-recloser applied in a distribution network integrated with DGs shall be conducted using a robust optimization algorithm. This research study uses the DE algorithm to globally search for the optimal settings of the auto-recloser. These settings should minimize the operating time when applied to the distribution network integrated with a DG. An optimization model is framed in this subsection by formulating the problem and stating the objective. The time-dial and pick-up decision variables are subject to design constraints which limit the search within their minimum and maximum parameter setting [84-85].

### 4.9.1. Problem formulation

The blinding of protection, sympathetic tripping, and loss of coordination with other protection devices mal-operations of the auto-recloser are non-linear optimization problems since the auto-recloser's operation time is determined from a non-linear function expressed in (4.15). The problem with the operating time is an increase of the operating time in a faulted feeder, which requires minimization. Only the TD and  $I_p$  are unknown independent decision variables. A, B, and p are known [86].

$$T_{Ri} = (\frac{A}{(\frac{I_R}{I_{Pi}})^{p-1}} + B)TD_i \quad (4.15)$$

Where  $i$  is the auto-recloser identifier.

The objective is to minimize the operating time [12]. The form of the objective function is expressed in (4.16)

$$OF = \text{Min } T_{Ri} \quad (4.16)$$

### 4.9.2. Auto-recloser settings constraints

The range of auto-recloser settings from which feasible solutions are encountered is presented as constraints in (4.17) and (4.18) [78]. These are the constraints of the time-dial and pick-up of the auto-recloser.

$$TD_{min} \leq TD \leq TD_{max} \quad (4.17)$$

$$I_{Pmin} \leq I_P \leq I_{Pmax} \quad (4.18)$$

Where,  $TD_{min}$  is the minimum limit of the time-dial setting;  $TD_{max}$  is the maximum limit of the time-dial setting,  $I_{Pmin}$  is the minimum limit of the pick-up setting and  $I_{Pmax}$  is the maximum limit of pickup setting.

### 4.9.3. DE algorithm application

This optimization problem is a single-objective optimization problem and the global search for optimal settings of the time-dial and pick-up that should minimize the operating time and reduces the mal-operations of the auto-recloser in a distribution network integrated with DGs. This shall optimize the protection of the auto-recloser in prevailing voltage and fault conditions. The three commonly applied algorithms to optimize protection settings are the PSO, ACO, and DE algorithms. These algorithms can be applied to search for the Pareto optimal solutions of these settings [87]. With the PSO algorithm, the search continues only with the same particles and no other particles are substituted during iterations, which can limit its global search

for optimal solutions of the objective function [82]. The ACO algorithm performs better for a local search than for a global search and this is a shortfall for a global search of the time dial setting and pick-up setting [88-89]. The DE algorithm is a method that was proposed by Kenneth V. Price and R. Storn in 1997 [84]. It is a child of the Genetic Algorithm annealing, by the addition of the differential mutation operator. The DE algorithm was proposed for minimizing non-linear functions, it is a simple and efficient meta-heuristic algorithm for globally searching optimal solutions. The DE algorithm continues the search with the best vectors through mutation and selection operations and computes optimal solutions. Joymala Moirangthem, et. al [90] applies it to search for the optimal relay coordination settings in a DG network. There are four steps in the DE algorithm to achieve stochastic optimal solutions *viz.* Initialization, differential mutation, crossover, and selection. Initialization generates an initial population  $\mathbf{P}^0$ , which the three steps after the initialization of the setting parameters evolve  $\mathbf{P}^0$  to  $\mathbf{P}^1$  and  $\mathbf{P}^1$  to  $\mathbf{P}^2$  until the termination conditions are fulfilled (14) [85]. The best solution is given in the final generation of the decision variables that best meet the objective for the fitness function.

The algorithm used is the *DE/rand/1/bin*. The inputs of the DE algorithm are the lower bound ( $TD_{min}, I_{Pmin}$ ), upper bound ( $TD_{max}, I_{Pmax}$ ) of the decision variables, population size ( $P$ ), number of generations ( $G$ ), scaling factor ( $F$ ) and cross-over the property ( $Cr$ )[85-86,91].

*Step 1: Initializing the differential evolution parameters (random).*

The target vectors in (4.19) are initialized randomly in (4.20) to create a random population [84]. This is the random selection of the initial population for optimal solutions of the decision variables. These values are selected between their minimum and maximum limits.

$$\begin{pmatrix} TD_{(k)}^g \\ I_{p(k)}^g \end{pmatrix} = \begin{pmatrix} td_{(k,1)}^g, td_{(k,2)}^g \dots \dots \dots, td_{(k,i)}^g, \dots \dots \dots, td_{(P,D)}^g \\ I_{p(k,1)}^g, I_{p(k,2)}^g \dots \dots \dots, I_{p(k,i)}^g, \dots \dots \dots, I_{p(P,D)}^g \end{pmatrix} \quad (4.19)$$

$$\begin{pmatrix} td_{(k,i)}^g \\ I_{p(k,i)}^g \end{pmatrix} = \begin{pmatrix} td_{pi}^{min} \\ I_{pi}^{min} \end{pmatrix} + (rand_{(k,j)}) \times \begin{pmatrix} td_i^{max} - td_i^{min} \\ I_{pi}^{max} - I_{pi}^{min} \end{pmatrix} \quad (4.20)$$

Where,  $g = 1, 2, \dots, G$  is the maximum number of generations;  $i = 1, 2, \dots, D$  is the dimension of the problem and  $rand_{(k,i)}$  is the uniformly distributed random variable within the range of (0,1).

*Step 2: Differential mutation (one differential operator)*

*For*  $g = 1$  *to*  $G$  *do* loop for generation.  
*For*  $k = 1$  *to*  $P$  *do* loop for the population size.

The mutated vectors of the time-dial and pick-up decision variables are generated by using (4.21).

$$\begin{pmatrix} tdv_{(k,i)}^{g+1} \\ I_{pv(k,i)}^{g+1} \end{pmatrix} = \begin{pmatrix} td_{r1}^g \\ I_{pr1}^g \end{pmatrix} + F \times \begin{pmatrix} td_{r2}^g - td_{r3}^g \\ I_{pr2}^g - I_{pr3}^g \end{pmatrix} \quad (4.21)$$

Where,  $r_1, r_2$  and  $r_3 \in \{1, 2, \dots, \mathbf{P}\}$  are randomly chosen integers, different from each other and different from the running index  $i$  [91].

The mutated decision variables are presented in (4.22).

$$\begin{pmatrix} TDv_{(k)}^{g+1} \\ I_{pv(k)}^{g+1} \end{pmatrix} = \begin{pmatrix} tdv_{(k,1)}^{g+1}, tdv_{(k,2)}^{g+1} \dots \dots \dots, tdv_{(k,i)}^{g+1}, \dots \dots \dots, tdv_{(k,D)}^{g+1} \\ I_{pv(k,1)}^{g+1}, I_{pv(k,2)}^{g+1} \dots \dots \dots, I_{pv(k,i)}^{g+1}, \dots \dots \dots, I_{pv(k,D)}^{g+1} \end{pmatrix} \quad (4.22)$$

*Step 3: Crossover*

In the crossover, a trial vector is generated using an if statement. A trial vector is selected by (4.23) [92].

$$\begin{pmatrix} tdvnew_{(k,i)}^{g+1} \\ I_{pvnew(k,i)}^{g+1} \end{pmatrix} = \begin{cases} \begin{pmatrix} tdv_{(k,i)}^{g+1} \\ I_{pv(k,i)}^{g+1} \end{pmatrix} & \text{if } rand_{(k,i)} \leq Cr \text{ or } i = i_{rand} \\ \begin{pmatrix} td_{(k,i)}^g \\ I_{p(k,i)}^g \end{pmatrix} & \text{otherwise} \end{cases} \quad (4.23)$$

*end*

end loop for the population size.

*Step 4: Selection (binomial)*

*For i = 1 to D do*

To generate a new population with optimal solutions, the differential evolution replaces the target vector with the trial vector using (4.24).

$$\begin{pmatrix} TD_{(k)}^{g+1} \\ I_{p(k)}^{g+1} \end{pmatrix} = \begin{cases} \begin{pmatrix} tdvnew_{(k,i)}^{g+1} \\ I_{pvnew(k,i)}^{g+1} \end{pmatrix} & \text{if } T_r \left( \begin{pmatrix} tdvnew_{(k,i)}^{g+1} \\ I_{pvnew(k,i)}^{g+1} \end{pmatrix} \right) \leq T_r \left( \begin{pmatrix} td_{(k,i)}^g \\ I_{p(k,i)}^g \end{pmatrix} \right) \\ \begin{pmatrix} td_{(k)}^g \\ I_{p(k)}^g \end{pmatrix} & \text{otherwise} \end{cases} \quad (4.24)$$

*end*

end loop for selection.

*end*

end loop for generation.

## 4.10. Optimal settings and operation

The new line current and fault current detected by the auto-recloser in the presence of DG are used to obtain the optimal time-dial and pick-up settings for the third case and the fourth case. To obtain the best time-dial and pick-up setting, the code of the DE algorithm in subsection 4.9 is implemented in the MATLAB Script and runs for the network conditions of the third and fourth cases. Table 4-1 presents the results of the algorithm under these voltage and fault conditions. The performance of these settings is simulated and



compared with the conventional settings performance. The extremely inverse time-current characteristic curves of the conventional settings (not-optimized curves) and optimal settings (optimized curves) are presented in Fig. 14. The optimal settings show improved response compared to the conventional settings.

**Table 4-1 Optimal settings**

CT ratio (A)	Peak fault current (A)	Auto-recloser current (A)	Pick-up setting ( $I_{pvnew}$ in %)	Time-dial setting ( $tdvnew$ )
300/5	2930	1860	100	0.1
300/5	1649	80	100	0.45

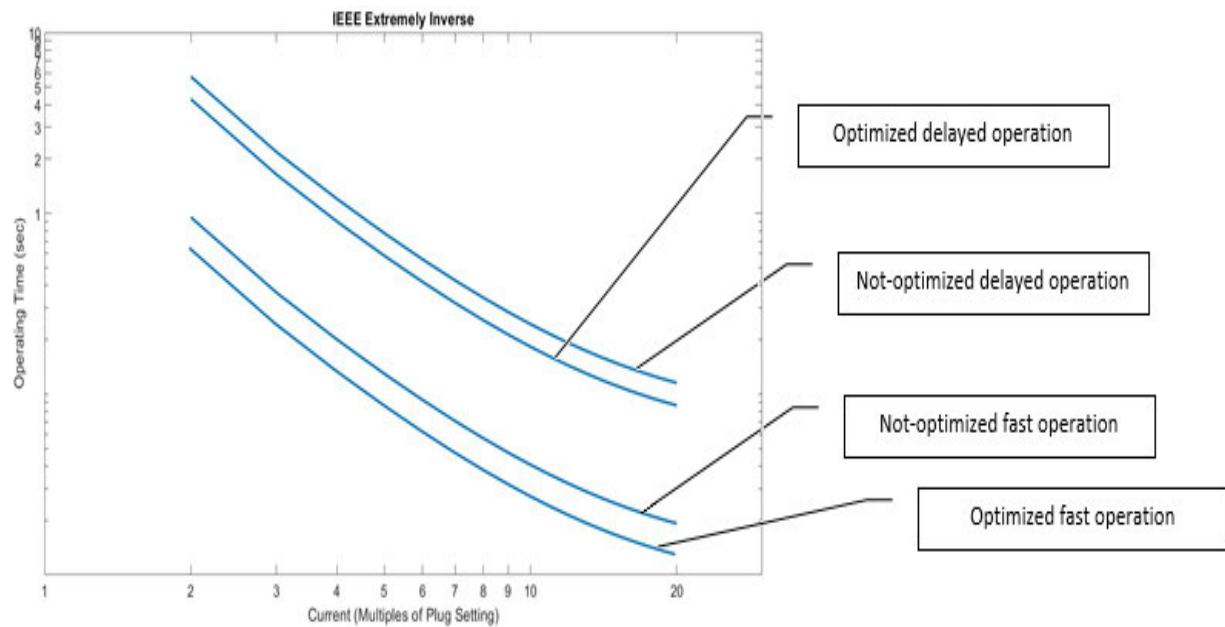


**Fig. 4-12 Comparison of the fast and delayed curves with conventional and optimal settings in case 3 and case 4**

#### 4.10.1. Optimal performance analysis for a temporary fault

The optimal settings are programmed in auto-recloser R1 to validate that they produce an improved performance for the new conditions of the distribution network. A temporary fault is simulated and the results are depicted in Fig. 4-13. It can be observed that the conventional settings do not clear the temporary fault and have a delayed response while the optimal settings can isolate the fault until it self clears and restore service. There is a difference of 0.1 sec in the operation time of the auto-recloser between the conventional settings and optimal settings. The requirements for selectivity, security, dependability and sensitivity are met [93].

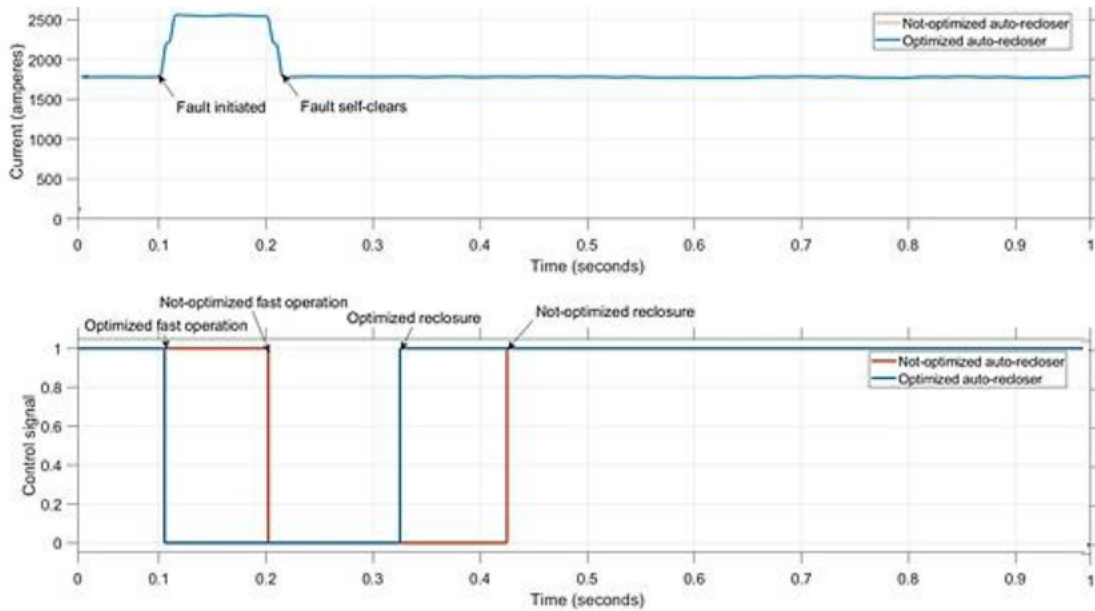
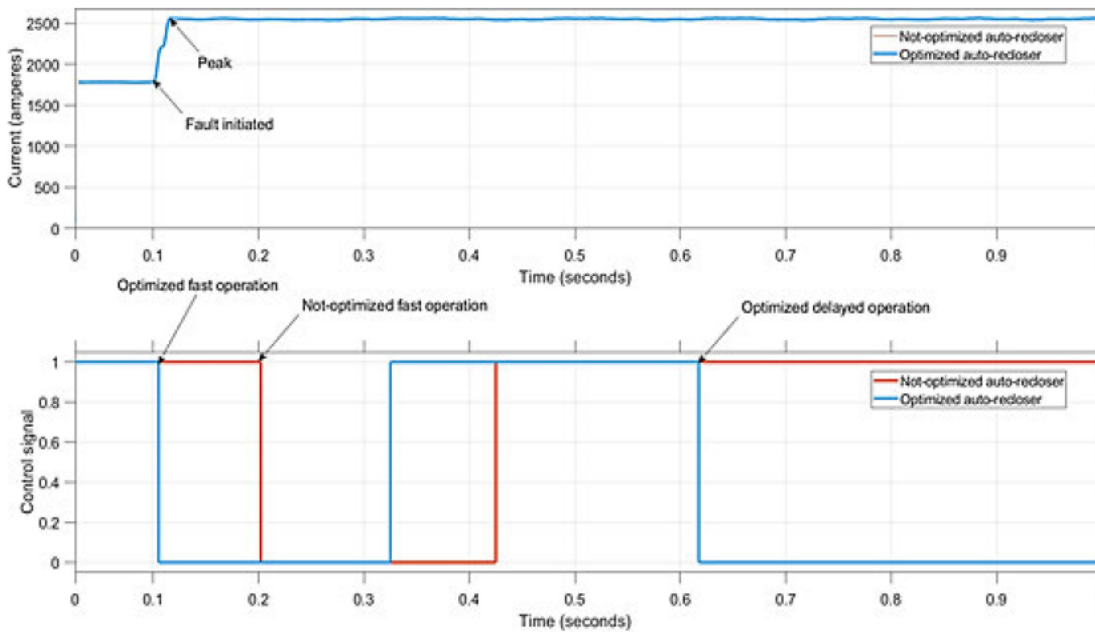


Fig. 4.13 Comparison of the not-optimized and optimized operation of auto-recloser R1 for a temporary fault

#### 4.10.2. Optimal performance analysis for permanent fault

The Fig. 4-14 below depicts the optimal operation for a permanent fault. The DG remains grid-connected and therefore continually feeds the fault as depicted. However, the fast and the delayed operating time of the auto-recloser have been enhanced. The auto-recloser responds quicker with the optimal settings compared to the conventional settings for both the fast and the delayed mode of operation. The requirements for selectivity, security, dependability, sensitivity and redundancy are met [93].



**Fig. 4-14 Comparison of the not-optimized and optimized operation of auto-recloser R1 for a permanent fault**

## **4.11. Conclusion**

The current contribution of DGs and its effects on the auto-recloser the pick-up and operating times have been investigated. An IEEE 13 node radial distribution feeder is used and the developed auto-recloser applied in two lateral feeders. DGs are integrated into nodes 33 and 75. Four cases were investigated by changing the location of the fault on the lateral feeders for auto-reclosers in a network with and without DGs. Each fault location yielded a different result of the voltage profile, current profile, pick-up activity, and operating times of auto-reclosers. These results were compared and it was found that the auto-recloser operates according to the set pick-up and time-dial in the passive distribution system. However, the integration of DGs showed mal-operations in the auto-reclosers, there was an abnormal pick-up in a healthy feeder and the operation times increased. The selectivity, security, dependability, sensitivity, and redundancy of the auto-recloser was degraded, this results in the blinding of protection, sympathetic tripping and loss of coordination with other protection devices. This required a search of optimal settings that shall mitigate or reduce the mal-operations. The DE algorithm was applied to search for optimal time-dial and pick-up settings. These settings were tested and the pick-up activity as well as the operating times improved.

The conclusions drawn in this chapter serve as a basis for optimizing the protection of the auto-recloser under different case studies presented in chapter 5.

# **Chapter 5 Optimizing Auto-recloser Protection**

## **5.1. Introduction**

There are four types of DG systems that can be integrated into the distribution network. The first type is capable of delivering only active power but may be required to deliver reactive power, the second type delivers both active and reactive power, the third type delivers only reactive power and the fourth type delivers active power and consumes reactive power [92]. The type and location of these DG systems determines their fault current contribution to the fault current level. Type one and type two supply additional active power into the grid for power loss reduction and are enabled to support the voltage profile through injection of the reactive power [94]. Each system can be configured to have a low voltage ride-through and can alter the voltage profile [27]. With the variation in the voltage profile, the optimization of the auto-recloser protection must be adequate to meet the requirements. This chapter applies the auto-recloser model of chapter four in different DG location, DG type, fault location and fault type case studies. The selection of optimal settings is performed by the DE algorithm and the modified DE algorithm schemes. The exploration and exploitation of the best performing schemes is balanced with the use of an exponential scale factor.

## **5.2. DG systems**

Type one and type four are to be integrated. Type one is a Solar PV system and type four is the Wind Turbine system. Each type of DG system operates to meet the requirements for supplying active power into the grid and to inject or absorb reactive power for voltage support in a grid-connected mode. The voltage, frequency and power factor requirements for distribution network integration shall be met to enable a synchronous voltage support in the case of voltage disturbances, voltage drops and voltage instability [95-96].

### **5.2.1. Solar PV system**

The output power of the Solar PV system is dependent on the size, number, temperature of the Solar PV panels and the solar irradiance. The inverter provides a two-way flow of power and communication between the distribution network and the Solar PV system [97]. The Solar PV system supports the distribution network voltage by supplying constant power at a unity power factor. It delivers the maximum available power to the distribution network by increasing the inverter output current even during faults or voltage

drop conditions [98].

### **5.2.2. Wind Turbine system**

The mode of the interfacing transformer for the Wind Turbine system is a neutral grounding by small resistance of 20 ohms, this is installed at the neutral point of the grounding transformer [99]. The output power is dependent on the wind speed. These are the conditions that the Wind Turbine system introduces into the distribution network. An appropriate interfacing transformer configuration and grounding scheme compatible with the distribution network is applied. The Wind Turbine system's power factor is also set to unity.

## **5.3. Integration**

The active distribution network is a local electrical power system 4 which is given in the IEEE 1547 standard [100]. The DG systems are hybridized by the integration of the energy storage system to balance the power supply, reduce intermittency and level the load [101]. The capacity factors of the Solar PV and Wind Turbine systems are taken to be 0.097 and 0.43 [29]. According to the IEEE 1547 standard, when a fault occurs, it is required that the low voltage ride-through is initiated for the DG system. This low voltage ride-through can be initiated for each system individually or for both systems [30].

## **5.4. DE modified schemes**

The auto-recloser is required to have an optimal fast operating time for temporary faults when DG remains grid-connected. To facilitate this optimal auto-recloser protection, the auto-recloser operation should be based on the minimum and maximum fault currents experienced by the feeder [24,93,102-103]. The auto-recloser should trip and reclose before the temporary fault extinguishes, it should operate to extinguish the fault prohibiting the operation of downstream protection devices. The auto-recloser should act selectively to clear temporary faults on the first shot [104]. The DE algorithm has been modified to design three schemes which should each individually enhance the protection of the auto-recloser to meet the requirements and reduce mal-operations. This is to find the best scheme and optimal settings for the different voltage and fault conditions case studies. The schemes make use of the weighted difference between two points. The mutation strategies and modification are presented in Table 5-1 and the time-dial and pick-up settings for optimizing auto-recloser protection are presented in Tables 5-2.

**Table 0-1 DE modified schemes**

DE scheme	Mutation strategy	Modification
MDE 1	DE/rand/2	$\begin{pmatrix} tdv_{(k,i)}^{g+1} \\ I_{pv(k,i)}^{g+1} \end{pmatrix} = \begin{pmatrix} td_{r1}^g \\ I_{pr1}^g \end{pmatrix} + F \times \begin{pmatrix} td_{r2}^g - td_{r3}^g \\ I_{pr2}^g - I_{pr3}^g \end{pmatrix} + F \times \begin{pmatrix} td_{r4}^g - td_{r5}^g \\ I_{pr4}^g - I_{pr5}^g \end{pmatrix}$
MDE 2	DE/best/1	$\begin{pmatrix} tdv_{(k,i)}^{g+1} \\ I_{pv(k,i)}^{g+1} \end{pmatrix} = \begin{pmatrix} td_{best}^g \\ I_{pbest}^g \end{pmatrix} + F \times \begin{pmatrix} td_{r1}^g - td_{r2}^g \\ I_{pr1}^g - I_{pr2}^g \end{pmatrix}$
MDE 3	DE/best/2	$\begin{pmatrix} tdv_{(k,i)}^{g+1} \\ I_{pv(k,i)}^{g+1} \end{pmatrix} = \begin{pmatrix} td_{best}^g \\ I_{pbest}^g \end{pmatrix} + F \times \begin{pmatrix} td_{r1}^g - td_{r2}^g \\ I_{pr1}^g - I_{pr2}^g \end{pmatrix} + F \times \begin{pmatrix} td_{r3}^g - td_{r4}^g \\ I_{pr3}^g - I_{pr4}^g \end{pmatrix}$

**Table 0-2 Conventional and Optimal Settings**

Scheme	Fast Time Dial setting (seconds)	Fast Pickup setting (%)	Delayed Time Dial setting (seconds)	Delayed Pickup setting (%)
Conventional	0.10	150	0.6	150
DE	0.15	150	0.45	100
MDE1	0.05	100	0.3	150
MDE2	0.8	100	0.6	150
MDE3	0.3	50	0.45	150

## 5.5. Case studies for optimal auto-recloser protection

This assessment of the auto-recloser when there is a variation in the voltage and fault current caused by the integration of DGs of two different types. This is to observe whether the injection of reactive power causes the voltage to remain steady, rise or fall. The voltage rise or fall must remain within the +/- 6% of the variation from the nominal voltage. The auto-recloser performance is assessed under the change of the voltage and fault current conditions. The mal-operations that may occur in the auto-recloser are assessed to identify the scheme settings can optimize the protection of the auto-recloser [93].

### 5.5.1. Case study 1: Temporary fault at F1 for no DG

In this case study, the distribution network does not have DGs integrated. The settings given in Table 5-2

are tested in a voltage profile depicted in Fig. 5-1. The performance of the protection settings provided by each scheme shall be observed and compared to determine which scheme can be used to obtain optimal settings in this case. When the fault strikes in the F1 location as depicted in Fig. 3-3, the voltage drops to 0 V, but does not remain at 0, there are transient rises in the voltage from 0 V. This is not caused by an integration of a DG as there is no DG connected. However, this only occurs during the temporary fault. The drop in the voltage shows that there is a short-circuit in the distribution feeder. The fault has a duration of 0.1 sec and the voltage rises back to the 14.6 kV RMS. There is no variation in the voltage. It can be observed in Fig. 5-2 how the current behaves in these voltage and fault conditions. It can be observed that the magnitude of the current rises to 23.110 kA at 0.1 sec. This is the peak of the fault current. The auto-recloser determines its operating time through the scheme settings it has been programmed. The pick-up activity of the auto-recloser can be observed in Fig. 5-2 according to these settings. The settings computed the operating times presented in Table 5-3 [93].

**Table 0-3 Auto-recloser operating times in case study 1**

<b>Scheme</b>	<b>Fast Operating Time (msec)</b>
Conventional	13.9
DE	20.9
MDE1	6.5
MDE2	103.7
MDE3	37.1

It can be observed in Fig. 5-3 and Table 5-3 that all the schemes cause the pick-up of the auto-recloser to remain within 200 msec. Therefore, they all provide an optimal operating time for the auto-recloser when there is no DG integrated. The scheme that had optimal settings when compared to all the schemes is MDE1. The auto-recloser responded the fastest compared to all the schemes when programmed with the settings computed by this scheme. There was no protection blinding or sympathetic tripping mal-operations for all the schemes [93].

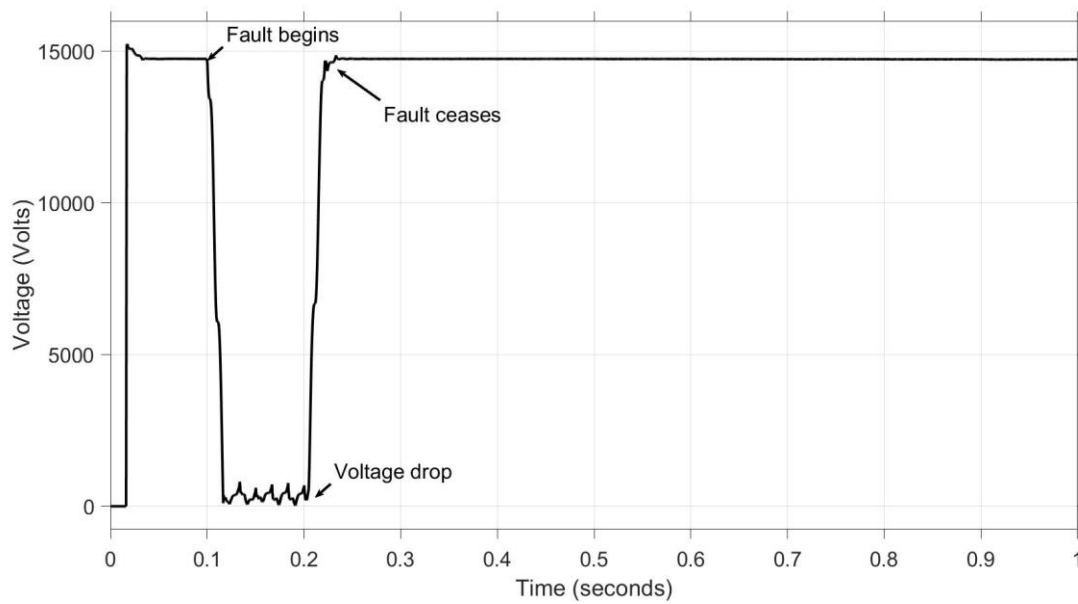


**Fig. 0-1 Voltage profile with no DG for a temporary fault in the F1 fault location**

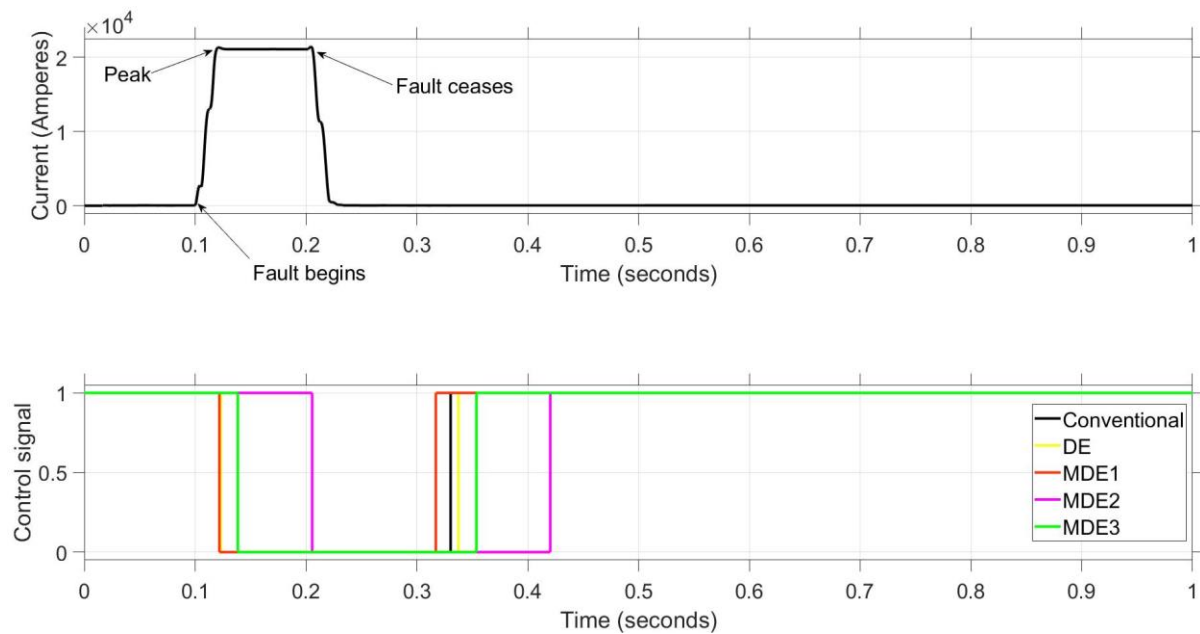


**Fig. 0-2 Auto-recloser pick-up activity for different schemes and settings in case study 1**

### 5.5.2. Case study 2: Temporary fault at F1 for the Solar PV system integration

In this case study, the distribution network has a Solar PV system integrated into it. The settings are tested in a voltage profile depicted in Fig. 5-3. The performance of the protection settings provided by each scheme



shall be observed and compared to determine which scheme can be used to obtain optimal settings in this case study. There is a minor increase in the voltage to 14.7 kV RMS from the first case study. The increase is 0.7% which is within the +/- 6% variation standard. When the fault strikes in the F1 location as depicted in Fig. 3-3, the voltage drops to 0 V, but it not steady at 0 V. This shows that there is a short-circuit in the distribution feeder. The fault has a duration of 0.1 sec and the voltage rises back its 14.7 kV when the fault ceases. The Solar PV system does not provide much support during the voltage drop. It can be observed in Fig. 5-4 how the current behaves in these voltage and fault conditions. It can be observed that the magnitude of the fault current is similar to the first case. The auto-recloser determines it's operating time through the settings it has been programmed with. The pick-up activity of the auto-recloser can be observed in Fig. 5-4 according to the settings from each scheme. The settings computed the operating times in Table 5-4 [93].

**Table 0-4 Auto-recloser operating times in case study 2**

<b>Scheme</b>	<b>Fast Operating Time (msec)</b>
Conventional	13.90
DE	20.85
MDE1	6.481
MDE2	103.7
MDE3	37.13

It can be observed in Fig. 5-4 that all the schemes stay within the optimal operating time as in the first case. There was not much change in the operating times. However, the Solar PV system is integrated far from the fault, this caused minor effect on the voltage and the fault current. The contribution of the Solar PV system did not cause any mal-operations using any of the settings in the auto-recloser, but it did reduce the operating times provided by DE and MDE1 settings. MDE1 still remained the scheme that had optimal settings when compared to all the schemes. There was no protection blinding or sympathetic tripping mal-operations for all the schemes.

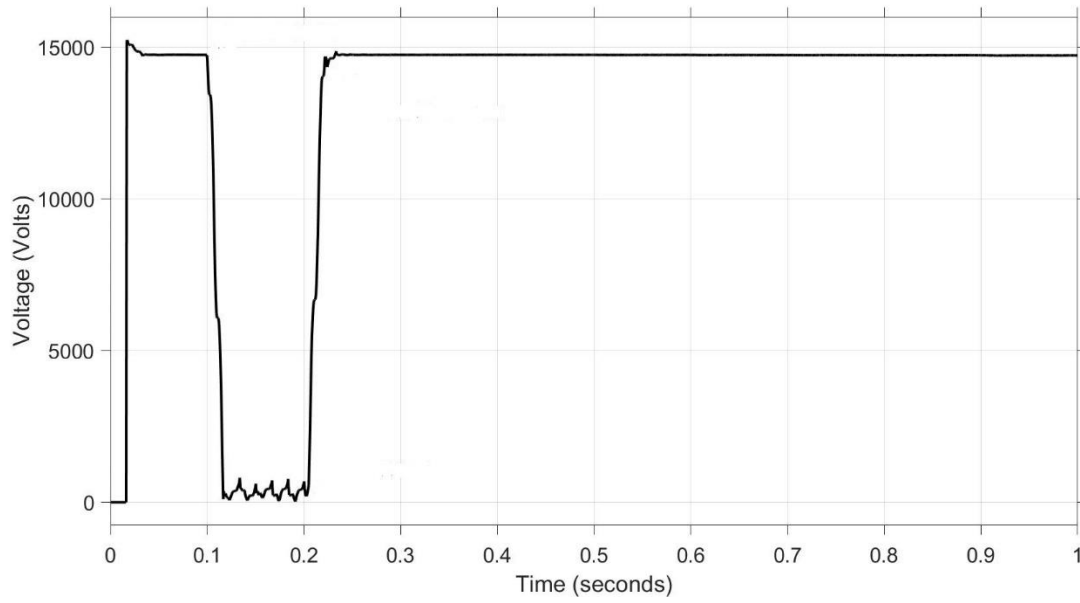


**Fig. 0-3 Voltage profile with Solar PV system integration for a temporary fault in the F1 fault location**

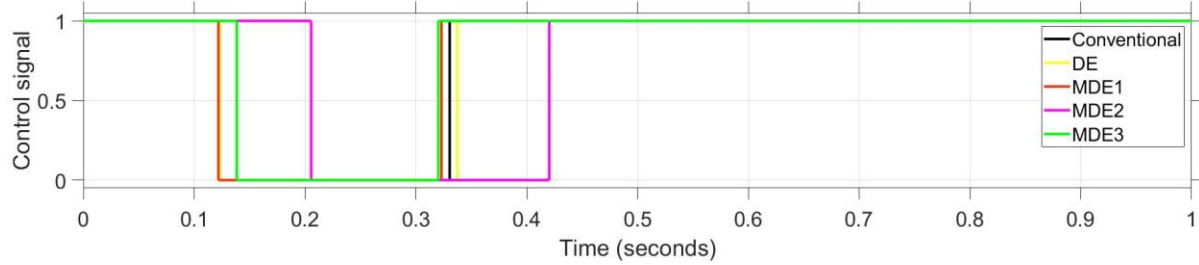
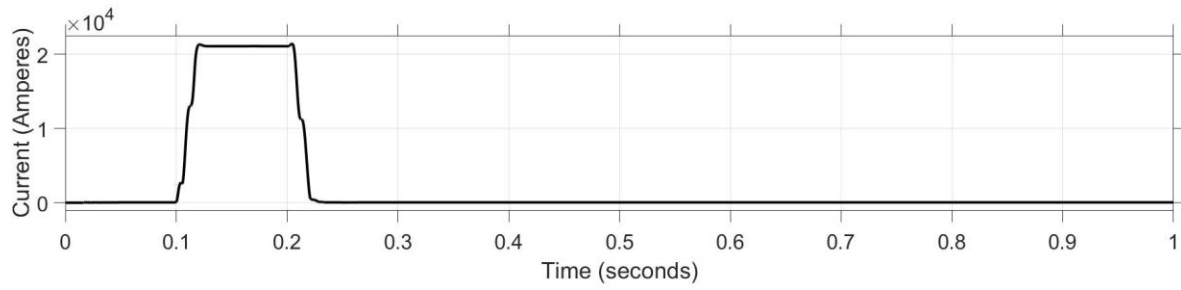


**Fig. 0-4 Auto-recloser pick-up activity for different schemes and settings in case study 2**

### 5.5.3. Case study 3: Temporary fault at F1 for the Solar PV and Wind Turbine systems integration

In case study 1, the pick-up activity of the auto-recloser was tested with no DG and in case study 2 the pick-up activity of the auto-recloser was tested when the distribution network is integrated with a Solar PV

system. The pick-up activity was tested with the settings computed by the schemes. The fault location remained the same. This case study is to test for an optimal protection of the auto-recloser when there is a different type of a DG system integrated in a different location.

The distribution network has a Wind Turbine system added. The settings are tested in a voltage profile depicted in Fig. 5-5. The voltage is not steady. There is a falling and a rising voltage profile in the distribution feeder. It rises to 16 kV between 0 to 3.25 sec, this is a 9.6 % voltage rise and false to 14 kV which is a 4.1 % fall. It rises to 16.2 kV at 3.25 sec, this is a 11 % voltage rise and begins to becomes steady. The performance of the protection settings provided by each scheme shall be observed and compared to determine which scheme can be used to obtain optimal settings in these conditions. When the fault strikes in the F1 location as depicted in Fig. 3-3, the voltage drops to 2 kV in this case study. This shows that there is a short-circuit in the distribution feeder but the Wind Turbine system remaining grid connected supports the utility generator by supplying a voltage of 2 kV during the temporary fault. The fault has a duration of 0.1 sec and the voltage rises back after the fault ceases. It can be observed in Fig. 5-6 how the current behaves in these voltage and fault conditions. It can be observed that the magnitude of the current rises to 23.11 kA at 0.1 sec. This is the peak of the fault current. The auto-recloser determines its operating time through the settings it has been programmed with. The pick-up activity of the auto-recloser can be observed in Fig. 5-6 according to the settings from each scheme. The settings computed the operating times in Table 5-5 [93].

**Table 0-5 Auto-recloser operating times in case study 3**

<b>Scheme</b>	<b>Fast Operating Time (msec)</b>
Conventional	3901
DE	5851
MDE1	786.6
MDE2	12080
MDE3	967.2

It can be observed in Fig. 5-6 that all schemes with their settings compute an operating time greater than 200 msec. But the two schemes that had a better performance amongst all the schemes are MDE1 and MDE3. The scheme that had optimal settings when compared to all the schemes is MDE1. The auto-recloser responded the fastest with these settings but it experienced sympathetic tripping in its delayed operating mode. The conventional, DE and MDE2 computed slower operating times which may cause a loss of coordination with other protection devices.

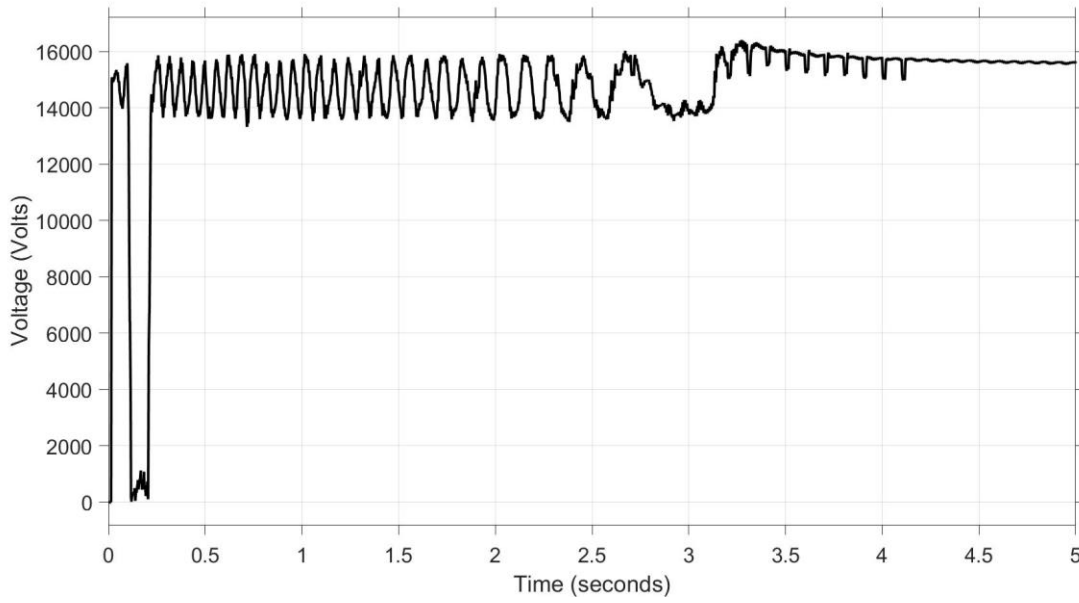


**Fig. 0-5 Voltage profile with Solar PV and Wind Turbine system integration for a temporary fault in the F1 fault location**

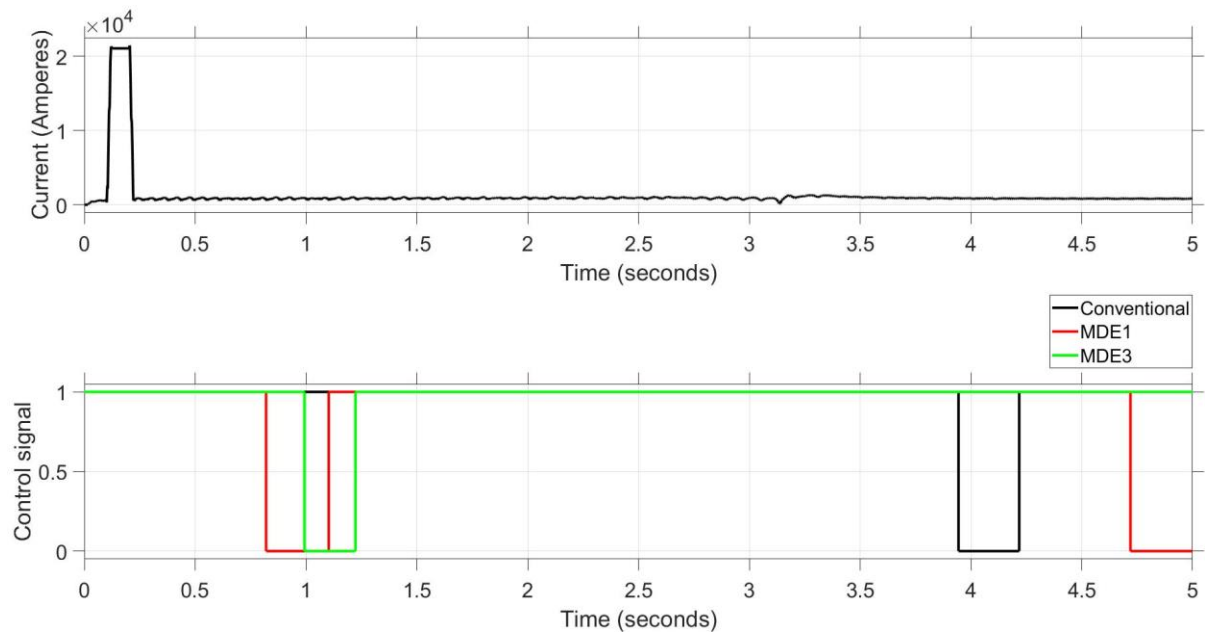


**Fig. 0-6 Auto-recloser pick-up activity for Conventional, MDE1 and MDE3 schemes and settings in case study 3**

#### 5.5.4. Case study 4: Temporary fault at F2 for no DG

In this case study the distribution network does not have DGs integrated. The settings are tested in a voltage profile depicted in Fig. 5-7. The location of the fault is changed to test the pick-up activity of the auto-recloser under new fault conditions. The performance of the protection settings provided by each scheme

shall be observed and compared to determine which scheme can be used to obtain optimal settings in this case. When the fault strikes in the F2 location as depicted in Fig. 3-3, the voltage drops to 11 kV. The fault has a duration of 0.1 sec and the voltage rises back to the 14.6 kV after the fault ceases. The change in the location of the fault caused the voltage to have a reduced voltage drop. It can be observed in Fig. 5-8 how the current behaves in these voltage and fault conditions. It can be observed that the magnitude of the current rises to 360 A at 0.1 sec which is a 22.75 kA reduction from case study 1. This is the new peak in the fault current. The auto-recloser determines its operating time through the settings it has been programmed with. The pick-up activity of the auto-recloser can be observed in Fig. 5-8 according to the settings from each scheme. The settings computed the operating times in Table 5-6 [93].

**Table 0-6 Auto-recloser operating times in case study 4**

<b>Scheme</b>	<b>Fast Operating Time (msec)</b>
Conventional	Infinity
DE	Infinity
MDE1	3979
MDE2	63660
MDE3	1939

In Fig. 5-8 it can be observed that only MDE1 and MDE3 provide settings that react the fastest. The conventional and DE schemes compute infinite operating times. Therefore, they cause the auto-recloser to mal-operate with protection blinding. The scheme that had settings that operate the auto-recloser faster when compared to all the schemes is MDE1. However, these settings do not isolate the 0.1 sec temporary fault and can cause a loss in coordination with other protection devices. MDE2 had a delayed reaction which can cause a loss of coordination with other protection devices.

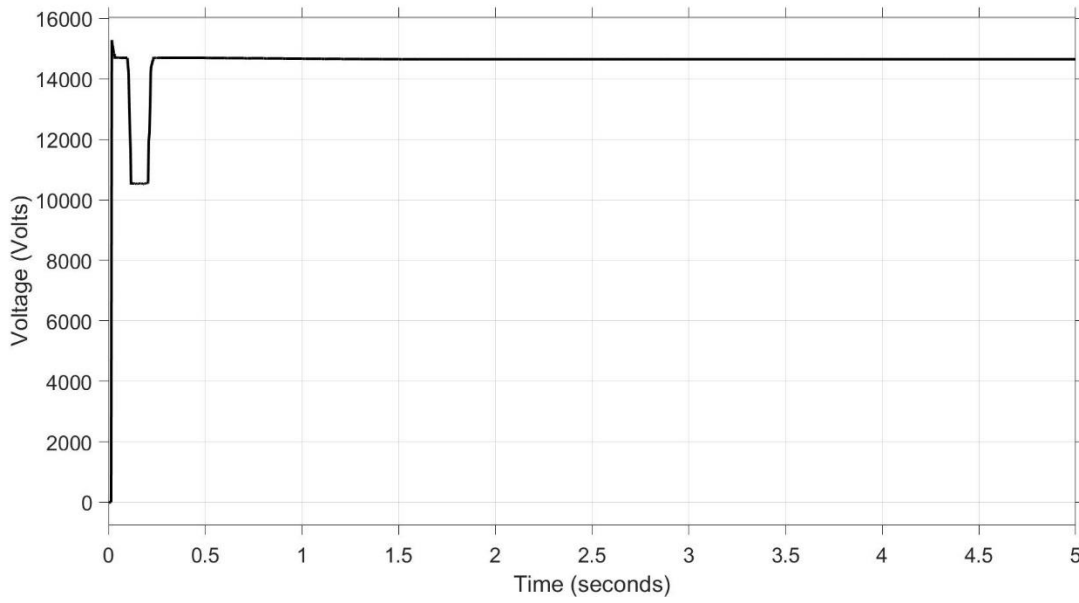


**Fig. 0-7 Voltage profile with no DG for a temporary fault in the F2 fault location**

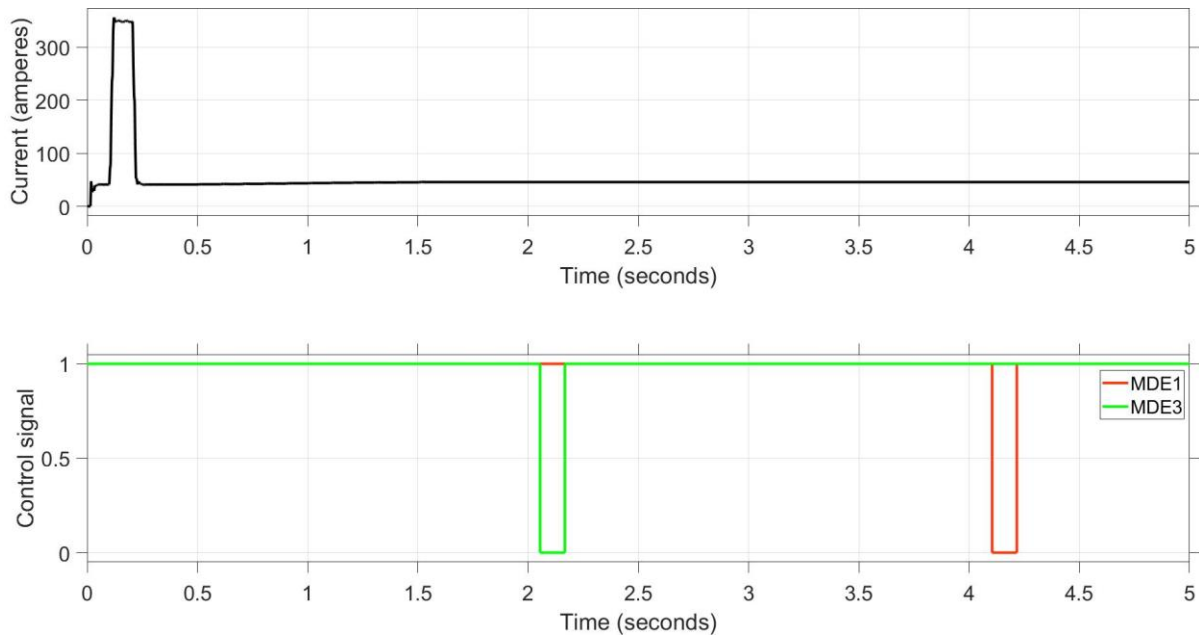


**Fig. 0-8 Auto-recloser pick-up activity for MDE1 and MDE3 schemes and settings in case study 4**

### 5.5.5. Case study 5: Temporary fault at F2 for a Solar PV system integration

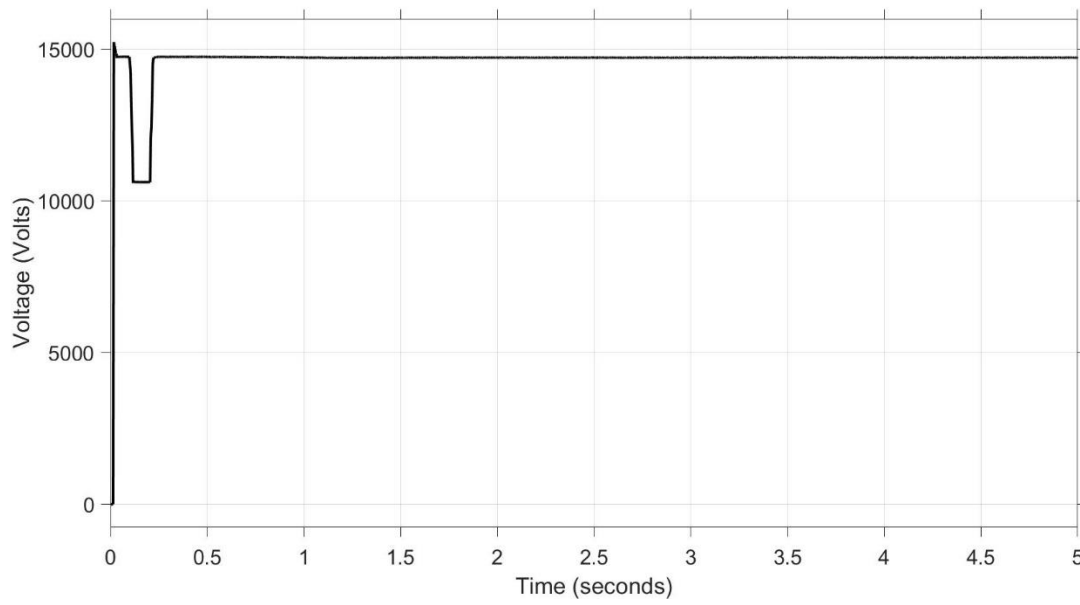
In this case study the distribution network has a Solar PV system integrated into it and the fault location is changed from F1 to F2 as can be seen in Fig. 3-3. The settings are tested in a voltage profile depicted in

Fig. 5-9. The impact on the voltage caused by the change in the fault location can be observed. The voltage drops to 10.9 kV. The location of the fault reduced the voltage drop. These are the voltage conditions that the auto-recloser is operating in. The performance of the protection settings provided by each scheme shall be observed and compared to determine which scheme can be used to obtain optimal settings in this case. The fault has a duration of 0.1 sec and the voltage rises back to 14.6 kV when the fault ceases. It can be observed in Fig. 5-10 how the current behaves in these voltage fault conditions. It can be observed that the magnitude of the fault current rises to 395 A. The pick-up activity of the auto-recloser can be observed in Fig. 5-10 according to the settings from each scheme. The settings computed the operating times in Table 5-7 [93].

**Table 0-7 Auto-recloser operating times in case study 5**

<b>Scheme</b>	<b>Fast Operating Time (msec)</b>
Conventional	Infinity
DE	Infinity
MDE1	2093
MDE2	32540
MDE3	1503

It can be observed in Fig. 5-10 and Table 5-7 that the two schemes that provide settings with better responses are MDE1 and MDE3 but they do not operate the auto-recloser to isolate the 0.1 sec temporary fault. The settings from the conventional and DE schemes give an infinite operating time. This is protection blinding. MDE2 settings may cause the loss of coordination because of the delayed response. The scheme that provided a faster operating time in this case is MDE3.



**Fig. 0-9 Voltage profile with Solar PV system integration for a temporary fault in the F2 fault location**

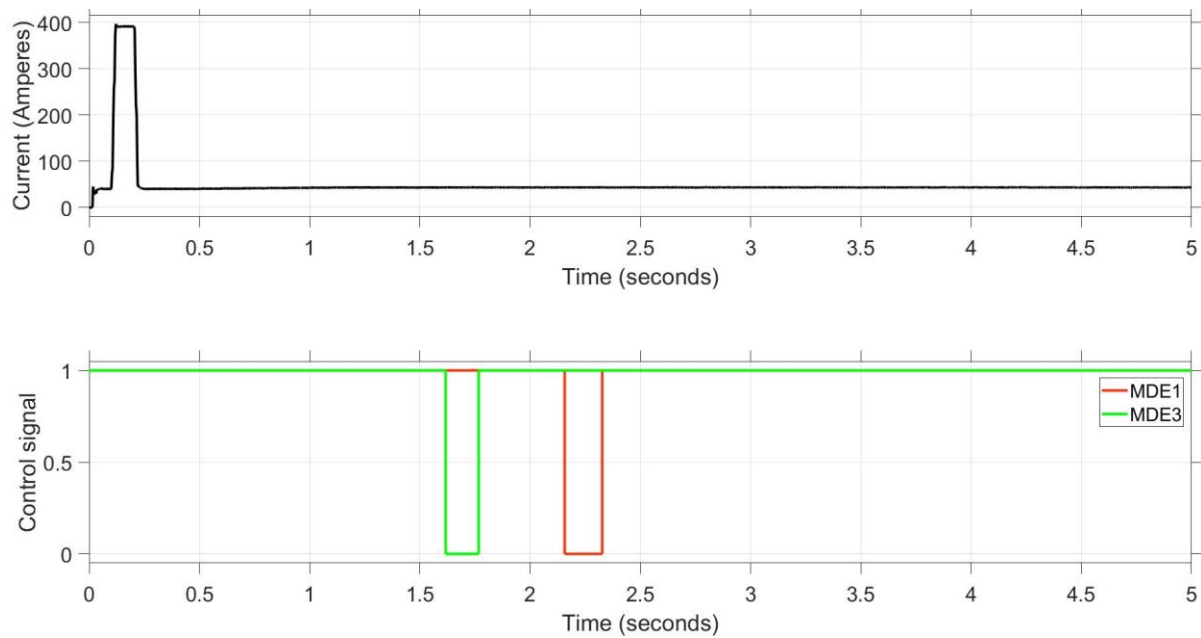


**Fig. 0-10 Auto-recloser pick-up activity for MDE1 and MDE3 schemes and settings in case study 5**

### 5.5.6. Case study 6: Temporary fault at F2 for a Solar PV and Wind Turbine system integration

As in case studies 4 and 5, the fault location is changed and a new fault location is F2 as depicted in Fig. 3-



3. The protection of the auto-recloser is tested in this new fault location and the settings are tested to find an optimal performance that can handle the temporary fault location. The location and type of the DG remains the same as in case study 3.

The distribution network has a Wind Turbine system added. The settings are tested in a voltage profile depicted in Fig. 5-11. The voltage is not steady. The performance of the protection settings provided by each scheme shall be observed and compared to determine which scheme can be used to obtain optimal settings in this case. When the fault strikes the voltage drops to 10 kV. The change in the location and type of the fault reduces the impact on the voltage drop. The fault has a duration of 0.1 sec and the voltage rises but it is not stable. It is fluctuating between 12 kV and 18 kV. It can be observed in Fig. 5-12 how the current behaves in these voltage and fault conditions. It can be observed that the magnitude of the current rises to 550 A at 0.1 sec, but the current is not in a steady state. The auto-recloser determines its operating time through the settings it has been programmed with. The settings computed the operating times in Table 5-8. Only the settings from MDE1 scheme showed a faster response to the fault, but not in the optimal operating time.

**Table 0-8 Auto-recloser operating times in case study 6**

<b>Scheme</b>	<b>Fast Operating Time (msec)</b>
Conventional	Infinity
DE	Infinity
MDE1	888.1
MDE2	14210
MDE3	7887

It can be observed in Fig. 5-12 and Table 5-8 that the only scheme that provides a faster operating time for the auto-recloser is MDE1. The fault location and type change has caused protection blinding when using settings from the conventional and DE schemes. They showed infinite operating times which caused the auto-recloser to not operate. The settings from the MDE2 and MDE3 schemes show that they can be a loss of coordination with other protection devices, as these reach thousand milliseconds. MDE1 showed a faster response compared to all the settings but exhibited sympathetic tripping. The fault ceased after 0.1 sec, but the delayed operating mode was triggered.

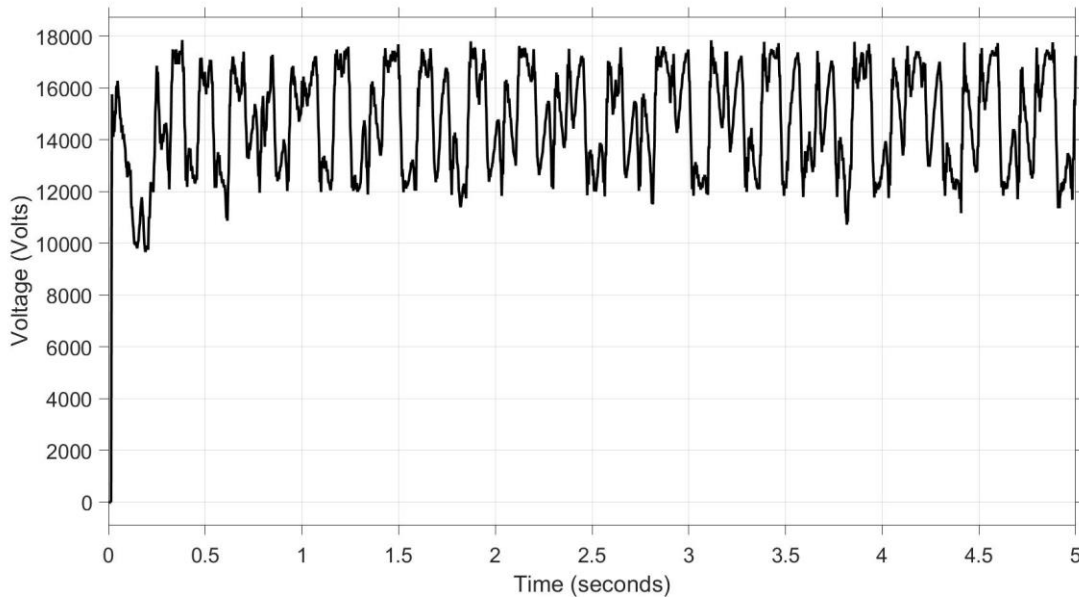


**Fig. 0-11 Voltage profile with Solar PV and Wind Turbine system integration for a temporary fault in the F2 fault location**

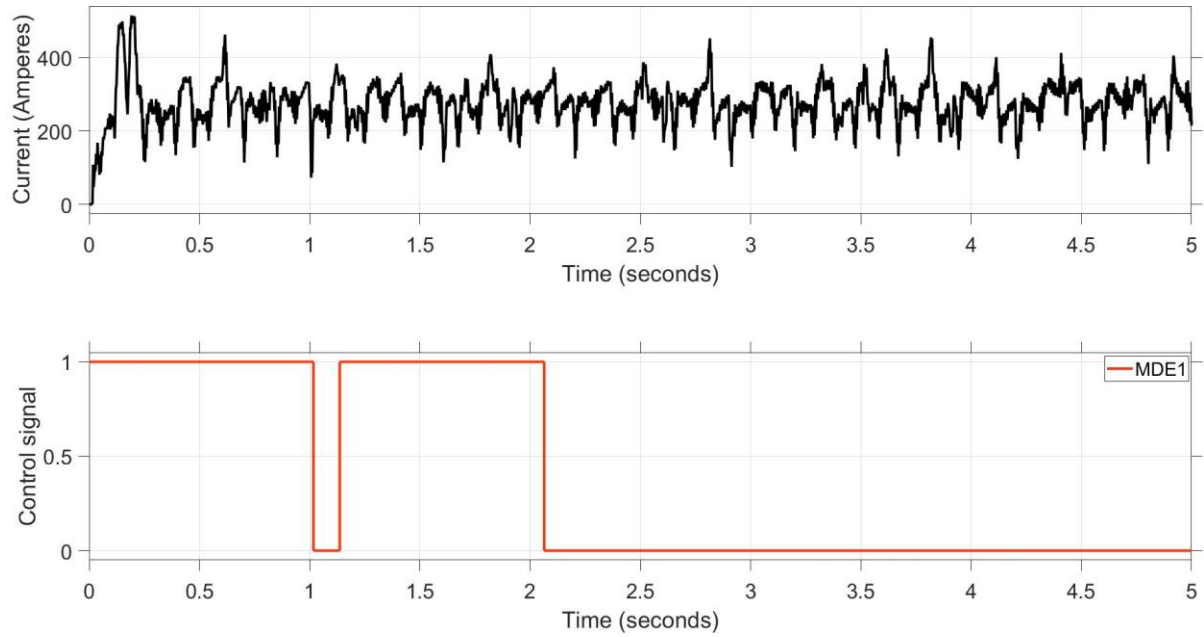


**Fig. 0-12 Auto-recloser pick-up activity for MDE1 scheme and settings in case study 6**

## 5.6. Case studies for the exponential scale factor application

The differential mutation is varied by applying a varied scale factor. The exploration and exploitation of

the DE algorithm shall be balanced by the scale factor variation. The DE algorithm has to be able to explore the time-dial and pick-up settings search space while having an optimal ability to refine the identified search area and find the optimal settings. To ensure a balanced exploration and exploitation ability, the scale factor is modified according to the equation (5.1). High values of the scale factor will enhance the exploration of the search space, as the scale factor decreases exponentially, the exploitation will be enhanced [19, 93].

$$F = \frac{1}{e^{(1 - \frac{(It_{max} - It)}{It_{max}})}} \quad (5.1)$$

Where  $It_{max}$  is the maximum number of iterations and  $It$  is the current iteration.

The two best performing schemes that have been identified are MDE1 and MDE3. For the MDE1 the new time-dial and pick-up settings using the exponential scale factor are 0,05 and 175 and for MDE3 the new time-dial and pick-up settings are 0.15 and 100. These settings are for the fast operating mode of the auto-recloser.

### 5.6.1. Exponential scale factor application for case study 1

The exponential scale factor is applied in case study 1. The voltage and fault conditions remain the same as in case study 1. The settings have changed for two schemes to be used in optimizing the protection of the auto-recloser. The pick-up activity of the auto-recloser can be observed in Fig. 5-13 according to the settings from each scheme. The settings computed the operating times presented in Table 5-9.

**Table 0-9 Auto-recloser operating times for exponential scale factor application in case study 1**

<b>Scheme</b>	<b>Fast Operating Time (msec)</b>
MDE1	7.244
MDE3	19.44

It can be observed in Fig. 5-13 that these settings from the two schemes cause the auto-recloser to operate within 200 msec. Therefore, they provide an optimal operating time for the auto-recloser when there is no DG integrated. The scheme that provided optimal protection is MDE1. It responded faster than MDE3. There was no protection blinding or sympathetic tripping mal-operations cause by the application of these settings.

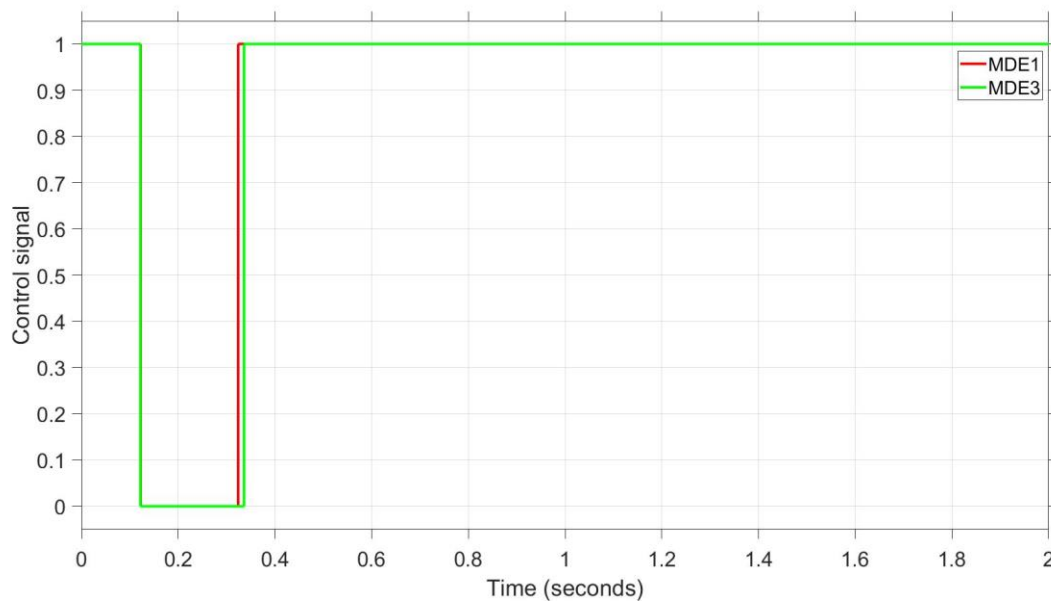


**Fig. 0-13 Auto-recloser pick-up activity for MDE1 and MDE3 schemes and settings with exponential scale factor in case study 1**

### 5.6.2. Exponential scale factor application for case study 2

The exponential scale factor is applied in case study 2. The voltage and fault conditions remain the same as in case study 2. The settings for two schemes have changed from the case study 2. The pick-up activity of the auto-recloser can be observed in Fig. 5-14 according to the settings from each scheme. The settings computed the operating times presented in Table 5-10. These operating times are similar to the application of the exponential scale factor in case study 1.

**Table 0-10 Auto-recloser operating times for exponential scale factor application in case study 2**

Scheme	Fast Operating Time (msec)
MDE1	7.244
MDE3	19.44

It can be observed in Fig. 5-14 that the settings from the two schemes are within 200 msec. Therefore, they provide an optimal operating time for the auto-recloser when there is a Solar Photovoltaic system integrated. The scheme that provided optimal protection is MDE1. It responded faster than MDE3. There was no protection blinding or sympathetic tripping mal-operations caused by the schemes.

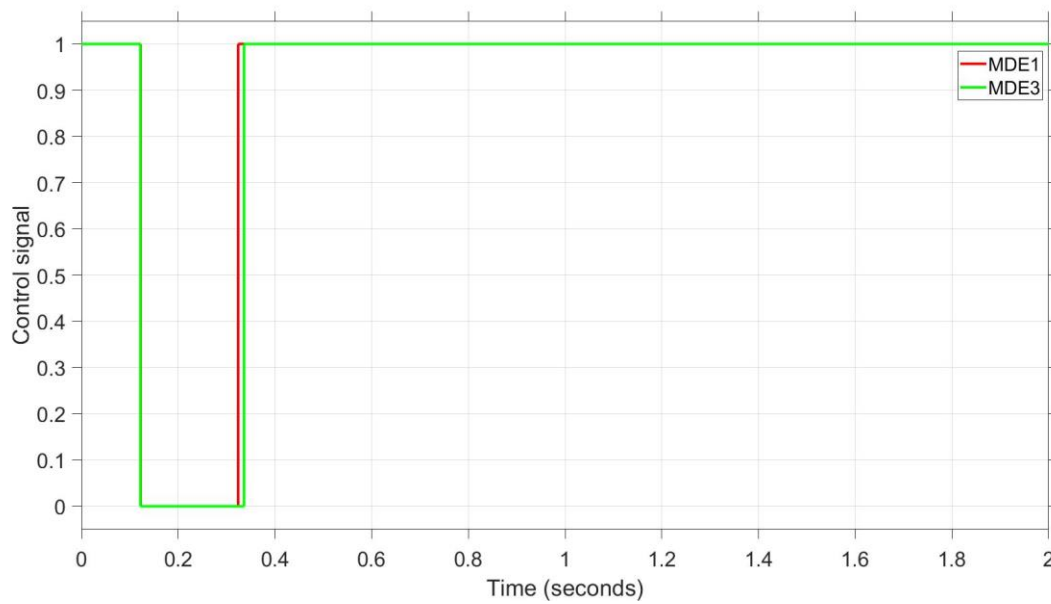


**Fig. 0-14 Auto-recloser pick-up activity for MDE1 and MDE3 schemes and settings with exponential scale factor in case study 2**

### 5.6.3. Exponential scale factor application for case study 3

The exponential scale factor is applied in case study 3. The voltage and fault conditions remain the same as in case study 3. The settings have changed for two schemes to be used for the MDE1 and MDE3 schemes. The performance of the auto-recloser can be observed in Fig. 5-15 according to the settings from each scheme. The settings computed the operating times in Table 5-9.

**Table 0-11 Auto-recloser operating times for exponential scale factor application in case study 3**

Scheme	Fast Operating Time (msec)
MDE1	5310
MDE3	2360

It can be observed in Fig. 5-15 that MDE3 has a delayed response and in Table 5-11 that the settings from the two schemes surpass 200 msec. The settings in this case are not optimal according to the 100 msec to 200 msec target to isolate the 0.1 sec temporary fault. The MDE3 scheme settings operated the auto-recloser faster than the MD1 scheme settings but did not provide optimal protection. There was no protection blinding or sympathetic tripping mal-operations in the auto-recloser using this scheme's settings but there could be a loss of coordination because of the increased delay in the pick-up activity.

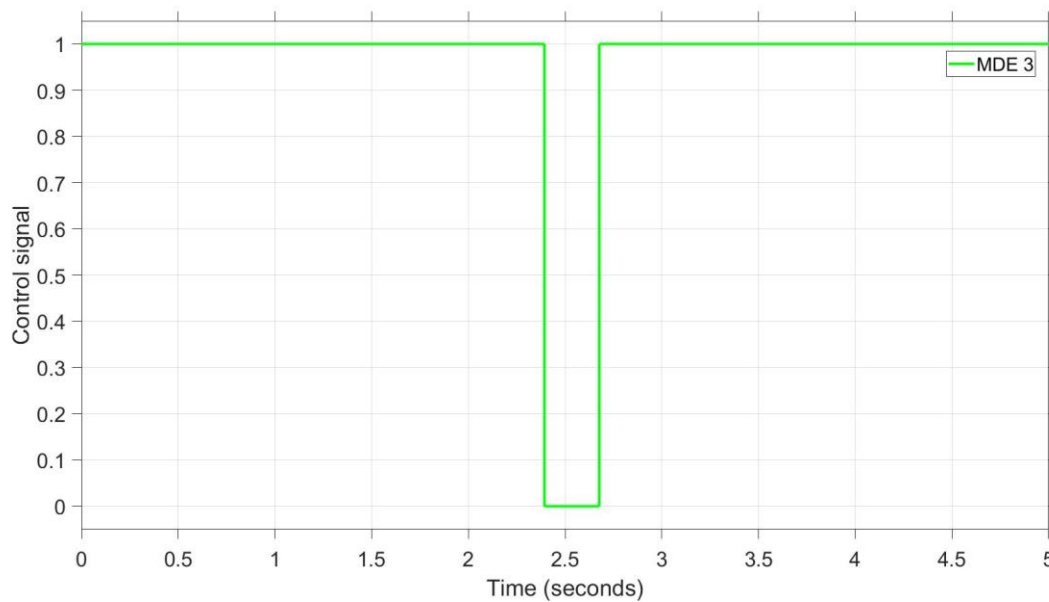


**Fig. 0-15 Auto-recloser pick-up activity for MDE3 scheme and settings for the exponential scale factor in case study 3**

#### 5.6.4. Exponential scale factor application for case study 4

The exponential scale factor is applied in case study 4. The voltage and fault conditions remain the same as in case study 4. The settings have changed for the MDE1 and MDE3 schemes. The pick-up activity is not shown for this case study. The settings computed the operating times in Table 5-12.

**Table 0-12 Auto-recloser operating times for exponential scale factor application in case study 4**

Scheme	Fast Operating Time (msec)
MDE1	Infinity
MDE3	11940

It can be observed in Table 5-12 that MD1 provides settings that do not cause the auto-recloser to operate, this is protection blinding. MDE3 does provide settings that can operate the auto-recloser, but with a very delayed operating time. This time can cause a loss of coordination with other protection devices. The settings do not isolate the 0.1 sec temporary fault.

#### 5.6.5. Exponential scale factor application for case study 5

The exponential scale factor is applied in case study 5. The voltage and fault conditions remain the same as in case study 5. The settings for MDE1 and MDE2 scheme have been changed. The pick-up activity of the

auto-recloser can be observed in Fig. 5-16 according to the scheme settings of MDE3. The pick-up activity of the auto-recloser with MDE1 scheme settings is not available because the auto-recloser does not operate. The settings computed the operating times in Table 5-13.

**Table 0-13 Auto-recloser operating times for exponential scale factor application in case study 5**

Scheme	Fast Operating Time (msec)
MDE1	Infinity
MDE3	6100

It can be observed in Fig. 5-17 how the auto-recloser responds with MDE3 settings. The settings from the two schemes do not operate the auto-recloser optimally in this case but MDE3 does provide a faster operating time compared to MDE1. MDE1 scheme settings cause the auto-recloser to have protection blinding, and MDE3 can cause loss of coordination.

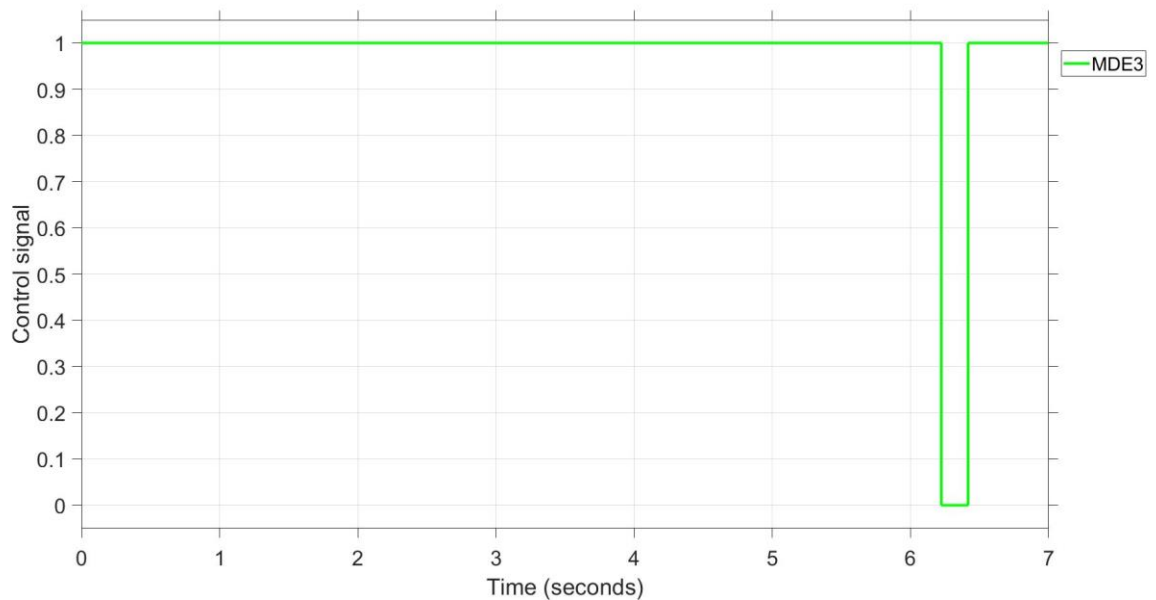


**Fig. 0-16 Auto-recloser pick-up activity for MDE3 scheme and settings with exponential scale factor in case study 5**

### 5.6.6. Exponential scale factor application for case study 6

The exponential scale factor is applied in case study 6. The voltage and fault conditions remain the same as in case study 6. The settings are changed for MDE1 and MDE3. The pick-up activity of the auto-recloser can be observed in Fig. 5-17 according to the settings from each scheme. The settings computed the operating times in Table 5-14.

**Table 0-14 Auto-recloser operating times for exponential scale factor application in case study 6**

Scheme	Fast Operating Time (msec)
MDE1	5361
MDE3	2361

It can be observed in Fig. 5-17 that the auto-recloser responds with a delayed operating time greater than 200 msec using the MDE1 and MDE3 scheme settings. They do not clear the 0.1 sec temporary fault. MDE3 scheme settings responds the fastest compared to the MDE1 scheme settings. Both of the scheme settings can cause a loss of coordination.

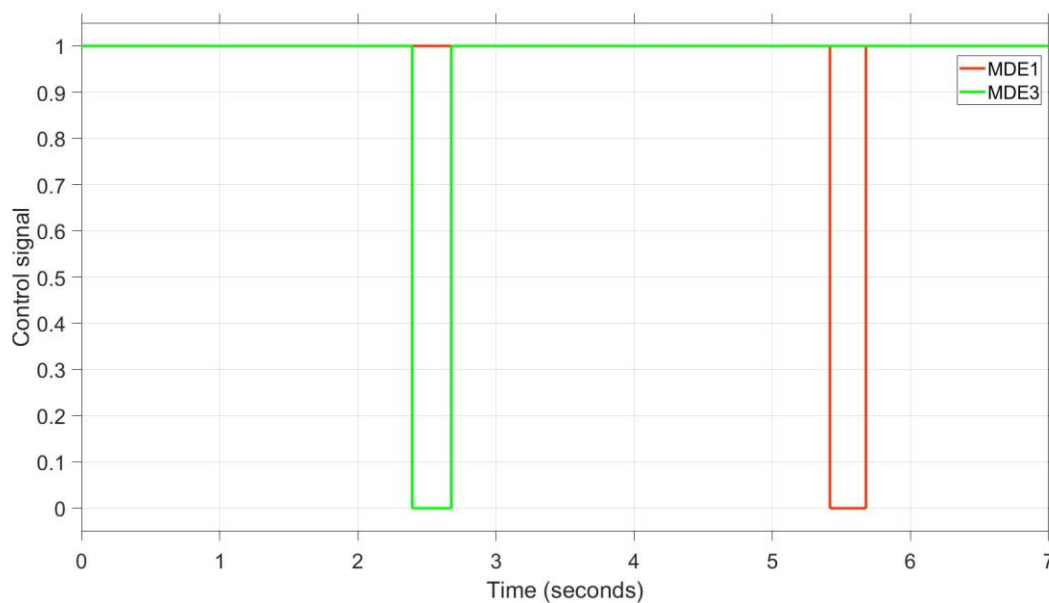


**Fig. 0-17 Auto-recloser pick-up activity for MDE1 and MDE3 schemes and settings with exponential scale factor in case study 6**

## 5.7. Discussion

Six case studies with different voltage and fault conditions in the distribution network have been simulated. The voltage profiles show the voltages at the node number 802 when there is a temporary fault. The fault is assumed to be 0.1 sec of duration. The temporary fault is located in F1 for three case studies and F2 for another three case studies. The fault located in F1 is a three-phase-to-ground fault and the fault located in F2 is a single-phase-to-ground fault. Five types of settings are applied to the auto-recloser to test the protection of the auto-recloser and obtain the settings that can best operate the auto-recloser to protect the distribution network under the conditions. These five set of settings are from the conventional method, DE



algorithm and MDE algorithms. The response of the current was taken from a single-phase to observe what the current level rises to. The pick-up activity of the auto-recloser was observed for different settings.

### **5.7.1. Comparison of scheme and settings performance for F1 fault location**

Fig. 5-18 presents the comparison of the auto-recloser operating time for the pick-up of the temporary fault in the location F1. The comparison is for each scheme and settings applied on the auto-recloser for the three case studies. The response of the auto-recloser is determined during the sub-transient state of the fault current. The conventional settings cause the auto-recloser to perform optimally in the first case study and in the second case study when there is an integration of the Solar PV system, but when the Wind Turbine system is integrated, the performance of the auto-recloser is degraded. The auto-recloser is not dependable in case study 3. The DE scheme settings show optimal operating times for case study 1 and case study 2 but show a delayed response in case study 3, they perform worse than the conventional settings. MDE1 scheme settings show an optimal performance for case study 1 and case study 2, but they also show a delayed response in case study 3. However, the operating time greatly reduced when compared to the conventional and DE schemes. This scheme can optimize the protection of the auto-recloser through the reduction of the operating time. MDE2 operates optimally for case study 1 and case study 2, but performs worse when compared to the conventional, DE and MDE1 schemes. In case study 3, the scheme computed the worst results of the operating time than all the schemes. The MDE3 scheme and settings computed optimal results for the first and the second case studies, but gave a delayed response in case study 3. All schemes and their settings in case study 3 surpass the 200 msec target for optimal protection of the auto-recloser. For faults that are within the 200 msec duration, this keeps the auto-recloser fault clearance within the instantaneous and adjustable instantaneous operating region. Integrating a Wind Turbine system proves to cause delayed pick-up on the auto-recloser, but for faults within 1 second, the MDE1 and MDE3 schemes can be applied, but MDE1 scheme causes the auto-recloser to have sympathetic tripping, the auto-recloser is sensitive to the voltage rise and falls introduced by the Wind Turbine system.

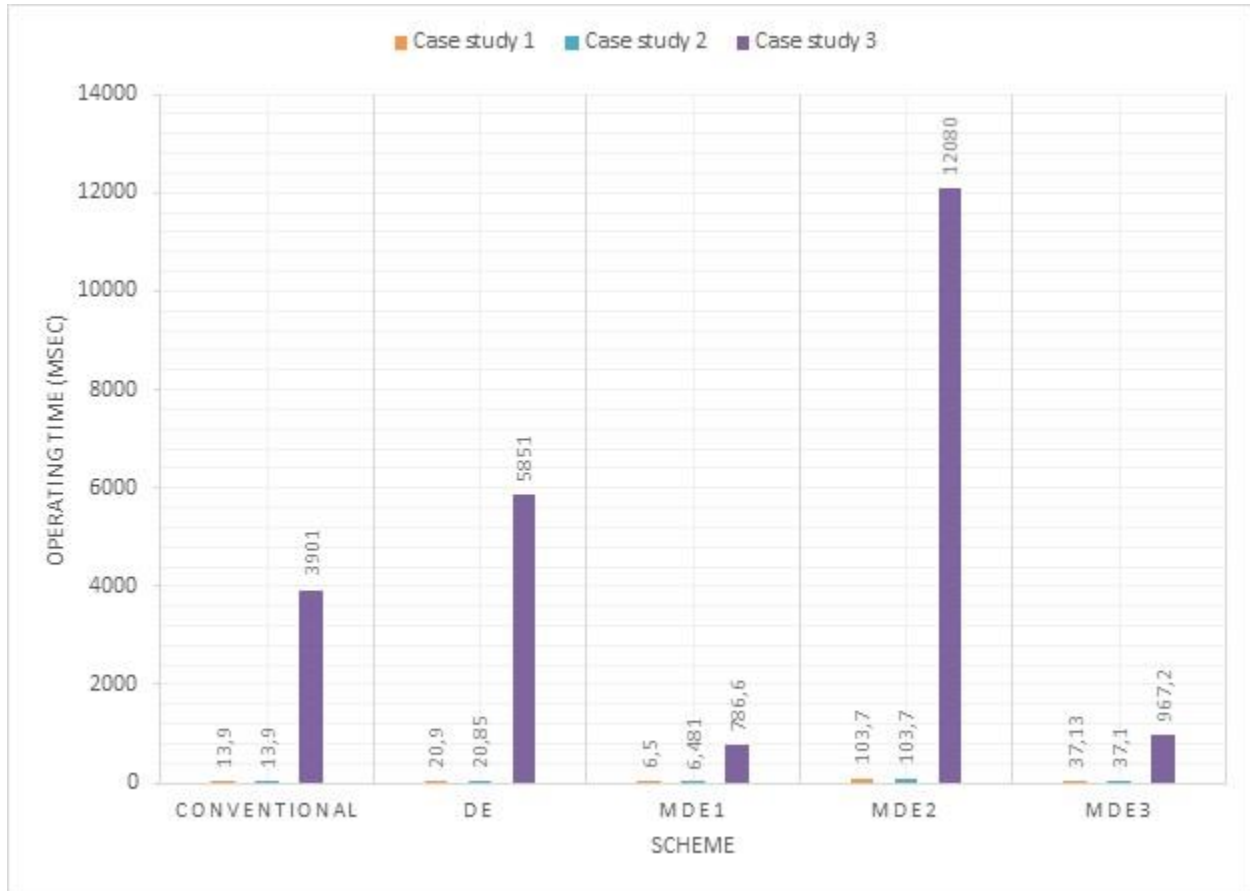


**Fig. 0-18 Scheme and settings performance for temporary fault at F1 location**

### **5.7.2. Comparison of scheme and settings performance for F2 fault location**

Fig. 5-19 presents the comparison of the auto-recloser operating time for the pick-up of the temporary fault in the location F2 for the three case studies. The response of the auto-recloser is determined during the sub-transient state of the fault current. The conventional and DE scheme settings cause the auto-recloser to compute an infinite operating time. The protection of the auto-recloser is blinded when there is a fault and it mal-operates for all three case studies. MDE1 scheme settings compute operating times for all the three cases but they are delayed responses and they surpass the 200 msec target for a fault lasting 0.1 sec. However, they cause a reduction in the operating time for case study 3 compared to the other two case studies. MDE2 gives high operating times for all the case studies, but performs better in case study 3 than in the other two case studies. MDE3 scheme settings computed delayed operating times for all the cases, but they showed a reduced operating time in case study 2. The MDE1, MDE2 and MDE3 scheme settings are likely to cause a loss of coordination depending on the coordination time interval. But for faults reaching up to a second of duration, MDE1 scheme settings can isolate the faults in case study 3. For faults that are

within the 200 msec duration, the auto-recloser does not have fault isolation within the instantaneous and adjustable instantaneous operating region for all the scheme settings. Changing the fault location caused a varied operating time for the pick-up of the auto-recloser for MDE1, MDE2 and MDE3. For the conventional and DE scheme settings it caused the auto-recloser to not pick-up the fault at all.

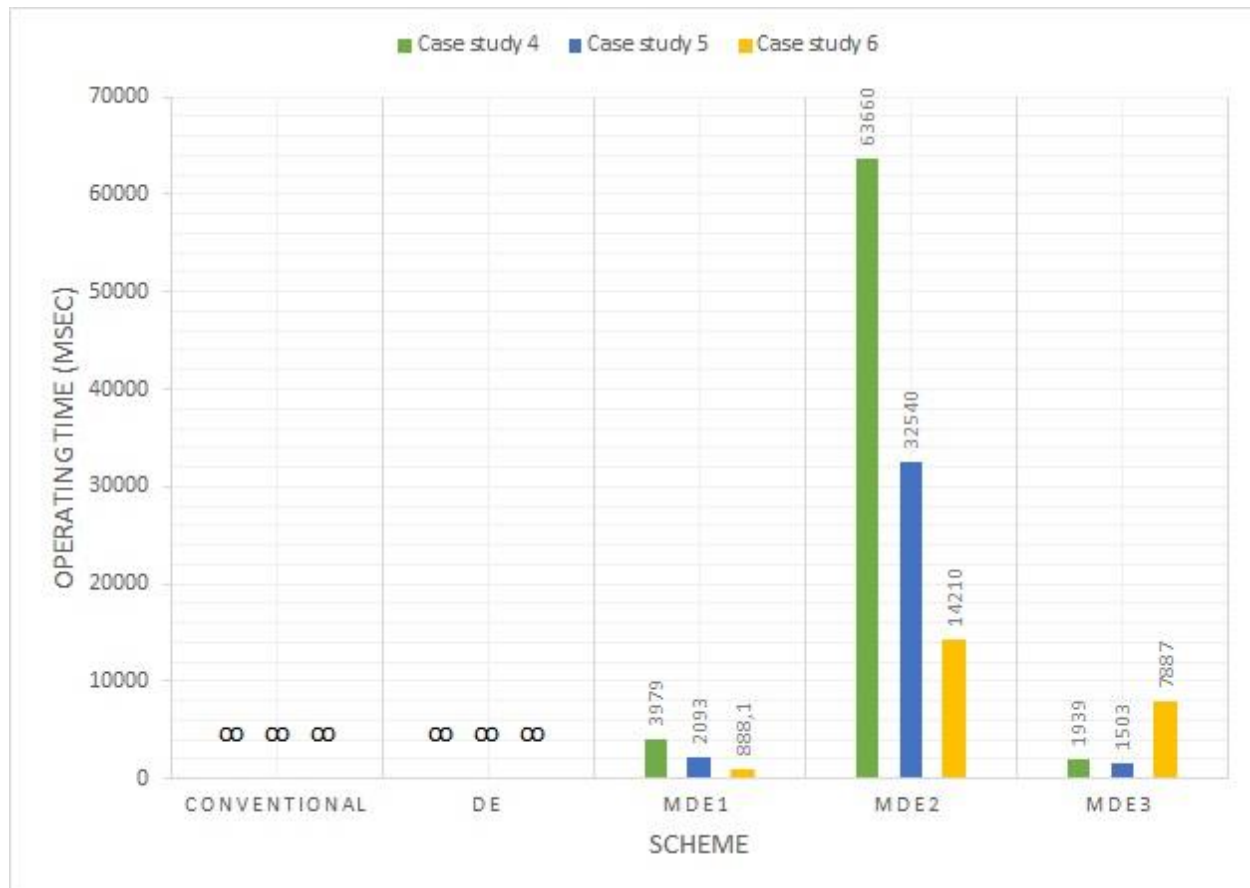


Fig. 0-19 Scheme and settings performance for temporary fault at F2 location

### 5.7.3. Comparison of scheme and settings performance with an exponential scale factor for F1 fault location

MDE1 and MDE3 are compared with each other in Fig. 5-20. The application of an exponential scale factor was to obtain balanced exploration and exploitation of the schemes. This is to obtain balanced settings that shall be tested for optimal protection in the auto-recloser. For case study 1, both scheme settings compute optimal operating times within the 200 msec target for a 0.1 sec temporary fault. When the Solar PV system is integrated in case study 2, both scheme settings compute optimal operating times for the auto-recloser, the time is within the 200 msec target. For faults that are within the 200 msec duration, this keeps the auto-

recloser fault isolation within the instantaneous and adjustable instantaneous operating region. In case study 3, the settings for both schemes gave a delayed pick-up of the auto-recloser, greater than the 200 msec target. The optimal scheme for settings is MDE3, but a better selection needs to be done for the change of type, location and increase in penetration of the distributed generation.

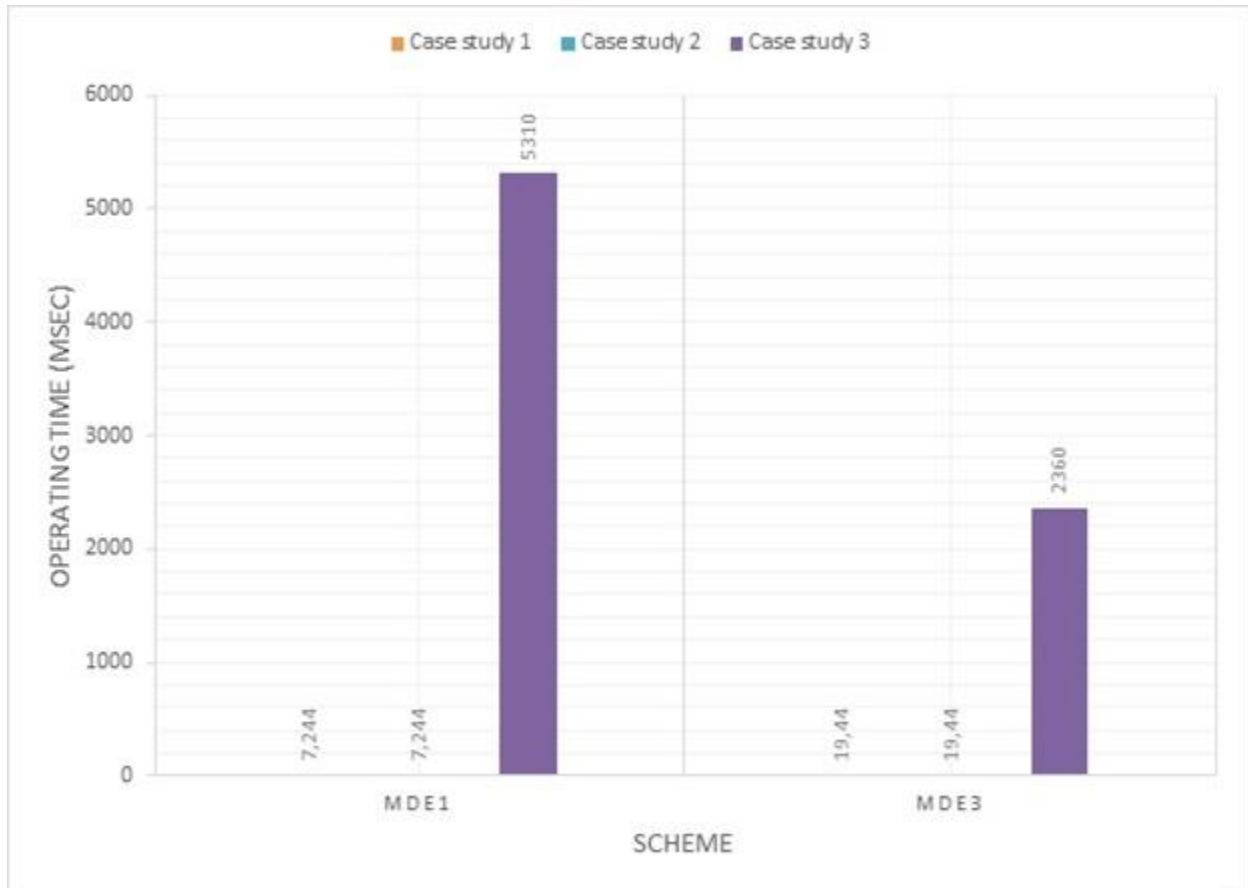


Fig. 5-20 Scheme and settings performance with an exponential scale factor for temporary fault at F1 location

#### 5.7.4. Comparison of scheme and settings performance with an exponential scale factor for F2 fault location

MDE1 and MDE3 are compared with each other for a change in the fault location as depicted in Fig. 5-21. For case study 1, MDE1 computes faster operating time than MDE3 but the operating time surpasses the 200 msec target and cannot isolate the temporary fault. For case study 2 and case study 3, MDE 1 computes an infinite operating time and mal-operates the auto-recloser. There is protection blinding. MDE3 computes high operating times for the auto-recloser, and they are not optimal. They may cause a loss of coordination.

For faults that are within the 200 msec duration, the auto-recloser fault isolation is not within the instantaneous and adjustable instantaneous operating region. The change in the fault location degraded the protection of the auto-recloser.

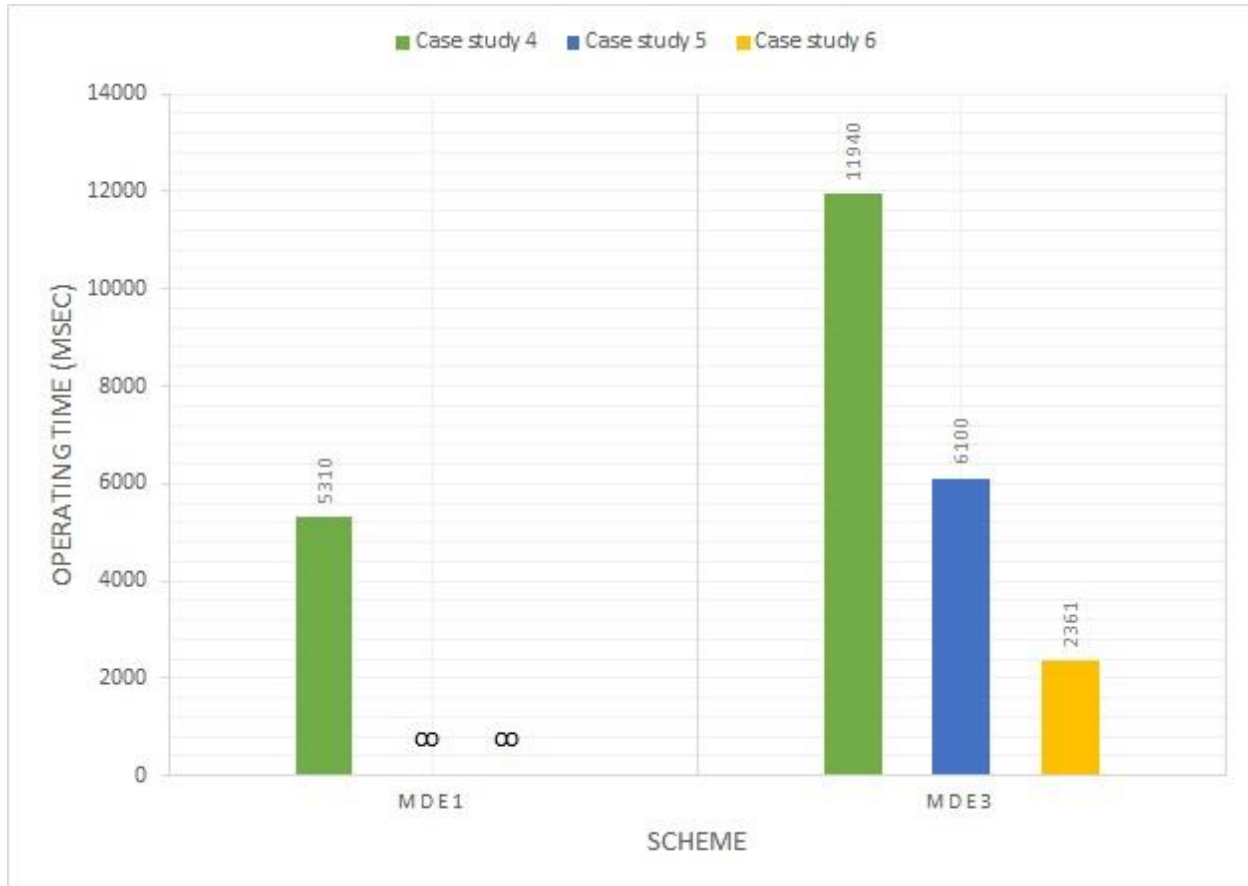


Fig. 0-21 Scheme and settings performance with an exponential scale factor for temporary fault at F2 location

## 5.8. Conclusion

Different case studies presented different scenarios of the factors that can cause an auto-recloser to mal-operate in a distribution network integrated with DG. This formed a foundation to optimize the auto-recloser in this distribution network for the automated responses in protecting it against temporary faults. The change in a type, location and penetration of DG systems in the IEEE 34 node distribution feeder presented voltage conditions that required settings to reduce the operating time for the pick-up activity in the auto-recloser. The fault location also became a factor in the operating time of the auto-recloser. This presented varied fault conditions. The requirement for an optimal protection of the auto-recloser is that the fast operating time should be in the range of 100 msec to 200 msec. This is to keep it from having mal-operations such as protection blinding and loss of coordination with other protection devices. Five settings were tested

and analysed in six case studies. Two of the settings from the MDE algorithm showed a better performance for these factors that can cause mal-operations. However, the scheme settings could not perform optimally for the change in type, location, increase in penetration of the DG and change in fault location and type.

The two modified schemes of the DE algorithm demonstrated capability to search and select optimal settings that can optimize the protection of the auto-recloser when there is an integration of the Solar PV system. However, there were mal-operations when there was an integration of the Wind Turbine system and change in the fault location and type. The selection, security, redundancy, sensitivity and dependability requirements were met for the integration of the Solar Photovoltaic but they were not met when the Wind Turbine system was integrated.

# **Chapter 6 Conclusion and Recommendation for future Research Works**

## **6.1. Introduction**

An auto-recloser, DE algorithm and MDE algorithm schemes have been successfully modelled in MATLAB Simulink and in the MATLAB Script. There were simulated performance results of the schemes settings that computed optimal performance but other results did not improve the performance to the optimal range of 100 msec to 200 msec. A DG integration, change in fault location and fault type case studies have been performed on the existing IEEE 34 node distribution feeder. This was to assess the impact of the settings obtained through the conventional settings and different DE algorithm schemes, in particular the pick-up activity of the auto-recloser when there is a temporary fault in an active distribution network. The feasibility of using the DE algorithm to obtain settings that can optimize the protection of the auto-recloser when a temporary fault occurs has been investigated.

## **6.2. Integration of DGs for the F1 fault location case studies**

Optimization of the auto-recloser protection for the integration of the Solar PV system was successfully performed when the temporary fault was a fault near the auto-recloser in the F1 location. With the constraints on settings of auto-recloser, the settings selected caused the pick-up activity of the auto-recloser to respond with an operating time within 200 msec during the temporary fault. The auto-recloser reclosed successfully and continued the supply of power. The MDE1 scheme settings showed a significant reduction in the operating time and became one of the schemes that can be applied to optimize the settings of the auto-recloser when there is an integration of a Solar PV system. This ensures that the requirements for selectivity, security, dependability, sensitivity and redundancy of the auto-recloser are met. However, when there was an integration of the Wind Turbine system, there was significant increase in the operating time of the auto-recloser and there was also sympathetic tripping in some cases. MDE1 scheme settings continued to show a reduction in the operating time compared to other scheme settings. The pick-up activity of the auto-recloser was delayed and surpassed the 200 msec target. The selectivity, dependability and security requirements were not met. The constant rise and fall voltage profile modes introduced by the Wind Turbine system caused the current to have the same profile. This caused the sympathetic tripping and failure of the auto-recloser to discriminate between a temporary fault and a permanent fault with the MDE1 scheme settings. But the reduction in the operating time of the auto-recloser by MDE1 and MDE3 give a possibility to apply the settings for temporary fault with a longer duration than 200 msec and within 1 sec. Therefore,

MDE1 and MDE3 are the recommended schemes in these case studies to optimize the auto-recloser protection.

### **6.3. Integration of DGs for the F2 fault location case studies**

Optimization of the auto-recloser protection for the integration of the Solar PV system was not successfully performed when the temporary fault was a fault far from the auto-recloser in the F2 location. The auto-recloser reclosed successfully and continued the supply of power, however with high operating times. The conventional and DE scheme settings had infinite operating times which cause the auto-recloser to have protection blinding. MDE1 and MDE3 scheme settings showed a reduced operating time compared to the MDE2 scheme settings and can be used for to optimizing the protection of the auto-recloser when there is an integration of a Solar PV system and Wind Turbine system. Although the requirements for selectivity, security, dependability, sensitivity and redundancy of the auto-recloser are not all met. The settings reduced the operating time of the auto-recloser when there was an integration of the Wind Turbine system. The constant rise and fall voltage profile modes introduced by the Wind Turbine system caused the current to have the same profile. This caused the sympathetic tripping and failure of the auto-recloser to discriminate between a temporary fault and a permanent fault for MDE1 scheme. But the reduction in the operating time of the auto-recloser by MDE1 give a possibility to apply the settings for temporary fault with a longer duration than 200 msec and within 1 sec. Therefore, MDE1 is the recommended scheme in these case studies to optimize the auto-recloser protection.

### **6.4. Integration of DGs with exponential scale factor application for the F1 fault location case studies**

These case studies investigated the feasibility of balancing the exploration and exploitation of the two schemes that performed better for obtaining optimal settings of the auto-recloser. This is to check the possibility of improving the schemes searching ability for balanced settings. The voltage and fault conditions remained the same as in the case studies that had the temporary fault in the F1 location. The scale factor of the schemes was exponentially varied. In these case studies, the MDE1 and MDE3 scheme settings were successfully applied to optimize the protection of the auto-recloser when the Solar PV systems was integrated. Again, MDE1 scheme exhibited best performance with regards to minimizing the operating time during the temporary fault, the operating time was within the 200 msec target. The scheme did not cause mal-operations and fully met the selectivity, security, dependability, sensitivity and redundancy requirements. However, when the Wind Turbine system was integrated, MDE1 scheme settings cause



protection blinding. MDE3 settings operate the auto-recloser without protection blinding in the case of the DGs having a change of type, location and penetration, but the operating time is not within the optimal target of 200 msec. MDE1 is recommended for the integration of a Solar PV system but MDE3 is recommended for the integration of the Wind Turbine system.

## **6.5. Integration of DGs with exponential scale factor application for F2 fault location case studies**

These case studies are to check the impact of a change in the fault location on auto-recloser when it is set with the MDE1 and MDE3 scheme settings obtained through the application of an exponential scale factor. The voltage and fault conditions remained the same as in the case studies that had the temporary fault in the F2 location. In these case studies, the MDE1 and MDE3 scheme settings did not perform optimally for both integrations of the DGs. When the auto-recloser was set with MDE1 scheme settings, it exhibited protection blinding when there was integration of the Solar PV system. The auto-recloser also exhibited protection blinding when there was an addition of the Wind Turbine system. MDE3 did not have protection blinding, but gave high operating times, however they reduced with the integration of the Solar PV system and addition of the Wind Turbine system. MDE3 is the scheme recommended in these case studies.

## **6.6. Recommendation for future Research Work**

The following future research work is proposed:

- Hardware-in-the-loop simulation and testing of the auto-recloser's pick-up activity.
- Applying adaptive protection scheme methods and use the schemes that optimized the protection of the auto-recloser. This is to automate the update of optimal settings in the auto-recloser when there is a change of conditions.
- Coordinating multiple auto-reclosers and finding the optimal coordination time interval for them to improve the distribution network response to different fault locations and types. The reach of the auto-recloser reduces when the fault is located far from the auto-recloser. This was evident when the fault location was changed to F2 and the fault current decreased. To further mitigate the blinding of protection due to the reach of the auto-recloser, future work on installing other auto-reclosers in a DG integrated network and optimizing them is proposed.

## References

- [1] A. Arafa, M. M. Aly and S. Kamel, "Impact of Distributed Generation on Recloser-Fuse Coordination of Radial Distribution Networks," in *2019 International Conference on Innovative Trends in Computer Engineering (ITCE)*, 2019.
- [2] U. Jamil, N. Qayyum, A. Mahmood and A. Amin, "Control Grid Strategies for Reduction of Real and Reactive Line Losses in Radial Power Distribution System," in *1st International Conference on Electrical, Communication and Computer Engineering (ICECCE)*, 2019.
- [3] N. Arava and V. R. Seshmasetti, "Voltage profile and loss analysis of radial distribution system in presence of Embedded generator with a case study in Mipower," in *IEEE Global Humanitarian Technology Conference (GHTC)*, 2013.
- [4] H. Yuan, F. Li, Y. Wei and J. Zhu, "Novel Linearized Power Flow and Linearized OPF Models for Active Distribution Networks With Application in Distribution LMP," in *IEEE Transactions on Smart Grid*, 2018.
- [5] M. J. Damghani, D. Faramarzi, H. A. Abyaneh and B. Vahidi, "Application of a Parallel-Resonance-Type FCL for Maintaining the Recloser-Fuse Coordination in a Power Distribution System with a Dispersed Generation," in *30th Power System Conference (PSC2015)*, 2015.
- [6] M. A. Velasquez, N. Quijano and A. I. Cadena, "Optimal placement of switches on DG enhanced feeders with short circuit constraints," in *Electric Power Systems Research*, 2016.
- [7] A. Ashour, "Modelling of Smart Auto-Recloser with Over Current Protection," in *Int. Journal of Engineering Research and Application*, 2018.
- [8] M.N. Alam, B. Das and V. Pant, "Protection scheme for reconfigurable radial distribution networks in presence of distributed generation," in *Electric Power Systems Research 192 (2021)*, 2021.
- [9] H. Bentarzi, M. Chafai, A. Ouadi and B. Harhati, "A New Computer Based Auto-recloser Framework," in *24th International Conference on Microelectronics (ICM)*, 2012.
- [10] O. Gorte, N. Kiryanova, M. Khmelik, A. Arestova, D. Baluev, G. Prankevich and V. Markin, "Assessment of Energy Storage Effect into Automatic Reclosing in Smart Grid," 2015.
- [11] F. T. Dai, "Impacts of Distributed Generation on Protection and Autoreclosing of Distribution Networks," in *10th IET International Conference on Developments in Power System Protection (DPSP 2010). Managing the Change*, 2010.
- [12] A. Abbasi, M. R. Haghifam and Ramin Dehghani, "An adaptive protection scheme in active distribution networks based on integrated protection," in *22nd International Conference on*

*Electricity Distribution (CIRED 2013)*, 2013.

- [13] L. F. F. Gutierrez, G. Cardoso Jr. and G. Marchesan, "Recloser-Fuse Coordination Protection for Distributed Generation Systems: Methodology and priorities for optimal disconnections," in *12th IET International Conference on Developments in Power System Protection (DPSP 2014)*, 2014.
- [14] S. F. Zarei and S. Khankalantary, "Protection of active distribution networks with conventional and inverter-based distributed generators," *International Journal of Electrical Power and Energy Systems*, vol. 129, pp. 1-13, 2021.
- [15] M. A. Dawoud, D. K. Ibrahim and M. Gilany, "Restoring recloser-fuse coordination in radial distribution networks with distributed generation," in *2017 Nineteenth International Middle East Power Systems Conference (MEPCON)*, 2017.
- [16] Md. Mahadi, H. S. Biswas and Md. A. A. Khan, "Study of Switching Transient Over Voltage due to Transient Short Circuit Fault in a Power Distribution Network," in *International Conference on Robotics,Electrical and Signal Processing Techniques (ICREST)*, 2019.
- [17] J. Kennedy, P. Ciufo and A. Agalgaonkar, "A review of protection systems for distribution networks embedded with renewable generation," in *Renewable and Sustainable Energy Reviews*, 2016.
- [18] V. Telukunta, J. Pradhan, A. Agrawal, M. Singh and S. G. Srivani, "Protection challenges under bulk penetration of renewable energy resources in power systems: A review," in *CSEE Journal of Power and Energy Systems*. 3, 2017.
- [19] H. M. Ashraf , M. F. Amjad, M. T. Arshad, M. I. Javaid and R. M. Asif, "Re-energizing of single phase by Protective scheme of parallel bi-Transmission Lines Using Fuzzy Logic Technique," in *5th International Conference on Renewable Energy: Generation and Applications (ICREGA)*, 2018.
- [20] J. H. He, Y. H. Cheng, J. Hu. and H. T. Yip, "An Accelerated Adaptive Overcurrent Protection for Distribution Networks with High DG Penetration," in *13th International Conference on Development in Power System Protection 2016 (DPSP)*, 2016.
- [21] S. Hemmati and J. Sadeh, "Applying Superconductive Fault Current Limiter to Minimize the Impacts of Distributed Generation on the Distribution Protection Systems," 2012.
- [22] H. BEDER, E. A. BADRAN aznd M. M. El-SAADAWI, "Investigation of the Impact of DG on the Behavior of NDEDG Protection Systems," in *22nd International Conference on Electricity Distribution*, 2013.
- [23] X. Wang, S.M. Strachan, S.D.J. McArthur and J.D. Kirkwood, "Automatic analysis of Pole Mounted Auto-Recloser data for fault diagnosis and prognosis," in *International Conference on Intelligent System Application to Power Systems (ISAP)*, 2015.

- [24] M. Njozela, S. Chowdhury, and S.P. Chowdhury, "Impacts of DG on the Operation of Auto-Reclosing Devices in a Power Network," in *2011 IEEE Power and Energy Society General Meeting*, 2011.
- [25] A. R. Haron, A. Mohamed, H. Shareef and Hadi Zayandehroodi, "Analysis and Solutions of Overcurrent Protection Issues in a Microgrid," in *IEEE International Conference on Power and Energy (PECon)*, 2012.
- [26] R. M. Chabanloo, M. G. Maleki, S. Mohammadi, M. Agah and E. M. Habashi, "Comprehensive coordination of radial distribution network protection in the presence of synchronous distributed generation using fault current limiter," in *International Journal of Electrical Power & Energy Systems*, 2018.
- [27] A. Chandra, G. K. Singh and V. Pant, "Protection of AC microgrid integrated with renewable energy sources – A research review and future trends," *Electric Power Systems Research* 193, pp. 1-28, 2021.
- [28] R. Thangaraj, M. Pant and A. Abraham, "New mutation schemes for differential evolution algorithm and their application to the optimization of directional over-current relay settings," in *Applied Mathematics and Computation*, 2010.
- [29] M. N. Hidayat and F. Li, "Impact of Distributed Generation Technologies on Generation Curtailment," in *2013 IEEE Power & Energy Society General Meeting*, 2013.
- [30] S. Das, A. Ray and S. De, "Optimum combination of renewable resources to meet local power demand in distributed generation: A case study for a remote place of India," 2020.
- [31] A. Dagar, P. Gupta and V. Niranjana, "Microgrid protection: A comprehensive review," in *Renewable and Sustainable Energy Reviews*, 2021.
- [32] A. Alam, V. Pant and B. Das, "Switch and recloser placement in distribution system considering uncertainties in loads, failure rates and repair," in *Electric Power Systems Research*, 2016.
- [33] Y. L. Baracy, L. F. Venturini, N. O. Branco, D. Issicaba and A. P. Grilo, "Recloser placement optimization using the cross-entropy method and reassessment of Monte Carlo sampled states," in *Electric Power Systems Research*, 2020.
- [34] L. Wright and L. Ayers, "Mitigation of Undesired Operation of Recloser Controls Due to Distribution Line Inrush," in *2015 IEEE Rural Electric Power Conference*, 2015.
- [35] T. P. Murray and A. Jones, "Field trials of Cutout mounted reclosers on single-phase spur lines in ESB networks," in *IEEE PES T&D 2010*, 2010.
- [36] N. Ji and S. Geiger, "Reducing outages in distribution by testing recloser controls," in *2014 China*

- International Conference on Electricity Distribution (CICED)*, 2014.
- [37] T. M. Krishna, B. Subrahmanyam, D. Reddy, N. V. Ramana and S. Kamakshaiah, "Power flow algorithm for radial distribution system with voltage sensitive loads," in *Annual IEEE India Conference(INDICON)*, 2012.
  - [38] Y. Tarid, Y. Wicaksono, A. S. Ramadhan and A. Purwanto, "Effect of Three Pole Auto-Reclose to Power System Transient Stability (Case Study: Jawa Timur and Bali System)," in *International Seminar on Intelligent Technology and Its Applications (ISITIA)*, 2018.
  - [39] A. A. Kusuma, P. A. A. Pramana, K. Gausultan H. M, and B. S, Munir, "Auto-reclose Performance Evalutation on 500kV Transmission Line with Four Circuits on One Tower," in *2018 International Conference on Smart Green Technology in Electrical and Information Systems (ICSGTEIS)*, 2018.
  - [40] M. P. Katti, S. H. Jangamshetti and A. Rege, "Modeling of Auto-recloser for Smart Grid," in *International Journal of Modern Engineering Research (IJMER)*, 2012.
  - [41] R. Ogden and J. Yang, "Impacts of Distributed Generation on Low-Voltage Distribution Network Protection," in *2015 50th International Universities Power Engineering Conference (UPEC)*, 2015.
  - [42] T. Thanasaksiri, "Modeling of recloser operation schemes under system ground fault using EMTP-ATPDraw," in *TENCON 2014 - 2014 IEEE Region 10 Conference*, 2014.
  - [43] J. D. Glover, M. S. Sarma and T. J. Overbye, *Power System Analysis and Design Fourth Edition*, Chris Carson, 2008.
  - [44] M.F. Alhajri and M. E. El-Hawary, "Exploiting the Radial Distribution Structure in Developing a Fast and Flexible Radial Power Flow for Unbalanced Three-Phase Networks," in *IEEE Transactions on Power Delivery*, 2010.
  - [45] H. Yazdanpanahi, Y. W. Li and W. Xu, "A New Control Strategy to Mitigate the Impact of Inverter-Based DGs on Protection System," in *IEEE Transactions on Smart Grid*, 2012.
  - [46] B. Fani, F. H. Mohammadi, M. Moazzamia and M. J. Morshed, "An adaptive current limiting strategy to prevent fuse-recloser miscoordination in PV-dominated distribution feeders," in *Electric Power Systems Research*, 2018.
  - [47] P. Mohammadi, H. El-Kishyky, M. Abdel-Akher and M. Abdel-Salam, "The Impacts of distributed generation on fault detection and voltage profile in power distribution networks," in *2014 IEEE International Power Modulator and High Voltage Conference (IPMHVC)*, 2014.
  - [48] R. A. Wilson and R. E. Catlett, "Reducing tripping times in medium voltage switchgear," in *2013 66th Annual Conference for Protective Relay Engineers*, 2013.

- [49] H. K. Karegar and S. Saberi, "Investigating of Wind Turbines Affects on Recloser Operation in Distribution Networks," in *IEEE International Conference on Power and Energy (PECon2010)*, 2010.
- [50] S. De Bruyn, J. Fadiran, S. Chowdhury, S. P Chowdhury and P. Kolhe, "The impact of wind power penetration on recloser operation in distribution networks," in *2012 47th International Universities Power Engineering Conference (UPEC)*, 2012.
- [51] M. Y. Shih, A. Conde, C. Angeles-Camacho, E. Fernandez and Z. M. Leonowicz, "Mitigating the impact of distributed generation and fault current limiter on directional overcurrent relay coordination by adaptive protection scheme," in *2019 IEEE International Conference on Environment and Electrical Engineering and 2019 IEEE Industrial and Commercial Power Systems Europe (EEEIC / I&CPS Europe)*, 2019.
- [52] V.A. Papaspiliotopoulos, V.A. Kleftakis, P.C. Kotsampopoulos, G.N. Korres, and N.D. Hatziaargyriou, "Hardware-in-the-Loop Simulation for Protection Blinding and Sympathetic Tripping in Distribution Grids with High Penetration of Distributed Generation," in *MedPower 2014*, 2014.
- [53] N. El Nailly, S. M. Saady, A. Elhaffar, T. Hussein, and F. A. Mohamedx, "Mitigating The Impact of Distributed Generator on Medium Distribution Network by Adaptive Protection Scheme," in *The 8th International Renewable Energy Congress (IREC 2017)*, 2017.
- [54] J. A. Martínez-Velasco, J. Martín-Arnedo and F. Castro-Aranda, "Modeling Protective Devices for Distribution Systems with Distributed Generation using an EMTP-Type Tool," in *Ingeniare. Revista chilena de ingeniería*, 2010.
- [55] K. Rana, U. Wani and H. Chaudhari, "Modified recloser settings for mitigating recloser-fuse miscoordination during distributed generation interconnections," in *IEEE International Conference on Power, Control, Signals and Instrumentation Engineering (ICPCSI-2017)*, 2017.
- [56] K. Bangash, M. E. Farag and A. Osman, "Impact of Energy Storage Systems on the Management of Fault Current at LV Network with High Penetration of Distributed Generation," in *International Journal of Smart Grid and Clean Energy*, 2017.
- [57] H. H. Zeineldin, H. M. Sharaf, D. K. Ibrahim and E. El-Din A. El-Zahab, "Optimal Protection Coordination for Meshed Distribution Systems With DG Using Dual Setting Directional Over-Current Relays," in *IEEE Transactions on Smart Grids*, 2015.
- [58] M.V. Tejeswini and B. C. Sujatha, "Optimal protection coordination of voltage-current time based inverse relay for PV based distribution system," in *2017 Second International Conference on*

*Electrical, Computer and Communication Technologies (ICECCT)*, 2017.

- [59] R. Benabid, M. Zellagui, A. Chaghi, and M. Boudour, "Optimal Coordination of IDMT Directional Overcurrent Relays in the Presence of Series Compensation using Differential Evolution," in *Proceedings of the 3rd International Conference on Systems and Control*, 2013.
- [60] H. Sedighneja and A. Jalilian, "Effect of protection device coordination on voltage sag characteristics of distribution networks," in *ISA Transactions*, 2010.
- [61] H. A. Abdel-Ghanya, A. M. Azmya, N. I. Elkalashy and E. M. Rashad, "Optimizing DG penetration in distribution networks concerning protection schemes and technical impact," in *Electric Power Systems Research* 128, 2015.
- [62] "Distribution System Analysis Subcommittee Report," <http://www.egr.unlv.edu/>.
- [63] S. Ghobadpour, M. Gandomkar and J. Nikoukar, "Determining Optimal Size of Superconducting Fault Current Limiters to Achieve Protection Coordination of Fuse-Recloser in Radial Distribution Networks with Synchronous DGs," in *Electric Power Systems Research*, 2020.
- [64] D. Kumar and S.R.Samantaray, "Design of an advanced electric power distribution systems using seeker optimization algorithm," in *International Journal of Electrical Power & Energy Systems*, 2014.
- [65] A. V. Pombo, J. Murta-Pinab and V. F. Pires, "Multiobjective planning of distribution networks incorporating switches and protective devices using a memetic optimization," in *Reliability Engineering & System Safety*, 2015.
- [66] S.P.S. Matos, M.C. Vargas, L.G.V. Fracalossi, L.F. Encarna and O.E. Batista , "Protection philosophy for distribution grids with high penetration of distributed generation," *Electric Power Systems Research*, vol. 196, 2021.
- [67] H. B. Funmilayo, J. A. Silva and K. L. Butler-Purpy, "Overcurrent Protection for the IEEE 34-Node Radial Test Feeder," *IEEE Transactions on Power Delivery*, vol. 27, no. 2, pp. 459-468, 2012.
- [68] Q. Cui and Y. Weng, "An environment-adaptive protection scheme with long-term reward for distribution networks," in *International Journal of Electrical Power & Energy Systems*, 2021.
- [69] G. Y. Sinishaw, B. Bantayirga and K. Abebe, "Analysis of smart grid technology application for power distribution system reliability enhancement: A case study on Bahir Dar power distribution," in *Scientific African* 12, 2021.
- [70] V. C. Ukwueze, J. N. Onah and T. C. Madueme, "A Frame Work for Over Current Relay Protection Optimization," in *International Journal of Engineering Research & Technology (IJERT)*, 2015.

- [71] Myoung-Hoo Kim, Sung-Hun Lim, and Jae-Chul Kim, "Improvement of Recloser-Fuse Operations and Coordination in a Power Distribution System With SFCL," *IEEE Transactions on Applied Superconductivity*, 2011.
- [72] "IEC/IEEE International Standard - High-voltage switchgear and controlgear - Part 111: Automatic circuit reclosers for alternating current systems up to and including 38 kV," *IEC 62271-111 and IEEE Std C37.60-2018*, no. 10.1109/IEEESTD.2019.8641507, pp. 1-272, 12 Feb 2019.
- [73] Nulec Industries A Schnieder Electric Company, "Recloser Application Notes," *Electrical Switchgear Engineers and Automation Specialists*, 2000.
- [74] X. Wang, S. D. J. McArthur, S. M. Strachan, J. D. Kirkwood and B. Paisley, "A Data Analytic Approach to Automatic Fault Diagnosis and Prognosis for Distribution Automation," in *IEEE Transactions on Smart Grid*, 2018.
- [75] F. Belloni, R. Chiumeo, C. Gandolfi and A. Villa, "A protection coordination scheme for active distribution networks," 2012 47th International Universities Power Engineering Conference (UPEC), 2012.
- [76] M. A. Redfern, W. T. Shang and R. O'Gorman, "Auto-reclose for remote breakers in networks containing distributed generators," in *10th IET International Conference on Developments in Power System Protection (DPSP 2010). Managing the Change*, 2010.
- [77] M. H. Kim, S. H. Lim, J. F. Moon, and J. C. Kim, "Method of Recloser-Fuse Coordination in a Power Distribution System With Superconducting Fault Current Limiter," *IEEE Transactions on Applied Superconductivity*, 2010.
- [78] M. Y. Shiha, A. Conde, C. Ángeles-Camacho, E. Fernández, Z. Leonowicz, F. Lezama and J. Chan, "A Two Stage Fault Current Limiter and Directional Overcurrent Relay Optimization for Adaptive Protection Resetting using Differential Evolution Multi-objective Algorithm in Presence of Distributed Generation," in *Electric Power Systems Research 190*, 2021.
- [79] H. S. Pandya, D. M. Pandeji, R. K. Iyer and M. Prathana, "Digital protection strategy of microgrid with relay time grading using particle swarm optimization," in *5th Nirma University International Conference on Engineering (NUICONE)*, 2015.
- [80] S. B. Gumede and A. K. Saha, "A Comparison of a Recloser Performance in a Passive and Active Distribution System," in *2021 International Conference on Electrical, Computer, Communications and Mechatronics Engineering (ICECCME)*, 2021.
- [81] P.Y. Wang, F.Y. Liang, J.Y. Song, L. Guo, J.F. Zhang, Y.Y. Xie and S.Z. Wang, "Fault current characteristics in active distribution networks with integrations of multiple PVs," in *2019 IEEE 8th*



- International Conference on Advanced Power System Automation*, Nanjing, 2019.
- [82] A. I. Atteya, A. M. El Zonkoly and H. A. Ashour, "Optimal Relay Coordination of an Adaptive Protection Scheme using Modified PSO Algorithm," in *2017 Nineteenth International Middle East Power Systems Conference (MEPCON)*, 2017.
  - [83] J. Kyle, B. Campbell and L. Martin, "Analysis of the Sympathetic Tripping Problem for Networks with High Penetrations of Distributed Generation," in *The International Conference on Advanced Power System Automation and Protection*, 2011.
  - [84] R. Madhumitha, P. Sharma, D. Mewara, O.V. G. Swathika and S. Hemamalini, "Optimum Coordination of Overcurrent Relays Using Dual Simplex and Genetic Algorithms," in *2015 International Conference on Computational Intelligence and Communication Networks (CICN)*, 2015.
  - [85] R. Thangaraj, T. R. Chelliah and M. Pant, "Overcurrent Relay Coordination by Differential Evolution Algorithm," in *2012 IEEE International Conference on Power Electronics, Drives and Energy Systems*, 2012.
  - [86] M. Klanac, D. Zarko and S. Stipetic, "Comparison of Ant Colony and Differential Evolution Optimization Methods Applied to a Design of Synchronous Reluctance Machine," in *International Conference on Electrical Drives & Power Electronics (EDPE)*, 2019.
  - [87] N. Li and S. Zhu, "Modified Particle Swarm Optimization and Its Application in Multimodal Function Optimization," in *International Conference on Transportation, Mechanical, and Electrical Engineering (TMEE)*, 2011.
  - [88] Ming-Gong Lee and Kun-Ming Yu, "Dynamic Path Planning Based on an Improved Ant Colony Optimization with Genetic Algorithm," in *2018 IEEE Asia-Pacific Conference on Antennas and Propagation (APCAP)*, 2018.
  - [89] R. Jangra and R. Kait, "Analysis and comparison among Ant System; Ant Colony System and Max-Min Ant System with different parameters setting," in *3rd International Conference on Computational Intelligence & Communication Technology (CICT)*, 2017.
  - [90] A. Ebrahimi, V. Dehdeleh, A. Boroumandnia and V. Seydi, "Improved Particle Swarm Optimization through Orthogonal Experimental Design," in *2nd Conference on Swarm Intelligence and Evolutionary Computation (CSIEC)*, 2017.
  - [91] S. Rodporn, D. Uthitsunthorn, T. Kulworawanichpong, R. Oonsivilai and A. Oonsivilai, "Optimal Coordination of Over-Current Relays Using Differential Evolution," in *9th International Conference on Electrical Engineering/Electronics, Computer, Telecommunications and Information*

*Technology*, 2012.

- [92] S. Ding, "Logistics network design optimization based on differential evolution algorithm," in *2010 International Conference on Logistics Systems and Intelligent Management (ICLSIM)*, 2010.
- [93] S. B. Gumede and A. K. Saha, "Optimizing Recloser Settings in an Active Distribution System Using the Differential Evolution Algorithm," in *Energies*, 2022.
- [94] R.P. Payasi, A.K. Singh and D. Singh, "Planning of Different types of distributed generation with seasonal mixed load models," *International Journal of Engineering, Science and Technology*, pp. 112-124, 2012.
- [95] M.L. Prasanna, A. Jain and J.R. Kumar, "Optimal Distributed Generation Placement Using Hybrid Technique," in *IEEE PES Asia-Pacific Power and Energy Engineering Conference (APPEEC)*, 2017.
- [96] G. Chen, F. L. Lewis, E. N. Feng and Y. Song, "Distributed Optimal Active Power Control of Multiple Generation Systems," *IEEE TRANSACTIONS ON INDUSTRIAL ELECTRONICS*, pp. 7079-7090, 2015.
- [97] F. Andr en, R. Br undlinger, and T. Strasser, Senior, "IEC 61850/61499 Control of Distributed Energy Resources: Concept, Guidelines, and Implementation," in *IEEE TRANSACTIONS ON ENERGY CONVERSION*, 2014.
- [98] M. Bouzguenda, A. Gastli, A. H. Al Badi and T. Salmi, "Solar Photovoltaic Inverter Requirements for Smart Grid Applications," in *IEEE PES Conference on Innovative Smart Grid Technologies - Middle East*, 2011.
- [99] J. Arrinda, J. A. Barrena, M. A. Rodr guez and A. Guerrero, "Analysis of massive integration of renewable power plants under new regulatory frameworks," in *3rd International Conference on Renewable Energy Research and Applications*, 2014.
- [100] S. Zhu, L. Geng, J. Zheng, X. Wang, D. Choi and Y. Li, "Selection Method of Transformer Interconnecting Distributed Generation and Distribution Networks," in *Transmission & Distribution Conference & Exposition: Asia and Pacific*, 2009.
- [101] J. Taylor, J. W. Smith and R. Dugan, "Distribution Modeling Requirements for Integration of PV, PEV, and Storage in a Smart Grid Environment," in *IEEE Power and Energy Society General Meeting*, 2011.
- [102] M. Ahmadi, O.B. Adewuyi, M.S.S. Danish, P. Mandal, A. Yona and T. Senjyu, "Optimum coordination of centralized and distributed renewable power generation incorporating battery storage system into the electric distribution network," *International Journal of Electrical Power &*

*Energy Systems* , vol. 125, 2020.

- [103] K.A. Wheeler, S.O. Faried and M. Elsamahy, "Assessment of Distributed Generation Influences on Fuse-Recloser Protection Systems in Radial Distribution Networks," in *IEEE/PES Transmission and Distribution Conference and Exposition (T&D)*, 2016.
- [104] B. Matthias, S. Eberlein and R. Krzysztof, "Design of an inverter model according to the network code requirements for low-voltage grids," in *Modern Electric Power Systems (MEPS)*, 2019.
- [105] R.R. Toledo, K.M. Silva and T.R. Honorato, "Evaluating Single-Phase Reclosing on Distribution Grid Voltage," in *4th Workshop on Communication Networks and Power Systems*, 2019.

